Universidad de Oviedo
Universidá d'Uviéu
University of Oviedo

Programa de doctorado: Ingeniería de Producción, Minero-Ambiental y de Proyectos

Tesis Doctoral

Algorithms for precision forest inventories based on terrestrial point clouds

Algoritmos para inventario forestal de precisión basados en nubes de puntos terrestres

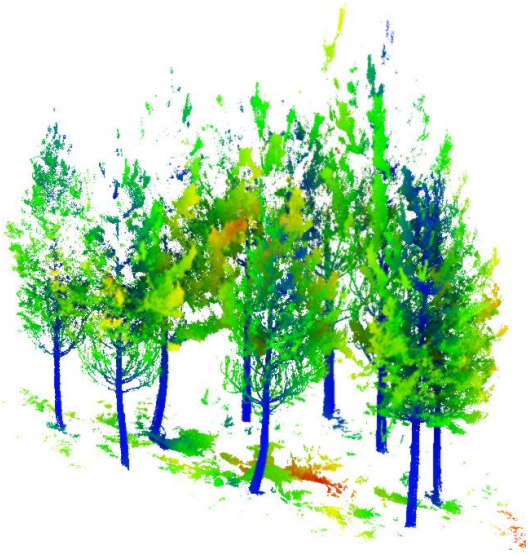

Covadonga Prendes Pérez

2022

Programa de doctorado: Ingeniería de Producción, Minero-Ambiental y de Proyectos

Tesis Doctoral

Algorithms for precision forest inventories based on terrestrial point clouds

Algoritmos para inventario forestal de precisión basados en nubes de puntos terrestres

Autora:

Covadonga Prendes Pérez

Directores:

Celestino Ordoñez Galán

Elena Canga Líbano

2022

Universidad de Oviedo

RESUMEN DEL CONTENIDO DE TESIS DOCTORAL

1.- Título de la Tesis	
Español/Otro Idioma: Algoritmos para inventario forestal de precisión basados en nubes de puntos terrestres	Inglés: Algorithms for precision forest inventories based on terrestrial point clouds

2.- Autor	
Nombre: Covadonga Prendes Pérez	
Programa de Doctorado: Ingeniería de Producción, Minero-Ambiental y de Proyectos	
Órgano responsable: Universidad de Oviedo	

RESUMEN (en español)

La gestión forestal sostenible ayuda a mitigar los efectos del cambio climático y es la base de un sector económico crucial. Optimizar las prácticas forestales facilita la sostenibilidad, pero requiere disponer de información de los recursos disponibles. Los inventarios tradicionales basados en muestreos periódicos del diámetro normal y la altura total seguidos de una generalización estadística no cubren las necesidades de información necesarias para una gestión sostenible multipropósito.

Esta tesis doctoral se centra en proporcionar nuevas herramientas para los inventarios forestales de precisión a través del desarrollo de algoritmos aplicables a nubes de puntos terrestres, que facilitan la obtención de una representación geométrica precisa de los árboles en un tiempo razonable. Además, esas mediciones eliminan la subjetividad asociada a los métodos tradicionales de inventario forestal. Específicamente, se desarrollaron algoritmos que proporcionan soluciones automáticas para aspectos clave de la gestión forestal: parametrización de ecuaciones de volumen, estimación de variables de forma del tronco y determinación del patrón óptimo de corte. Constituyen un flujo de trabajo secuencial en el sentido de que cada algoritmo utiliza datos del anterior para funcionar.

El primero calcula las variables básicas que caracterizan a los árboles geométricamente: (i) diámetros a lo largo del tronco; (ii) coordenadas del centro de la sección (XYZ); (iii) altura total del árbol. Los diámetros a lo largo del tronco y la altura se usan luego para parametrizar las ecuaciones de volumen. El segundo algoritmo estima variables de forma del tronco dividiéndolo en secciones espaciadas uniformemente cuyos diámetros y centros son calculados y se usan como variables de entrada para calcular automáticamente la curvatura, sinuosidad e inclinación de cada árbol. El tercer algoritmo determina el patrón de corte óptimo para cada fuste, maximizando el valor económico de cada árbol en base a una serie de productos comerciales. Se basa en el modelado tridimensional de los fustes e incluye el diámetro y la curvatura de cada troza.

El funcionamiento de los algoritmos se evaluó en varias parcelas y las ventajas y desventajas de cada uno fueron comparadas con los métodos tradicionales. Las pruebas de validación del Algoritmo 1 (parametrización de ecuaciones de volumen de madera) se llevaron a cabo en una parcela de *Pinus pinaster* con pendiente elevada, ramas bajas y sotobosque denso, y el 97% de los árboles fueron detectados automáticamente con un error medio cuadrático (*RMSE*) para la altura y las estimaciones de diámetros e 1.52 m y 1.14 cm respectivamente. Una ecuación de razón fue seleccionada de forma automática como la mejor opción para la parcela de validación. El *RMSE* de las estimaciones automáticas de volumen fue de 0.0233 m3 y 0.0149 m3 cuando los diámetros fueron previamente revisados por un operador y las secciones anómalas redibujadas. El Algoritmo 2 (estimación de variables de forma) se evaluó en una parcela de mejora genética de *Pinus pinaster* y los resultados obtenidos se compararon con mediciones de campo de la rectitud la inclinación basadas en una clasificación visual. La metodología se mostró robusta a los errores en la estimación de los centros de las secciones, la base para estimar variables de forma. Además, la precisión mejora sustancialmente con

respecto a las técnicas tradicionales donde la clasificación errónea es frecuente. La evaluación del Algoritmo 3 (tronzado óptimo de fustes) se realizó en una parcela de *Pinus radiata* con 120 árboles, y los resultados se compararon con los obtenidos al utilizar como datos de entrada solo los diámetros estimados con TLS y con funciones de perfil. El uso del TLS incluyendo la curvatura proporcionó una solución de tronzado óptimo más realista dando lugar a una estimación más baja del volumen comercial

Los tres algoritmos tienen una aplicación directa en la planificación forestal, respaldando el uso del TLS en inventarios forestales de precisión. Son completamente automáticos, pretenden ser aplicables a cualquier especie o tipo de nube de puntos terrestres y eliminan la subjetividad en las medidas de campo y en la estimación de variables. Aunque todos muestran resultados muy prometedores, sería deseable realizar una investigación sistemática en parcelas más grandes con distintas técnicas de escaneo y distintas condiciones forestales

RESUMEN (en Inglés)

Sustainable forest management helps mitigate climate change and supports a crucial economic sector. Optimizing forest management practice facilitates sustainability, but requires quality information on available resources. Traditional inventories based on periodic field sampling of diameter at breast height and total height and statistical generalization, do not meet current information needs for sustainable multipurpose management.

This doctoral thesis focuses on providing new tools for precision forestry inventories through developing algorithms applicable to terrestrial point clouds, which facilitates obtaining accurate geometric representations of trees in a reasonable time. Moreover, such measurements avoid the observer subjectivity of traditional forest inventory methods. In addition, 3D TLS point clouds can be processed automatically, or semi-automatically, by means of mathematical algorithms. Specifically, we developed algorithms which provide automatic solutions for three key issues in forest management: volume equation parametrization, stem shape variables estimation and optimal bucking pattern determination. They constitute a staged workflow in the sense that each algorithm builds on the previous one.

The first calculates the basic variables that characterize trees geometrically: (i) diameters of the sections along the stem; (ii) coordinates of the centre of the section (XYZ) and (ii) total height of the tree. Diameters along the stem and height are later used to parametrize wood volume equations. The second algorithm estimates stem shape variables by splitting the stem into evenly spaced sections whose diameters and centres are calculated and used as input variables to automatically calculate the maximum sagitta, sinuosity, and lean of each tree. The third algorithm determines the optimal bucking pattern of each stem, maximizing each tree's economic value in terms of several timber products. It is based on the three-dimensional modelling of stems and includes the diameter and curvature of each log.

Algorithm performance was tested in various plots and the advantages and disadvantages of each was compared to traditional techniques. Validation tests for Algorithm 1 (wood volume equation parametrization) were carried out in a *Pinus pinaster* plot with steep slopes, low branches and dense understory, and 97% of trees were automatically detected and RMSE of the height and diameter estimations was 1.52 m and 1.14 cm, respectively. A volume ratio equation was automatically selected as the best option for the test dataset. Root mean square error (*RMSE*) in automatic volume estimations was 0.0233 m^3 and 0.0149 m^3 when diameters were previously reviewed by an operator and anomalous sections redrawn. Algorithm 2 (stem shape variables estimation) was tested in a breeding trial plot of *Pinus pinaster*, and the results obtained compared with field measurements of straightness and lean based on visual classification. The methodology was robust to errors in estimating section centres, the basis for calculating shape parameters. Besides, its accuracy compared favourably with traditional field techniques, where misclassification is frequent. Testing of Algorithm 3 (optimal bucking of stems) was in a *Pinus radiata* plot of 120 trees, and the results compared with those obtained with input data that only consider diameters estimated from TLS measurements and taper equations, not take curvature into account. Using TLS and including curvature measurements, provided a more realistic optimal bucking solution and tended to result in lower estimations of commercial value.

All three algorithms have a direct application in forest planning, supporting the use of TLS in precision forest inventories. They are completely automatic, aim to be applicable to any species or terrestrial point cloud type and eliminate subjectivity in field measurements and the estimation of variables. Although all show promising results, the systematic investigation of larger test sites with different scanning techniques and forest conditions is desirable.

SR. PRESIDENTE DE LA COMISIÓN ACADÉMICA DEL PROGRAMA DE DOCTORADO EN _____

AGRADECIMIENTOS

A Juan Majada por darme la oportunidad de hacer esta tesis en el CETEMAS.

A mis directores Elena y Celestino por estar siempre dispuestos a guiarme y animarme.

A Carlos Cabo por su implicación en esta tesis aportando su conocimiento y su trabajo y por estar siempre disponible para ayudarme a mejorar.

A Mauricio por su colaboración en el Capítulo 4 y por estar siempre dispuesto a aportar.

A Ronnie Lendrum por su ayuda con el inglés y su buen hacer.

A la gente de Swansea y Trento que ayudó a sentirme como en casa.

A todos mis compañeros del SERMAS que han hecho que estos años de trabajo fueran mucho más llevaderos, es un orgullo ser parte de esta pequeña familia y sobre todo del equipo de Geomáticos.

En especial a mis chicas del CETEMAS por los paseos y las risas que tan necesarias son cuando una no ve la luz al final del túnel.

Gracias a Ernesto y Manu, compañeros de aventuras droniles durante estos años, por enseñarme siempre con paciencia y aguantar a este "Fardín" por el mundo.

A mi familia por darme la oportunidad de tener unos estudios y por confiar siempre en mi capacidad y en mi buen juicio. Tengo mucha suerte de teneros.

A mis amigos de todas las etapas por ser un pilar fundamental en mi vida.

A Pedro por tu cariño y por hacerme la vida más fácil soportando todos los "Python-dramas" con paciencia y una sonrisa.

Gracias a todos

FUNDING

The works carried out in this Doctoral Thesis were developed at the Forestry and Wood Technology Center of Asturias (CETEMAS) and co-founded by the Spanish Department of Rural and Forest Infrastructure, Regional Department of the Environment and Land Management of Asturias.

Specifically, the work presented in Chapters 2 and 3 was also funded by the National Institute of Agricultural and Food Research and Technology (INIA) within the framework of the RTA2017-00063-C04-02 (2017) project entitled: “Evaluation of relevant characters for the sustainable management of *Pinus pinaster* Ait. and their interaction under new climatic scenarios” and co-founded

STRUCTURE OF THE THESIS

This PhD thesis is divided into 5 chapters, which are summarised as follows:

1) **Chapter 1**: General introduction and objectives; The section includes the background and justification of the thesis followed by the defining of aims.
2) **Chapter 2**: An algorithm for the automatic parametrization of wood volume equations from TLS point clouds is presented and tested in a *Pinus pinaster* plot.
3) **Chapter 3**: An algorithm for the automatic assessment of individual stem shape parameters in forest stands from TLS point clouds is developed and tested in a *Pinus pinaster* plot.
4) **Chapter 4:** An algorithm for the optimal bucking of stems from terrestrial laser scanning data is presented and tested in a *Pinus radiata* plot.
5) **Chapter 5:** Conclusions.

Bibliography references in this thesis are included at the end of the manuscript to facilitate the literature search.

Note: This thesis has been written in a bilingual format of English-Spanish to meet the requirements of the International PhD Mention.

GRAPHICAL ABSTRACT

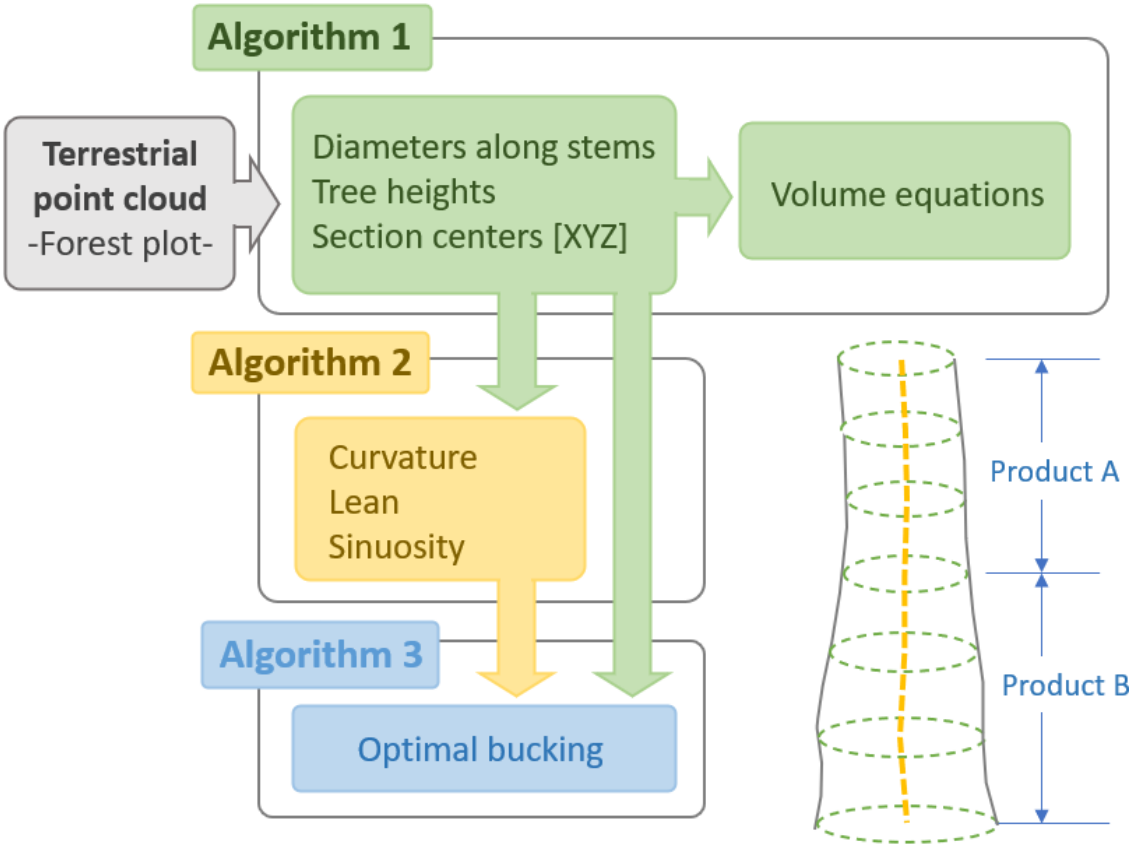

TABLE OF CONTENTS

INDEX OF FIGURES

INDEX OF TABLES

CHAPTER 1:

INTRODUCTION AND OBJECTIVES

CHAPTER 1: INTRODUCTION AND OBJECTIVES

1.1 JUSTIFICATION

The European Union recognizes that sustainable forest management can help to mitigate climate change while supporting a crucial economic sector. Accordingly, the use and management of forest resources must guarantee the sustainability of both environmental and economic roles. Sustainability can be ensured by optimizing forest management practices, which in turn requires quality information on available resources. In this sense, the proper characterization of forest ecosystems and the accurate and updated monitoring of the spatial-temporal distribution of forest stocks through inventories at the local, regional and global scale are crucial to deal with current threats such as the loss of biodiversity, diseases and pests, forest fires and global climate change by developing better management plans and mitigation policies.

Traditional inventories based on periodic field sampling of diameter at breast height (*dbh*, measured at approximately 1.30 m) and total height (*h*), followed by statistical generalization, do not meet current information needs for sustainable multipurpose management. In addition, they are costly in both economic and human terms, which is why they are usually limited to small areas of forest and a high sampling intensity. Furthermore, traditional field work often relies heavily on the skills of the operator, and careless measurements can lead to large errors. In this sense, remote sensing data can provide accurate, robust, and spatially explicit data over large areas through inexpensive and relatively quick surveys. More specifically, the use of TLS (Terrestrial Laser Scanning) allows high-quality information on the structure of trees, and more specifically the stems, to be obtained. In the last decade, there has been steady progress in terms of the study of the application of TLS in forest inventories. It is already possible to measure traditional tree attributes such as *dbh* and *h* from point cloud data, but they also offer the possibility of getting new data that are not measurable using conventional tools (straightness, lean, branches angle insertion, etc.). In this regard, the methods, experiments and techniques developed here have demonstrated that TLS can be used in a practical way to accurately collect certain tree attributes in sample plots.

However, after a decade of active research, TLS has not yet been accepted as an operational tool in forest inventories. Its application is hampered mainly by difficulties in the automation of the point cloud processing that provide~~s~~ convincing measurement results of the most important forest inventory parameters. There is still a lack of automatic and accurate methods to detect certain important tree attributes such as tree species and height, which needs further study. Other important factors that limit the use of this technology include the relatively high cost of the instrument, the limited software and the lack of personnel training. Additionally, it should be noted that acceptable results obtained from using TLS for forest inventories, from a forester's perspective, have only recently begin to appear. Therefore, it will take some time before foresters start using TLS operationally, and sufficient time is required to build the necessary software.

Having tools to process TLS data is essential to be able to transform these data into useful information for forest management: tools based on objective measurements and reproducible methodologies that allow us to have comparable multitemporal data. In this regard, this doctoral thesis is focused on providing new tools for precision forestry inventories through the development of algorithms to process terrestrial point clouds. Specifically, we have developed algorithms for three key issues in forest management: volume equation parametrization, stem shape variables estimation and optimal bucking pattern determination.

1.2 HISTORY OF FOREST INVENTORIES

The term forest inventory refers to the process of collecting information about the extent and condition of forest resources within a specified area (Kangas and Maltamo 2006). Interest in gathering information about forest resources goes far back in time. In fact, the first regulations to protect trees and forests date back to the 14th and 15th centuries, when the first attempts at forest inventory were carried out. These attempts were closely related to mining activity, which required large amounts of wood for the construction of mine shafts and galleries. Consequently, there were severe deforestation problems in areas surrounding mining infrastructures. However, these primitive inventories bear no resemblance to those we have now. It was not until the 18th when the Enlightenment started to place importance on the study of forests from a wider perspective. In times when coal and oil could not be exploited, wood was the only fuel that enabled industries to develop (foundries, glass production), as well as the material needed to pack merchandise (barrels), leather tanning, the building of factories and cities, the shoring of mines and shipbuilding. As such, the forest became a fundamental source of resources for the project of social change. But, in order to rationally exploit forests in such a way as to provide all these resources in a sustained manner over time and at the same time as they continue to fulfil their role as regulators of the hydrological cycle and protector of erosion, it was necessary to increase human knowledge of their structure and dynamics. Regarding tree breeding, agriculture treatments have been used since Roman times, although there was no knowledge about how to quantify and exploit forest resources without completely destroying them. With this objective, people began to inventory trees, laying the foundations for modern forest inventories: in Spain the first forest inventory was performed in 1748 (Alberdi, Cañellas, and Bombín 2017). However, these inventories were not done systematically following a specific methodology.

In fact, it is not until 150 years later, at the beginning of the 20th century, that systematic forest inventories started to be carried out. The pioneers in this respect were the Nordic countries and from there they spread around the world (Breidenbach et al. 2020). These early forest inventories contributed considerably to the development of statistical sampling theory and played their part in establishing a standard methodology to facilitate comparisons in both space and time. Basically, in a forest inventory, today, fixed plots of similar size and distributed within the study area are sampled, and the same kind of measurements taken: number of trees, species, the size of trees that exceed a certain diameter, state of regeneration, understory species, etc. All this information is very valuable for forest management, planning and exploitation because it enhances the characterization of forest stands structure, the calculation of wood volume, the state of health and regeneration of the stands and their evolution over time, among others.

Traditionally, forest inventories were primarily carried out to determine the quantity of available timber (Smith 2002). Over the years, however, the scope of inventories has been expanded to include ecological variables such as measures of the quality of habitat provided by different species. Other information relevant to the development of forest management plans includes descriptions of forest ownership, access and transport infrastructure, topography, hydrology, and soil characteristics.

Ideally, forest inventory should be based on a complete census. i.e., one that measures every tree in a given area. However, this is usually impossible in forestry due to the large areas involved (Kangas and Maltamo 2006). Therefore, the acquisition of information is typically based on sampling, which means only a small portion of the population is inspected. The measurements

for the rest of the population are inferred from this sample. The size and number of such samples is defined by the scope of the work and its scale. The largest scale corresponds to global inventories that are aimed at determining the extent and status of forest resources at the global level (for example, the Forest Resources Assessment carried out by Food and Agriculture Organization (FAO) since 1946, which also serves as a mechanism to harmonize terminology and definitions). On a smaller scale are the National Forest Inventories (NFIs), whose role is to provide continuously updated information regarding the state of a given nation's forest resources, including their timber volumes, species composition and sustainable development (Tomppo et al. 2010). Inventories at smaller scales are often carried out for more specific purposes, frequently related to forestry planning and operations. These include regional inventories (i.e., in Spain, inventories of autonomous regions), reconnaissance inventories (a rough analysis of the forest resources of a limited area), diagnostic sampling to guide forest management and forestry operations, logging studies (focusing on assessing the availability of harvestable wood and planning felling and harvesting operations), post-harvest inventories (to analyse regeneration and damage caused by forest harvesting operations), and monitoring of forest health (often linked to sanitary felling operations).

1.3 MEASUREMENT TECHNIQUES IN TRADITIONAL INVENTORIES

In the 19th century, forest inventories were already an established component of forest planning (Kotilainen and Rytteri 2011). Data gathering was based mainly on visual estimation. Since then, measurement techniques have been evolving to become increasingly more specific and now involve a wide range of measurement devices with different characteristics. Of all the variables that can be measured in a forest inventory the most important are *dbh* and *h,* although measurements of diameters at different heights can also be collected. In the case of *h*, the most common approach is to measure the total height of the tree, although other heights such as first live branch (which marks the beginning of the crown) or dominant height (helps to deal with issues of site classification) are sometimes measured. From such measurements, a set of forest variables of interest are derived, including total volume, basal area and height to diameter ratio.

Diameter measurements have traditionally been performed by means of a measuring tape, diameter tape (pi tape) or callipers. In the case of diameter tape, circular tree stem shape is assumed so diameter value is obtained directly in one measurement. From those three options, callipers are the most efficient to measure *dbh* directly whenever there is direct access. In cases where taper curve is a variable of interest it is also possible to measure upper diameters along the stem at various heights.

Upper stem diameters are most easily observed on felled trees; however, most of the time it is preferable to not cut the tree but to collect measurements on a standing tree (i.e., trees with high ecological value and young trees which are not ready to be cut). There are several instruments/devices to do this. The simplest is the Finnish parabolic calliper (Figure 1A), which consists of a calliper mounted on a pole. It is relatively difficult to transport in the forest because the device consists of several callipers and various poles that are put together for the measurement. Moreover, for practical reasons, 7 m has been found to be the maximum manageable height. Another option is the optical calliper (Figure 1D) which consists of two pentaprisms: one fixed, the other movable. Its design allows parallel beams to be generated that correspondent to the arms of a mechanical calliper. The sighting is situated at the position of the fixed prism and is separated into two parts. Through the upper part, the observer aims directly at the left-hand side of the stem.

There are also more sophisticated devices which provide more measurements in addition to diameters. One of the most well-known due to its versatility is the Bitterlich mirror relascope (Bitterlich 1984) (Figure 1B). Apart from diameters, the relascope provides measurements of height, slope, distance, and basal area of the stand. Following this line, there is also a more modern device the Criterion 400 (Figure 1C). It is a laser instrument manufactured by Laser Technology, Inc. (Fairweather 1994) which combines laser technology, a fluxgate compass and inclinometer, and software in a hand-held tripod mounted device to facilitate basic trees measurements and land survey measurements. The instrument has computing, editing and storage capabilities. It offers a flexible alternative for measuring tree diameters at any point along the stem because the user does not need to be at specified distance from the tree.

Figure 1. A) Finnish calliper B) Bitterlich relascope C) Criterion D) Optical calliper

All these techniques have common problems, which is their difficulty of use and the fact that the reliability of the measurements depends fundamentally on good training of the personnel in charge of them. Besides, even with an experienced field team, according to Salas, Reyes, and Bassaber (2005) the Finnish calliper tends to overestimate diameters and the relascope, the optical calliper as well as the Criterion have an increasing bias with increasing height.

Height measurements can be carried out by direct or indirect methods. The direct method involves climbing or using height measuring rods. Due to its difficulty of application, it is rarely used and then only for small trees. In the case of young trees, the use of a topographic survey is also common. As for indirect methods, they can be classified into two groups: one based on geometric principle and one based on the trigonometric principle. The most commonly used methods are from the second group: hypsometers (Suunto and Silva), altimeters (Haga), and clinometers (Blume-leiss). With all of them, the user needs to stand at a fixed horizontal distance from the base of the tree and point first at the top of the tree and then at the bottom and then read the value. The total height of the tree is calculated as the top reading minus the bottom

reading. Nowadays the most extensively employed method is the use of the sonic clinometer Vertex® (Haglof; Madison, Mississippi) (Thies and Spiecker 2004), which measures distances based on ultrasonic sound and angles. It enables the direct measurement of tree height based on the trigonometric principle. For the measurement of distances, a transponder is needed which is fixed to the tree and is an active component that emits a signal back to the Vertex. To determine the horizontal distance to the tree, the transponder has to be fixed at a certain height (default 1.3 metres).

Regardless of the instrument used, when using the trigonometric principle there are two main potential sources of error in height measurement: (i) error due to a failure to correctly identify the top of the tree, and (ii), in the case of leaning trees the maximum height is underestimated when the tree leans away from the observer, and vice versa.

From all of the above, it follows that traditional techniques of forest inventorying have several problems that need to be resolved: they can be inaccurate, expensive, time-consuming, and require a large number of qualified personnel (Apostol et al. 2018). As a result, they are limited to statistically established sample plots, resulting in low representativity at larger scales.

1.4 REMOTE SENSING TECHNIQUES IN FORESTRY: THE DATA REVOLUTION

The conventional methods of measuring the structural characteristics of the forest can provide direct measurement, but the cost of producing them is quite high. In this regard, getting fast data at minimal cost has become a necessity (Apostol et al. 2018). To overcome the limitations mentioned previously, alternative solutions and measuring methodologies were sought in the remote-sensing field (Dobre et al. 2021). In recent decades, fieldwork has been enhanced by global satellite positioning systems, automatic measuring devices, field computers and wireless data transfer, and modern remote sensing. As a result, cost-efficient spatial digital data that are more accurate than ever before are readily achievable (Holopainen and Kalliovirta 2006).

Initially, remote systems were limited to satellite imagery. Five decades have passed since the launch of the first international satellite sensor programme designed to monitor Earth's resources (the ERTS) in 1972. Since then, hundreds of Earth Observation Satellites have been sent into orbit and they are delivering assorted remotely sensed data from the local to the global scale (Wang et al. 2012). The most common sensor mounted on satellites is an optical imaging system, which is similar in design and application to a standard digital camera except that it can collect data beyond the visible wavelengths (i.e., infrared and thermal wavelengths) across the electromagnetic spectrum. According to Boyd and Danson (2005), from the resources perspective satellite remote sensing is useful to provide three levels of information. The first level refers to information on the spatial extent of forest cover, which can be used to assess the spatial dynamics of that cover; the second level comprises information on forest type, and the third level provides information on the biophysical and biochemical properties of forests. In the last level, forest variables are estimated indirectly by using mathematical models which relate spectral response with some forest variable of interest (i.e., above ground biomass, tree height, and canopy closure) (Li et al. 2020; Ghosh, Behera, and Paramanik 2020; Zhang et al. 2020; Zhao et al. 2019; Xie et al. 2022). Despite the profusion of such variables and its promising evolution, passive remote sensing technology still needs the development of innovative approaches to address the requirements of ecologically important indicators (Dobre et al. 2021). The main disadvantage of most passive remote-sensing systems is the constant need for ground measurement calibration. Besides, when fitting regression models assume several assumptions regarding the relationship between forest characteristics and image values/digital levels must

be made. In cases where these assumptions are incorrect or inaccurate, they can lead to important errors in the interpretation of the results (Zhang et al. 2021)

An alternative or a complement (depending on the situation) to passive remote-sensing systems may be active remote-sensing, especially laser scanning technologies, which provide different approaches for estimating tree characteristics from point clouds. More specifically, they produce tridimensional coordinates directly from the objects that are measured which, by themselves or through local geometric variables derived from them (e.g. normal and planarity), allow analyses that enable species classification, point cloud segmentation to identify trees or stem reconstruction, among other applications (Pascu et al. 2020; Cabo et al. 2018a; Dobre et al. 2021). In the 1970_s and 1980_s, the basic principles of using lasers for remote sensing were established, although it was not until the 1990_s that the first experiments with laser scanning instruments were carried out. LiDAR measurement systems began to join together optical-mechanical scanning/scanning systems, global positioning elements and inertial measurement units, thus constituting the first airborne laser scanners (Bufton 1989). Since then, aerial and terrestrial lasers have evolved rapidly, and nowadays laser scanning remote sensing provides optimal solutions for describing forest stands through structural indicators based on point cloud processing.

In parallel to the development of new sensors, new platforms on which to mount them have appeared in the forestry scenario, gradually gaining visibility. This is the case with the Unmanned Aerial Vehicles (UAVs), which can transport both passive and active sensors (mainly laser scanners). Regardless of the type of sensor they transport, their strong points are: i) their ease of assembly and transportation, which enables the capture of customized data, ii) their ability to capture extremely high-resolution data, and iii) their capacity to capture useful imagery /point clouds even in the presence of cloud cover. UAVs cannot rival traditional platforms (airplanes or satellites) in terms of spatial extent; however, with appropriate processing and analysis frameworks, data from UAVs are likely to offer substantial opportunities to augment and enhance data collected from these more traditional platforms (Dash, Pearse, and Watt 2018).

The combination of the different types of sensors and platforms provides a wide variety of options for studying forest resources, which have been triggered through the large number of scientific contributions related to different aspects of forestry, the most common being: forest ecology and management (Lechner, Foody, and Boyd 2020; Roughgarden, Running, and Matson 1991), land cover analysis (Rogan and Chen 2004; Buján et al. 2012), biomass estimation (Li et al. 2020; Kankare et al. 2013), hazard identification (Fraser and Li 2002; González-Olabarria et al. 2012), forest structure assessment (Maier, Tiede, and Dorren 2008; Morin et al. 2019) , and ecological indicators (Bagaram et al. 2018; Corbane et al. 2015).

1.5 LIDAR TECHNOLOGY AT THE SERVICE OF FORESTS

1.5.1 Airborne laser scanning (ALS)

The term airborne laser is frequently used to distinguish between systems that acquire LiDAR data from various types of aircraft and those systems that use spaceborne or terrestrial platforms (Maltamo, Næsset, and Vauhkonen 2014). The basis of all ALS systems is the emission of a short-duration pulse of laser light and the measurement of the elapsed time between emission and detection of the light reflected back to the sensor (Vauhkonen et al. 2014). As the speed of light is known, the distance from the point of emission to the underlying object from which the light was reflected can be easily calculated. At the same time, the position and the orientation of the sensor are recorded using a GPS and INS (Inertial Navigation System) so each

point within the point cloud has a set of 3D coordinates (XYZ) that constitute a detailed representation of the scanned objects.

In the specific case of forestry applications, ALS is well known for is its ability to accurately characterize the three-dimensional (3D) structure of the forest canopy at medium-large scales. More precisely, height and density metrics derived from ALS point clouds provide valuable information about the horizontal and vertical distribution of vegetation. Canopy height, subcanopy topography, and vertical distributions of canopies (Lim et al. 2003) are the most common attributes that can be directly retrieved from LiDAR data (Lim et al. 2003). But probably the greatest potential of LiDAR lies in the possibility of estimating a great number of attributes that can be predicted using empirical models, including above-ground biomass, basal area, mean stem diameter, vertical foliar profiles, and canopy volume, among others. As a consequence, there is a rich variety of studies covering topics such as single tree detection (Aubry-Kientz et al. 2019; Apostol et al. 2020), canopy variables estimation (Andersen, McGaughey, and Reutebuch 2005; Jarron et al. 2020), biomass estimation (Gonzalez de Tanago et al. 2018; Xu et al. 2021), height estimation (Mielcarek, Stereńczak, and Khosravipour 2018; Rodríguez-Puerta et al. 2021), and habitat characterization (Bourgouin, Valeria, and Fenton 2022; Santopuoli et al. 2020; Prada et al. 2022).

Finally, more and more countries are starting to acquire LiDAR data from parts of their territory (i.e., Italy, Canada and Brazil) or from the whole country (i.e., Finland, France and Germany). In most of these countries, these data are available to users at no cost through their national cartographic servers. As a consequence, the number of users who can potentially work with these data has increased rapidly in recent years. In the specific case of Spain, there is a plan for the periodic acquisition of LiDAR data within the framework of the project PNOA-LiDAR. Its objective is to cover the entire territory (in a 6-year cycle) through 3D colored point clouds obtained through airborne LiDAR sensors. The first coverage was acquired between 2009 and 2015 and the second began in 2015 and finished in 2021. The point density is 0.5 points/m² in the first coverage and 0.5-4 points/m² in the second, with some exceptions where the density is even higher (i.e., the autonomous region of Navarra, at 14 points/m^2). The availability of temporal series of data is a very powerful tool for the study of forest dynamics and evolution (including disturbances).

1.5.2 Terrestrial laser scanning (TLS)

TLS is based on the same principle as ALS, but in this case the scanning is performed from a device placed on the ground, which is why this technique is also known as "Ground Based Lidar Technology (Pfeifer and Briese 2007)**.** TLS scanners use tachymetric measurements, which combine the measurement of distances and angles. The scanner sweeps its entire field of view (FoV), varying the direction of the laser beam in order to scan the different points to be measured, either by rotating the device itself or by using a system of rotating mirrors. This last method is the most frequently used since mirrors are lighter and can rotate quickly and with great precision. The deflection system points the laser beam in the direction to be measured after which the laser beam is emitted and the reflected laser light is detected. The accuracy of distance measurements depends mainly on the intensity of the reflected laser light and therefore directly on the reflectivity of the object surface (Fröhlich and Mettenleiter 2004). The reflectivity depends on the angle of incidence and surface properties.

For each reflected signal, two angles representing distance an intensity (α and θ, respectively) are registered. Based on these angles it is possible to define the position of each one of the

points of the scene in a polar coordinate system, which is internally transformed to a cartesian system. In addition, the intensity of the returned signal is also stored, intensity being a measure of the energy received by each point. As a result, TLS creates a point cloud where each point is determined by its position (XYZ) (Wilkes et al. 2017). The technique is characterized by high measurement repeatability as well as the capacity to map 3D surfaces with millimetric accuracy (Van Leeuwen and Nieuwenhuis 2010) which enables the detailed study of the entire scanned surface as well as the detection of small features.

Regarding data acquisition, the equipment is stationed at a fixed point, which greatly simplifies the design of sensor required since it is not necessary to have an inertial system. The only thing that is needed is the scanner itself mounted on a tripod and a reference instrument that allows absolute coordinates to be obtained, generally a GPS (although this is not mandatory as analysis can be performed using relative coordinates). There are two different methods that can be used in TLS measurement: single-scan and multi-scan. In the single-scan approach, the laser scanner is placed at the center of the plot, and one full field-of-view (i.e., 360-degrees-by-310-degrees) scan is made, meaning that objects behind the nearest surfaces in the direction of the laser beams are missed (Liang and Hyyppä 2013). In the multi-scan method, several scans are made simultaneously inside and outside of the sample plot, so it is necessary to establish a series of points with known coordinates (sufficient in number of points and coordinates) that are identifiable from the scan points. These points are usually marked with spheres or targets whose coordinates are recorded in the field with a GPS. This allows the point clouds collected from each scan to be merged at a later point and based on the same coordinate system.

Technological breakthroughs in the field of terrestrial laser scanning area have led to the expansion of the stationary laser units which, when bundled with localization and mapping systems, can become mobile laser units known either as MLS (Mobile Laser Scanner) or mobile-TLS (Kukko et al. 2012). A typical MLS system has the capacity to localize and map by itself thanks to both the Global Navigation Satellite System (GNSS) receiver and the Inertial Measurement Unit (IMU) implemented in it (Liang and Hyyppä 2013). In this regard the performance of MLS is more similar to ALS than to TLS.

1.5.3 ALS vs TLS

Despite both ALS and TLS both being very valuable tools for assessing canopy structure, each has its own advantages and disadvantages. On the one hand, the strongest point of ALS is that it can cover large geographical areas and provide detailed information on canopy area and canopy height, as well as vegetation strata, due to the capacity of the beam of light to penetrate through branches and leaves. However, it is not possible to quantitatively assess interior canopy structure (i.e., stem variables such as *dbh* and branch architecture). Terrestrial devices on the other hand, unlike aerial devices, facilitate the observation of parts of trees that are not easily accessible from the sky, such as stems, branches and even low vegetation. In addition, the density of point clouds and their accuracy is, as a rule, higher with TLS (Fahey et al. 2016).

Regardless of the type of scanner employed, the point clouds are stored in an internal data format and each manufacturer offers product-specific software for data collection. Therefore, the customer needs special software which allows the raw data to be read and treated after the scanning. However, there are exchange formats, such as .las/.laz and .txt, among others , that facilitate the sharing of data captured with different scanners , meaning that they can therefore be analyzed with different software.

In this doctoral thesis, data captured with a TLS Scanner FAROFocus3D (Faro,2018) and a Leica P40 (Leica, 2021) have been used. Chapters 2 and 3 include a more detailed description of each of these systems.

1.6 PRECISION FORESTRY: A REVOLUTION IN THE WOODS

Digital transformation is reaching all sectors, and forestry is no exception. Inspired by advances in agriculture, forest managers globally have started to use new technologies to improve forest planning yields. Within the industry, this approach has been termed “precision forestry” which can be defined as the use of modern tools and technology to get as much real information as possible in order to improve decision making process and to ensure current goals of forest management (Kovácsová and Antalová 2010) . The best known and most frequently used tools are remote sensing, navigation systems and geographic information systems. The scope of precision forestry is very wide, and is constantly expanding, some of the most important topics currently being: forest monitoring, wood quality assessment, the fight against illegal logging and deforestation, pests and diseases, waste reduction, fighting wildfires, habitat conservation, land management and profits increase. One of the strongest aspects of precision forestry is its scalability, meaning it has a range of users, from private individuals to organizations and companies to regional and national governments. This new approach to forestry aims, in the first instance, to improve and complement the traditional system, although in the near future it is highly probable that precision forestry becomes established as the dominant mode due to its capacity to provide solutions to new challenges (Figure 2).

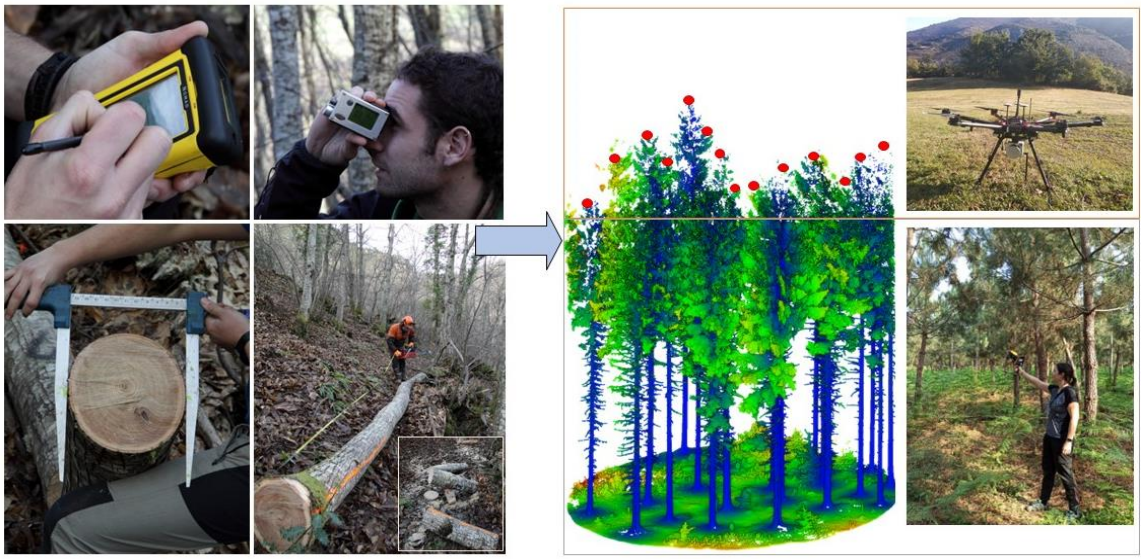

Figure 2. Change of paradigm in forestry: from traditional inventory devices to precision forestry techniques

Indeed, according to Fardusi, Chianucci, and Barbati (2017), the use of precision forestry is no longer simply a choice in forestry management and the provision of products, it is a necessity. However, the forestry industry is not adopting digital technology as quickly as most other industries, including agriculture. The explanation for this can be found in certain peculiarities of the forestry sector, which faces several challenges in introducing advances in technology in terms of forest inventory techniques and in forest management in general (Choudhry and O’Kelly 2018). Some of the most serious are explained below.

In the first place, public-private partnerships in relation to forest management is insufficient; consequently, there is little corporate involvement in forestry (76 percent of forests globally are

publicly owned, and most of the remainder are held by small-scale private owners who typically hold, on average, less than one hectare).

Secondly, and contrary to what happens in agriculture, commercial forests are located in remote and difficult terrains (high slope, hard-to-reach areas, dense understory, etc.), which presents many challenges for the adoption of new technologies.

Finally, the fact that the traditional system has been active for more than 300 years has generated a cadence that makes both public and private stakeholders/managers follow the conservative management/traditional system. According to Choudhry and O'Kelly (2018) for forest managers, precision forestry involves "a paradigm shift, from a highly manual and analogue system with broad-brush management prescriptions to a system with digital data capture and planning, granular management prescriptions, and tight operational control" based on objective and highly accurate data. It is a fact that many forest users lack experience in implementing and using accurate forestry technologies. Subsequently, while a wide range of precision forestry technologies exists, relatively few practical examples are up and running, but only a few seem to know how to take advantage of these technologies in real projects.

The field of forest inventories, and more specifically the use of terrestrial point clouds for inventory variables estimations, is not an exception, and despite their potential to produce objective assessments of the 3D forest structure (Van Leeuwen and Nieuwenhuis 2010) the technique is not fully implemented. Apart from the previous reasons there are other specific ones in the case of terrestrial point clouds, all of which are explained in detail in Chapters 2, 3, and 4. As an advance, many researchers agree that affordability (in the broad sense of the word) is the main key challenge to be overcome (Molina-Valero et al. 2020). In this context, affordability implies the automation of point cloud processing with attainable and easy-to-use software able to extract information related to important forest attributes. This is essential and must be the roadmap to follow.

1.7 BACKGROUND ON THE CREATION OF AUTOMATIC TLS-BASED INVENTORIES TOOLS

The use of TLS devices provides a reliable representation of the structure of the trees within the stands at the time when the data are collected (Liang and Hyyppä 2013). The fact that data are collected from the ground makes this technology especially suitable for studying stem profiles (Dassot et al. 2012). However, due to the large size and complexity of the high resolution three-dimensional point clouds, there is an increasing demand for methods for the automatic measurement of inventory variables, especially those which focus on the estimation of variables related to the stem and branches (Ghimire, Xystrakis, and Koutsias 2017). Researchers, and to some extent foresters, are trying to meet this demand by creating algorithms and methodologies based on terrestrial point clouds that are being applied in different fields of the forestry field. A good example of this are the "precision forestry" inventory methodologies that go beyond classic inventories, which were mainly focused on *dbh* (Pfeifer and Winterhalder 2004; de Conto et al. 2017; Hackenberg et al. 2014; Thies et al. 2004b; You et al. 2016) and *h* estimations (Cabo et al. 2018ab; Hauglin et al. 2014; Ghimire, Xystrakis, and Koutsias 2017). The new methodologies not only increase the accuracy of estimations of these to variables, but also try to estimate new ones, such as curvature and straightness of the stem, that condition the price of the timber in the market. In the case of *dbh* estimation one of the most important studies is that performed by Liang et al. (2018), who detailed a vast range of automatic or semi-automatic forest inventory methods focused on stem detection and *dbh* calculations. The high accuracy of the diameter estimations obtained in previous studies (*RMSE* values ranging from

0.71 to 2.64 cm; Hollaus, Mokroš, and Wang 2019) confirms that TLS is a suitable technique for precision inventories, and also meets the accuracy requirements for the vast majority of applications. Although there are many studies where stems are modelled, this number is drastically reduced when it comes to extracting diameters at different heights (Torresan et al. 2021).

In the case of height, TLS estimations are not as accurate as for diameters, some studies showing a tendency toward slight overestimation when comparing TLS measurements against field measurements (Olofsson and Holmgren 2016; Hopkinson et al. 2004; Maas et al. 2008). This was attributed to the presence of canopy shadow effects and obstructions resulting from complex multiple scan positions (Ghimire, Xystrakis, and Koutsias 2017). These results indicate the need for the refinement of the current methodologies and the further development of automatic feature identification and data extraction techniques.

The fact that TLS allows the estimation of diameters along the stem and height in a relatively simple and objective way broadens the range of variables that can be obtained from the point clouds. One of the most useful applications is the direct estimation of tree volume (Dassot et al. 2012; Saarinen et al. 2017). But in addition to this, it is possible to use the measurements obtained with the scanner for the parameterization of volume equations. On the one hand, this *modus operandi* avoids the traditional destructive sampling approach, which has several problems (Barker and Pinard 2001), the most evident among them being the destruction of the stand. In addition, the resultant volume equations can be used in stands with similar characteristics to those of the sample parameterized without the need to scan them, this consequently saving of time and money. Despite the great potential of TLS in this field, however, very few works have developed in this line (Li et al. 2021; Gabriel 2017; Sun et al. 2016).

In addition to stem volume, another of the main parameters that influence the use that wood obtained from a forest can be used for (and therefore its economic value) are the those related to the shape of the stem (straightness, sinuosity, lean, etc.). Specifically, tree stem curve holds a significant position in forestry, as it is one of the most important attributes for defining stem value (Liang et al. 2016).
In this same line, TLS also opens the door to quickly and easily measuring parameters that have a strong influence on stem value but are not currently measured due to technical difficulties or high cost. At the present time there are only a few studies that have focused their efforts on the calculation of shape variables such as straightness and lean (Murphy, Acuna, and Dumbrell 2010; Hamner, White, and Araman 2007; Dwivedi et al. 2019; Garms et al. 2020) or to the study of the presence and distribution of branches (Dassot et al. 2012; Kankare et al. 2013; Raumonen, Kaasalainen, Åkerblom, et al. 2013; Zhou et al. 2019)

The possibility of obtaining diameters along the stem, total heights and also curvature parameters open up the possibility of analysing the stem in an integral way with a number of variables, something that was unthinkable until recently. In fact, in the last fifteen years, the forest industry has shown increasing interest in laser scanning techniques and the performance of TLS systems for the volumetric measurement of timber assortments (Kankare et al. 2014). One of the main fields of interest is the optimal bucking of stems. In this regard, poor decisions in terms of cutting patterns lead to great losses in the value of the products obtained from the tree, therefore ruining previous silvicultural efforts to obtain good quality wood. In the field of optimal bucking, the number of studies where bucking algorithms are fed with data collected with TLS are rare. One of the few authors who has worked in this line is Murphy (2008) who determined stand value and log product yields using TLS and optimal bucking, and then

compared the results with estimates from actual stem profiles. The study revealed that TLS-derived estimates of average stand value and log product yields were within 7% of actual estimates. Later on, Murphy et al. (2010) collected information of stem profiles using three methods: (1) TLS scans, (2) Atlas Cruiser inventory procedure (Atlas Technology, 2010), and (3) manual measurements after harvesting. TLS volume and value recovery were within 8% and 7%, respectively, of actual harvester recovery, while Cruiser volume and value estimates were both within 4% of actual harvester recovery. Apart from this, the most recent study to investigate the potential of TLS data for optimising bucking algorithms, to our knowledge, is the one by Kankare et al. (2014). This study assessed the accuracy of high-density laser scanning techniques to estimate tree-level diameter distribution and timber assortments by combining ALS (Aerial Laser Scanning) and TLS for timber assortment estimation. The results showed that accurate tree-level timber assortments and diameter distributions can be obtained using TLS or a combination of TLS and ALS.

In this doctoral thesis three algorithms for precision forestry inventories based on terrestrial point clouds are developed that involve volume equation parametrization, stem shape variables estimation and the optimal bucking of stems. In Chapters 2, 3 and 4 all the limitations and possible improvements of previous studies dealing with these three topics are considered and discussed in detail, as are the theoretical and computational aspects of the three algorithms developed, the tests carried out to validate them, and the results obtained.

1.8 OBJECTIVES

This doctoral thesis is focused on providing new tools for precision forestry inventories. Specifically, three algorithms applicable to terrestrial point clouds which provide automatic solutions for three key issues in forest management were developed: volume equation parametrization, stem shape variables estimation and optimal bucking pattern determination.

In order to achieve this, the general objective was divided into the following specific objectives:

1) To design, implement, and test a fully automated algorithm for the parametrization of stem volume equations (stem taper and/or volume ratio equations). This is accomplished using data from TLS point clouds to automatically detect individual trees and measure diameters along the stem (d_i) and total height (h) at the individual tree level.
2) To design, implement, and test a fully automated algorithm that allows the estimation of straightness (maximum sagitta and sinuosity) and lean at the individual tree level from data captured with TLS.
3) To implement the two previous methodologies in a bucking algorithm for the optimal bucking of stems, based on their external characteristics (diameters and curvature), which maximize the economic value of a stand using data from TLS point clouds.
4) To analyse the advantages and disadvantages of the performance of each algorithm compared to traditional techniques

CHAPTER 2:

AUTOMATIC PARAMETRIZATION OF WOOD VOLUME EQUATIONS

CHAPTER 2: AN ALGORITHM FOR THE AUTOMATIC PARAMETRIZATION OF WOOD VOLUME EQUATIONS FROM TLS POINT CLOUDS: APPLICATION IN *PINUS PINASTER*

2.1 INTRODUCTION

Estimating merchantable volume as accurately as possible is essential in forest management in order to know the amount of wood available for the various uses that industry demands. There are basically two different methodologies for determining merchantable volume: stem taper equations and volume-ratio equations (Álvarez González, Gadow, and Real Hermosilla 2001; Trincado, Von Gadow, and Sandoval 1997). Stem taper equations rely on the mathematical relationships between diameters along the stem and the height at which they are located (Newnham 1992), while volume ratio equations estimate the volume of the tree up to a certain point in the stem (defined by its diameter or height) as a percentage of its total volume (Cao, Burkhart, and Max 1980; Van Deusen, Sullivan, and Matvey 1981). In both cases, tree stems are divided into logs which are assimilated as a cylinder, and the top section is modelled as a cone. Total stem volume is obtained by summing the log volumes and the volume of the top section. In the few published studies where the two methodologies are compared, no significant differences between them have been obtained (Parresol, Hotvedt, and Cao 1987; Trincado, Von Gadow, and Sandoval 1997). In order to develop these types of equations, large and comprehensive mass data is required to ensure that variability in the population, as well as in the geographic areas, is covered, so that the models can be applied in different stand typologies (Picard, Saint-André, and Henry 2012). Traditionally, to obtain such measurements, destructive techniques have been used, according to which a number of suitable trees (not forked nor excessively branched) that provide a representative distribution of diameter and height classes are selected and felled. They are then cut into logs of variable length and two perpendicular diameters are measured for each cross section (Menéndez-Miguélez et al. 2014) up to a top diameter of 7 cm. These techniques are resource-intensive (Corral-Rivas et al. 2007; Crecente-Campo, Alboreca, and Diéguez-Aranda 2009), since they require the felling of trees and consequently, stem-volume models for many tree species are non-existent and/or have only been developed for certain specific geographical areas, thus limiting their applicability.

The use of remote sensing techniques, more specifically, Terrestrial Laser Scanning (TLS), is gaining great importance in the estimation of variables related to stems and branches. This is mainly due to the high resolution and precision of the information it provides at the plot level, making possible the 3D modelling (Zong et al. 2021) and reconstruction of the trees (Liang et al. 2016) without the need for felling. As a result, since the early 2000_s the possibilities offered by TLS in the forestry sector are increasingly being recognized for research and commercial ends (Fröhlich and Mettenleiter 2004), particularly in terms of compiling forest inventories (Hollaus, Mokroš, and Wang 2019). Although manual extraction processes are still sometimes used (Holopainen et al. 2011; Kankare et al. 2014) the general trend is to use automatic procedures (Liang et al. 2012; Raumonen et al. 2015). Liang et al. (2018) detail a wide range of automatic or semi-automatic forest inventory methods focused on stem detection and diameter at breast height (*dbh*) calculations.

Regarding parameter extraction, most studies focus on the estimation of stem variables such as diameters (d_i) at different height positions, including *dbh* and *h* (Cabo et al. 2016; de Conto et al. 2017; Hackenberg et al. 2014; Hauglin et al. 2014; Henning and Radtke 2006; Pfeifer and Winterhalder 2004; Thies et al. 2004; You et al. 2016) but there are some authors who have also

studied crown variables (Jung et al. 2011; Mohammed, Majid, and Izah 2018). In the case of *dbh*, TLS-based estimations have provided *RMSE* values ranging from 0.71 to 2.64 cm (Hollaus, Mokroš, and Wang 2019) which fulfil the requirements of many practical applications, e.g., national forest inventories (Liang et al. 2018). This high accuracy makes TLS a suitable technique to develop locally adjusted merchantable volume equations (Sun et al. 2016; Trincado and Burkhart 2006).

Although there are many studies where stems are modelled, this number is drastically reduced when it comes to extracting diameter at different heights for merchantable volume equations. There are, in addition, only a few studies evaluating the performance of TLS in contrast to field data in the measurement of stem taper (Henning and Radtke 2006; Liang et al. 2014; Maas et al. 2008; Mengesha, Hawkins, and Nieuwenhuis 2015). That said, some authors have put their efforts into the use of TLS for the estimation of variables of great importance for the wood industry such as branch architecture (Laurin et al. 2016), solid wood volume (Dassot et al. 2012) and taper equation construction (Gabriel 2017; Olofsson and Holmgren 2016; Sun et al. 2016).

The consistent increase in popularity of LiDAR devices, linked to their decreasing cost and rapid developments in their associated computer hardware and scanner technology in recent years, will make 3D point cloud data easily available for a wider range of users. Indeed, robust, time efficient and flexible software for data processing is already being demanded (de Conto et al. 2017), especially in the field of forestry. Within this context, the automated processing of TLS forestry data remains a challenge, particularly in regard to the efficient storage and analysis of voluminous merged scan data, the filtering of noise and unwanted data, and methods for dealing with the partial and complete occlusion that is common in forest plots (Calders et al. 2020; Li et al. 2020; Pitkänen, Raumonen, and Kangas 2019). Another challenge is to reduce the time invested in data collection and processing to make it similar to or less than the time required to parametrize conventional volume equations. This depends largely on the level of automation that can be attained by the software-aided analysis of the scanned plots (Thies et al. 2004).

The aim of this study is to design, implement and test a fully automated methodology for the parametrization of stem volume equations (stem taper and/or volume ratio equations). This is accomplished using data from TLS point clouds to automatically detect individual trees and measure diameters along the stem (d_i) and total height (h) at the individual tree level.

2.2 METHODOLOGY

Figure 3 shows a workflow of the methodology detailing the steps involved the automatic parametrization of volume equations, including the input/output data needed and the procedures to be followed. In Section 2.2.1, the procedure for obtaining h and d_i in a fully automatic way from the TLS point cloud is explained in detail, including the identification and individualization of the stems, and the subsequent estimation of their geolocation. Section 2.2.2 details the procedure followed for the parametrization of the volume equations.

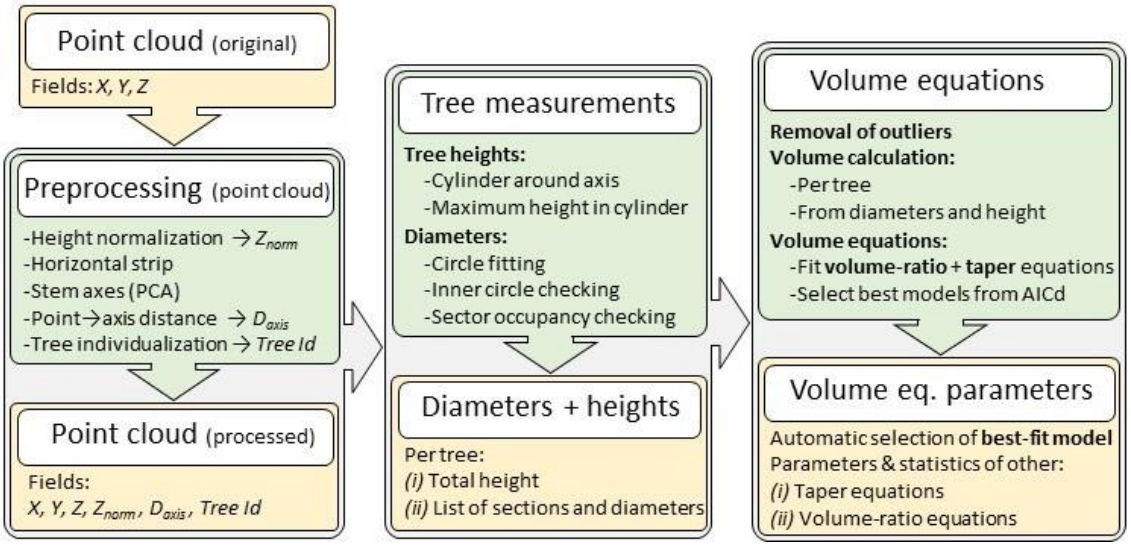

Figure 3.Workflow of the methodology proposed for the volume equations parametrization from TLS point clouds (Input/output data are shown in yellow and procedures in green)

2.2.1 Automatic estimation of dendrometric variables

2.2.1.1 Preprocessing of point cloud data

This part of the methodology encompasses all the steps that need to be followed to process the 3D point cloud prior to the automatic estimation of d_i and *h:* the aim is to automatically detect individual trees in the plot, then isolate and identify all points belonging to each tree and extract those points which are along the stem. The workflow can be itemized as follows (see Figure 4).

1) Construction of a digital elevation model (DEM) to define the ground.
2) Height normalization of the point cloud to obtain Z coordinate, which refers to the ground (Z_{norm}).
3) Selection of candidate point groups along a horizontal strip (equal height from the horizontal ground), and where no scrub or branches are expected, on the basis of clustering of points using the DBSCAN algorithm (Birant and Kut 2007). The consistency of the groups in the horizontal strip is checked according to the methods described in Cabo et al. (2018ab).
4) Location of stem axis through the determination of the centroid and PC1 of detected stems: The methodology assumes that candidate tree stems are essentially linear features. As such, in the principal component (PC) analysis of the XYZ coordinates of each stem-candidate point group, the first PC (PC1) aligns with the direction of the maximum variance from the XYZ coordinates of each group. Then, PC1 is used to define the direction of each stem axis. The other two principal components (PC2 and PC3) are, by definition, perpendicular to each other and to PC1 (Oviedo-de la Fuente et al. 2021) and can therefore be used as local/tree coordinate axes to calculate the distance of any point from the PC1 axis.
5) Calculation and storage of distances from each point to the closest axis: D_{axis}. This has various applications, but the most obvious is that it allows the points of each tree to be filtered by their distance from the axis, making the separation of the main parts of each individual tree into crown/branches and stem relatively straightforward.
6) Tree individualization. All the points are assigned and linked to their closest axis (*Tree Id*)

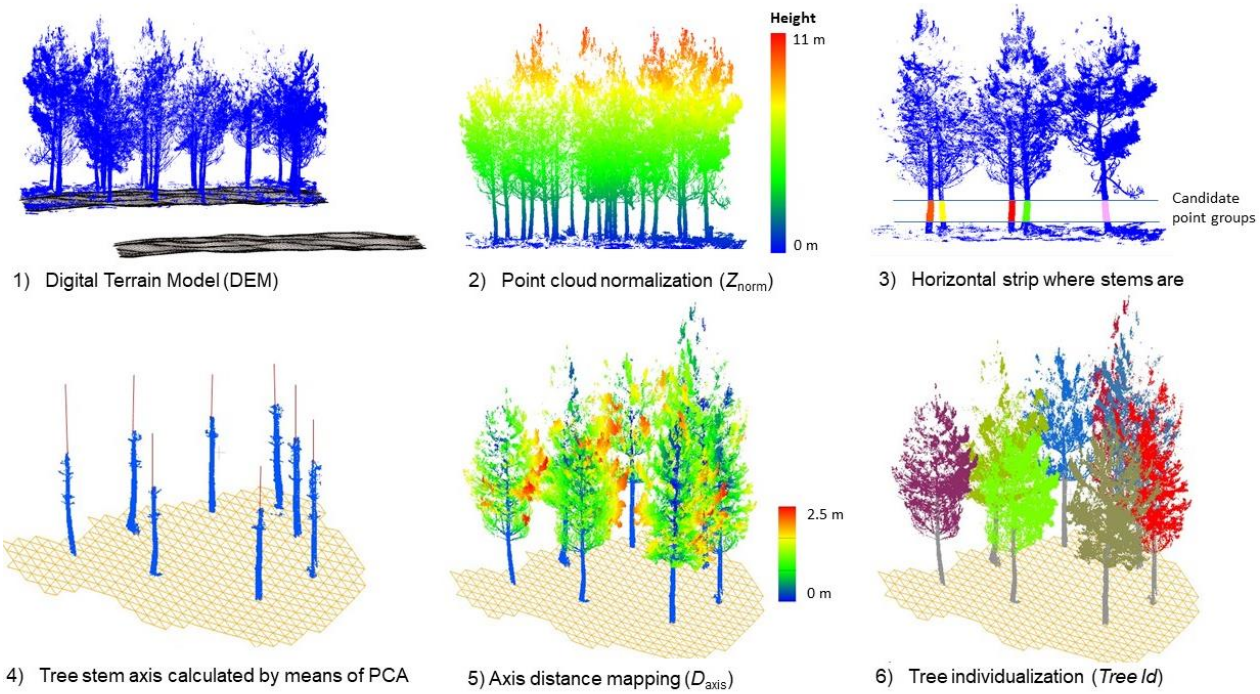

Figure 4. Workflow for the identification of tree stems prior to automatic estimation of d_i and h. 1) DEM generation 2) Point cloud normalization (Z_{norm}) 3) Strip on the height normalized point cloud where the groups of candidate points likely to be tree stems are identified 4) Tree stem axes resulting from PCA analysis, where the PC1 is represented by a red line 5) Axis distance mapping of each tree (D_{axis}) 6) Tree individualization procedure, where all the points are labelled with a tree identifier (Tree Id)

2.2.1.2 Tree height estimation

The estimation of tree height is based on the determination of the highest point in the crown in the proximity of each stem axis. For this, the points belonging to each tree (Figure 5A) are first clustered. From the resulting groups, those that are few in number and far from the stem, which may correspond to noise, artifacts, or canopy from higher neighbour trees, are automatically removed. The remaining points are filtered by distance from the tree axis in order to only consider those closest to the axis for the tree height estimation. This is done based on a threshold distance that delimits a cylinder around the top part of the tree, and can be varied for different species, conditions or environments. *h* is finally estimated as the elevation above the ground of the highest point inside the cylinder (Figure 5B), which reduces the probability that *h* corresponds to the top of another higher tree, and allows appropriate estimations, even for tilted trees (Figure 5C). A default distance threshold value can be set as half of the average distance between neighbour trees in the plot. However, this value can be altered, generally reduced, if the stems are essentially straight and/or there is a high diversity in terms of tree height within the plot.

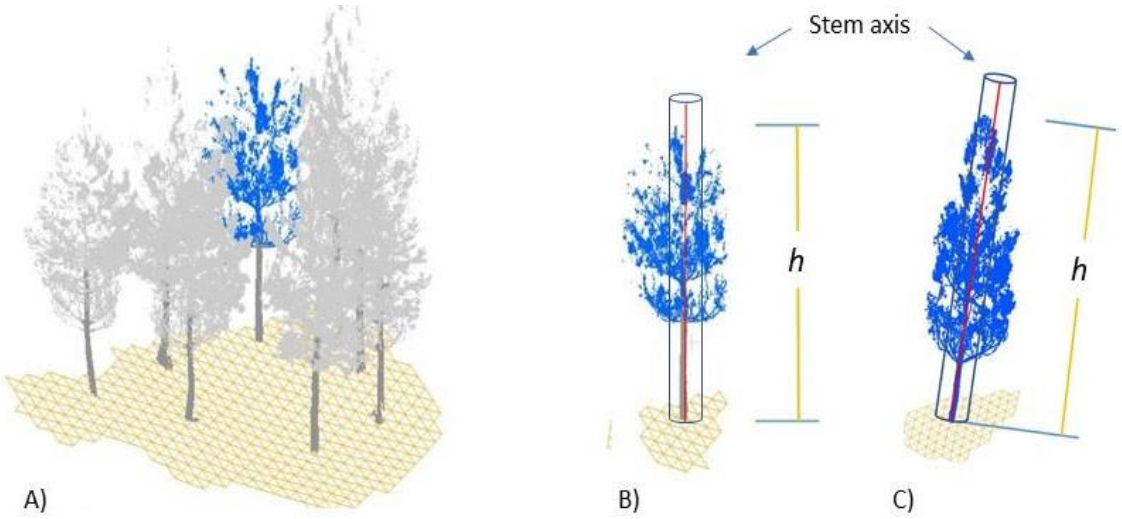

Figure 5. Tree height estimation procedure, where h is estimated for each individualized tree (A) as the highest point within the area of a delimited cylinder around the tree axis after noise filtering (B) and which is also valid for tilted trees (C)

2.2.1.3 Diameter estimation along the stem

The tree stem is initially segmented by extracting the points that are within a certain distance of each axis. This distance is set as the maximum stem radius expected in the plot. Then, diameters at different heights along each stem (d_i) are measured at a user defined interval starting from the ground (Figure 6A). To do so, each d_i is measured in a slice, which comprises all the points in a thin horizontal section of stem of uniform thickness. The maximum height with points in these sections strongly depends on the quality of the results obtained in the stem filtering step, which, in turn, is mainly dependent on occlusions, the point cloud density and the presence of artifacts around the stem, such as branches or understory. These three factors are interrelated and their influence on the resulting d_i is expected to be stronger in the upper sections of the stem. As well as the height interval for slice extraction, the thickness of the slices and the upper height limit can be specifically set for different species and/or conditions, environments or studies (Figure 6B).

For the initial diameter estimation, the algorithm computes the diameters by fitting a circle to the points in each slice in each tree stem (Figure 6C). The circle fitting method is described in detail in Cabo et al. (2018ab). The algorithm calculates the diameter and the X and Y coordinates of each section center, thus their position along the stem is defined and stored.

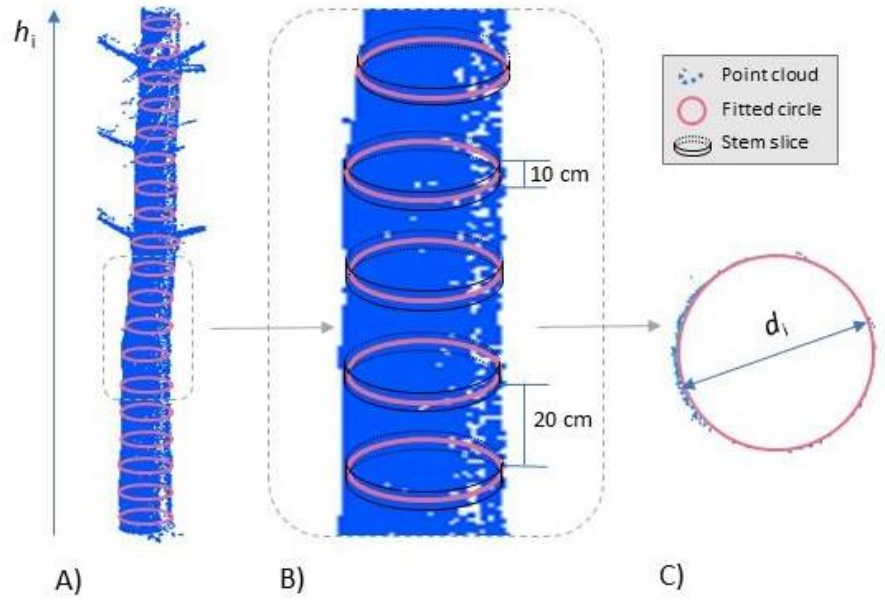

Figure 6. A) Cross-sections along the stem B) Detail of stem slices showing height interval for their extraction, and their thickness C) Circle fitting to the points of a stem slice

Automatic identification and labelling of anomalous sections.

Frequently, the horizontal sections at different heights used to fit the circles contain points that do not belong to the stem but to other parts of the tree, such as branches, leaves or other artifacts. In those cases, the circle fitting may result in an erroneous estimation of the stem radius (r). The algorithm includes two complementary functions that allow, on the one hand, the identification and labelling of the anomalous sections, and, on the other, automatic correction in those cases where it is possible. Both functions are explained in detail below:

Inner circle (IC): this function was presented for the first time in Cabo et al. (2018a). Here, a concentric inner circle with radius r' = r/2 is set up in the fitted section (Figure 7). If the position and size of the circle fitted is correct, no points are expected inside the inner circle.

Sector occupancy (SO): this function is based on the assumption that the points within a section follow a close-to-circular distribution and, except in cases of very severe occlusions, almost half of each tree section should be covered by points if it is measured from only one TLS setup, but more if it its measured from several setups. In order to verify that the circle fitting is compatible with this point coverage around the stem sections, an annulus divided into sectors is created around the position of each initially fitted circle (Figure 7). The width of the annulus can be varied if irregularities on the stem/bark are expected. If the position and size of the circle fit is correct, at least half minus one of the sectors should be occupied by points: this also allows circle fittings in stem sections that are only reached from one scan position, while the shape of the point group is continuously checked.

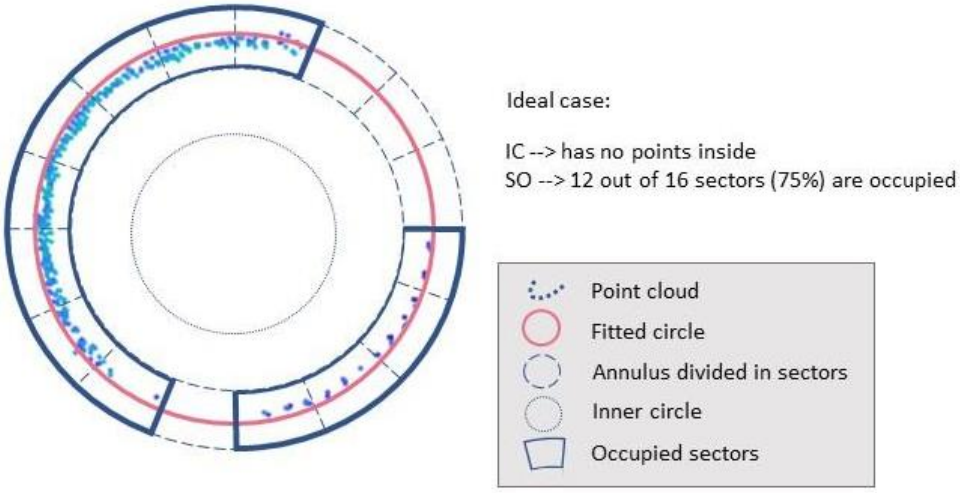

Figure 7. Checking functions of the circle fitting step in each section (IC +SO) showing an example of an ideal case, where the section would be labelled as correct.

If in the first circle fitting of a section there are no points in the inner circle, and there are sufficient sectors occupied, the diameter estimation is considered correct. However, if there are points within the inner circle, or there are not sufficient sectors occupied in the annulus, it is highly probable that the diameter fitting is not correct. To resolve this, all the points within the section are clustered based on the distance between them. Then, the circle fitting is carried out again using only the cluster with the largest number of points, which is more likely to contain a higher percentage of points on the stem (Cabo et al. 2018a). This gives a new estimation for the diameter and position of the section of the stem. The new circle fitting is then checked again (i.e., IC and SO).

If a section passes the validation functions (either in the first or second round), it is labelled as “correct (C)”. If both the first and second round of validation functions fail, the section is labelled as “flagged (F)”. If in the first or the second round of validation functions there are not enough points to perform the circle fitting, the section is labelled as “not enough data (ND)”.

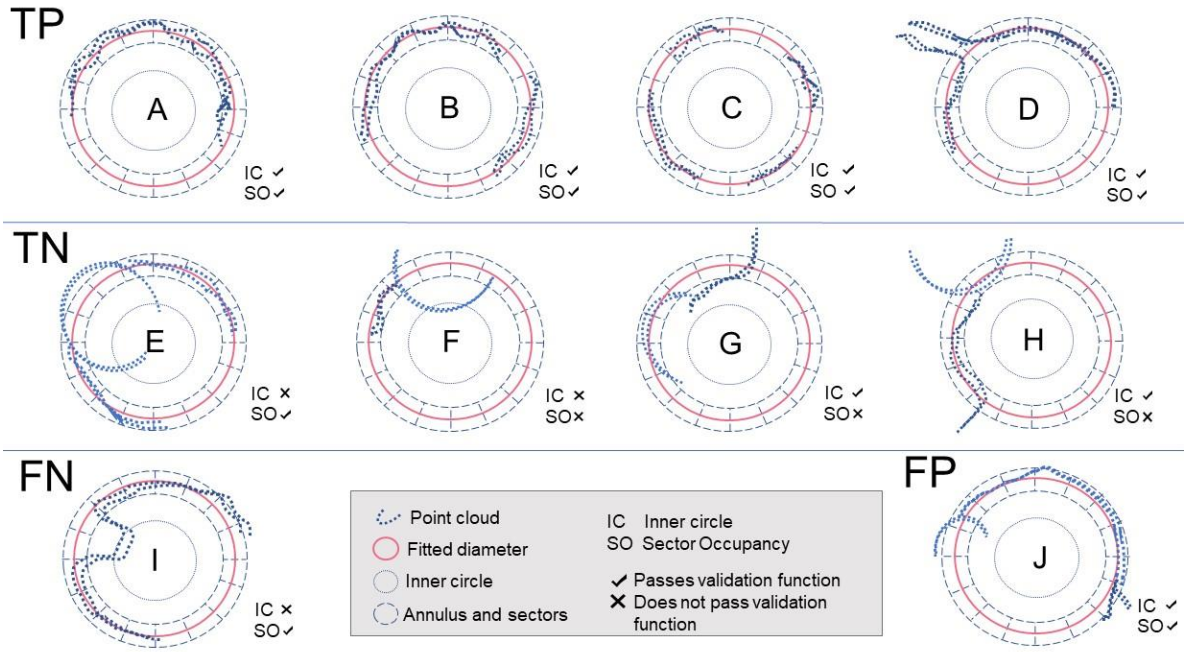

Figure 8. Algorithm for diameter estimation performance when labelling sections. Sections can be classified into 4 categories, TP) True positives: labelled as C when they indeed are; TN) True negatives: labelled as F when they indeed are; FP) False positives: labelled as C when they should be F; and FN) False Negative: labelled as F when they should be C.

Figure 8 shows 10 different hypothetical section scenarios and the behaviour of the circle fitting and validation functions in each case. They are classified into four groups: True positives (TP), True negatives (TN), False positives (FP) and False negatives (FN). TP are correct estimations (from the first or second fitting round) and they are automatically stored as correct diameters (Figure 8. (A, B, C, D)). TN (i.e., those sections correctly labelled as F or ND) can be either left to be inspected visually by an operator or eliminated straightaway (Figure 8. (E, F, G, H)). FP and FN correspond to rare situations in which the algorithm would wrongly classify the results. For example, Figure 8I correspond to an irregular stem section, while Figure 8J represents a branch with a quasi-circular section. However, these specific misassignments could be avoided by changing the parameters of the checking functions/tests (diameter of the inner circle, annulus width, and/or minimum number of occupied sectors).

2.2.2 Parametrization of volume equations

The merchantable volume can be calculated using different types of volume equations: mainly stem taper and volume-ratio equations, which are similar in terms of accuracy with respect to merchantable volume. In order to parametrize either of them, it is necessary to have a longitudinal data structure, that is, multiple diameter measurements for each individual at different heights along the stem (d_i, h_i) as well as the total height (h). The estimated dbh, d_i and h obtained from TLS data following the methodology described are used as input values to estimate merchantable volume using volume equations. For each type of volume equation, a large number of models (i.e., different specific expressions of the general volume equation) and parameter estimation approaches have been proposed in recent decades (Westfall and Scott 2010).

The first type of equation, a system of taper and volume equations, describe stem taper by providing (i) a taper equation with the diameter at any point along the stem or the height of the

stem for a fixed diameter (eq.1), (ii) merchantable volume to any top diameter and from any height or individual volume for logs of any length at any height above the ground (eq.2) and (iii) total volume by integration of taper equation (eq.3). Taper equations can be classified into: simple taper equations, segmented taper equations and variable exponent taper equations. Of these, segmented taper equations have the greatest flexibility, as well as the capacity to describe the total volume efficiently (Pang et al. 2016). Ideally, a taper equation should be compatible, meaning that the volume computed by integration of the taper equation should be equal to that calculated by a total volume equation (Clutter 1980; Demaerschalk 1972). The specific model included in this work, that proposed by Fang et al (2000), meets this requirement as it include a segmented taper equation (specific to f_1, eq.1), and complementary formulations to directly calculate total and merchantable volumes (specific to f_2, eq.2; specific to f_3, eq.3).

$$d_i = f_1(dbh, h, h_i) \quad \text{eq. 1}$$

$$v_i = f_2(dbh, h, d_i) \quad \text{eq. 2}$$

$$v = f_3(dbh, h) \quad \text{eq. 3}$$

It is important to consider that, in spite of the versatility and accuracy of stem taper equations, their practical use is limited unless they are embedded within a computer program (Larsen 2017). Moreover, when the data source is TLS, it is highly probable that the convergence in the iterations needed to calibrate the taper equation could be compromised due to the difficulty of d_i extraction in the upper stem because of branch occlusions in the crown, which leads to poor delimitation of the stem profile.

The second type of equations, volume ratio equations are, in contrast to taper equations, directly targeted at estimating wood volume up to a predefined diameter depending on its merchantable volume. They are very easy to both develop and use (Crecente-Campo, Alboreca, and Diéguez-Aranda 2009), and a hypothetical lack of upper stem data would not have a strong influence on their parametrization. Volume estimations from volume ratio equations, whose general expression is shown in eq. 4-6, are based on the combined use of two equations—a total volume equation (v) (eq. 4) and a ratio equation, R_i (eq. 5)—to estimate the portion of volume up to a certain point (limit diameter d_i or height h_i) with values from 0 to 1, and, as such, the merchantable volume (v_i) is their product (eq. 6):

$$v = g_1(dbh, h) \quad \text{eq. 4}$$

$$R_i = g_2(dbh, d_i) \quad \text{eq. 5}$$

$$v_i = v \cdot R_i \quad \text{eq. 6}$$

The algorithm developed in the current work, includes five total volume models (*v;* specific to g_1, eq.4) and four ratio models (R_i*;* specific to g_2, eq.5). The five specific total volume models (v, g1) are the linearized allometric model and four other models proposed by Spurr (1952): combined variable, generalized combined variable, quadratic and cubic polynomial. The four ratio models (R_i*;* g_2, eq.5) included are the ones described in Burkhart (1977); Clark and Thomas (1984); Reed and Green (1984); Van Deusen, Sullivan, and Matvey (1981). Finally, the algorithm processes all the models and selects and integrates one of the total volume models (eq.4) and one of the ratio models (eq.5) into a volume ratio equation (eq.6), based on statistical criteria.

Considering all the above, the steps implemented in the algorithm are synthesized as follows:

1) In the first step, outliers in the stem analysis data (d_i, h_i) are detected following the systematic procedure proposed by Bi and Long (2001). A nonparametric taper curve is fitted using local regression with a typical smoothing factor value (0.25). Then, those values which fall below a point equivalent to the lower quartile minus twice the interquartile range, or above a point corresponding to the upper quartile plus twice the interquartile range were removed owing to the fact that most of these data points correspond to stem deformations, and volume equations are not intended for deformed trees (Rodríguez, Lizarralde, and Bravo 2015).
2) The models implemented in the methodology (stem taper equation and the volume ratio models) are fitted and the algorithm calculates the values and significance of parameters (fitting by generalized least squares for non-linear models), the goodness-of-fit statistics of every model (coefficient of determination R^2, root mean square error *RMSE*, Akaike´s information criterion, *AIC*) are used to select the best model and measure the quality of the fittings, which can also be checked by graphical analysis (residual versus predicted values and predicted versus observed values and a scatterplot of relative diameter (d_i/dbh) vs relative height (h_i/h)).
3) After the debugging of the data set, total volume is calculated using a cone equation for the top section and, for each log, the Smalian equation (a formula that calculates the volume for each log by multiplying the average of the areas of the two end cross-sections by the section's length). This total volume then becomes the dependent variable in the parametrization of the different equations.
4) The algorithm automatically selects the model with the lowest *AICd* (that is, the smallest *AIC* value in the set of models) where all parameters are significant as its candidate for the final merchantable volume equation. The user can either accept the algorithm choice or reject it and select any of the other proposed models according to their own preferences or specific requirements on the basis of all the goodness-of-fit statistics and graphical behaviour of each model.

2.3. CASE STUDY

2.3.1 Study area and data

The methodology explained above was tested in a coniferous stand (*Pinus pinaster*) located in the autonomous region of Asturias (Figure 9A), where *Pinus pinaster* is the third species in terms of wood volume logging, representing 21% of total coniferous wood felled in Asturias (SADEI 2018).

The study plot, which has an approximate area of 5700 m^2 (Figure 9B), is part of a breeding program where the growth of different families and provenances of *Pinus pinaster* is being evaluated (RTA2017-00063-C04-02, 2017). Initially, in 2005, 900 trees were planted following a gridded distribution. A thinning treatment was made in 2018, reducing the number of trees to 428. Regarding the stand characteristics, density is 806 trees/ha with an average *dbh* and *h of* 18 cm and 10.5 m, respectively while average canopy cover fraction is 44%. The terrain is irregular with a slope of 60% and dense cover of different species of scrub such as *Ulex, Ericas*, *Pteridium* among others (average height is 50 cm, canopy cover is 80%) (Figure 9C).

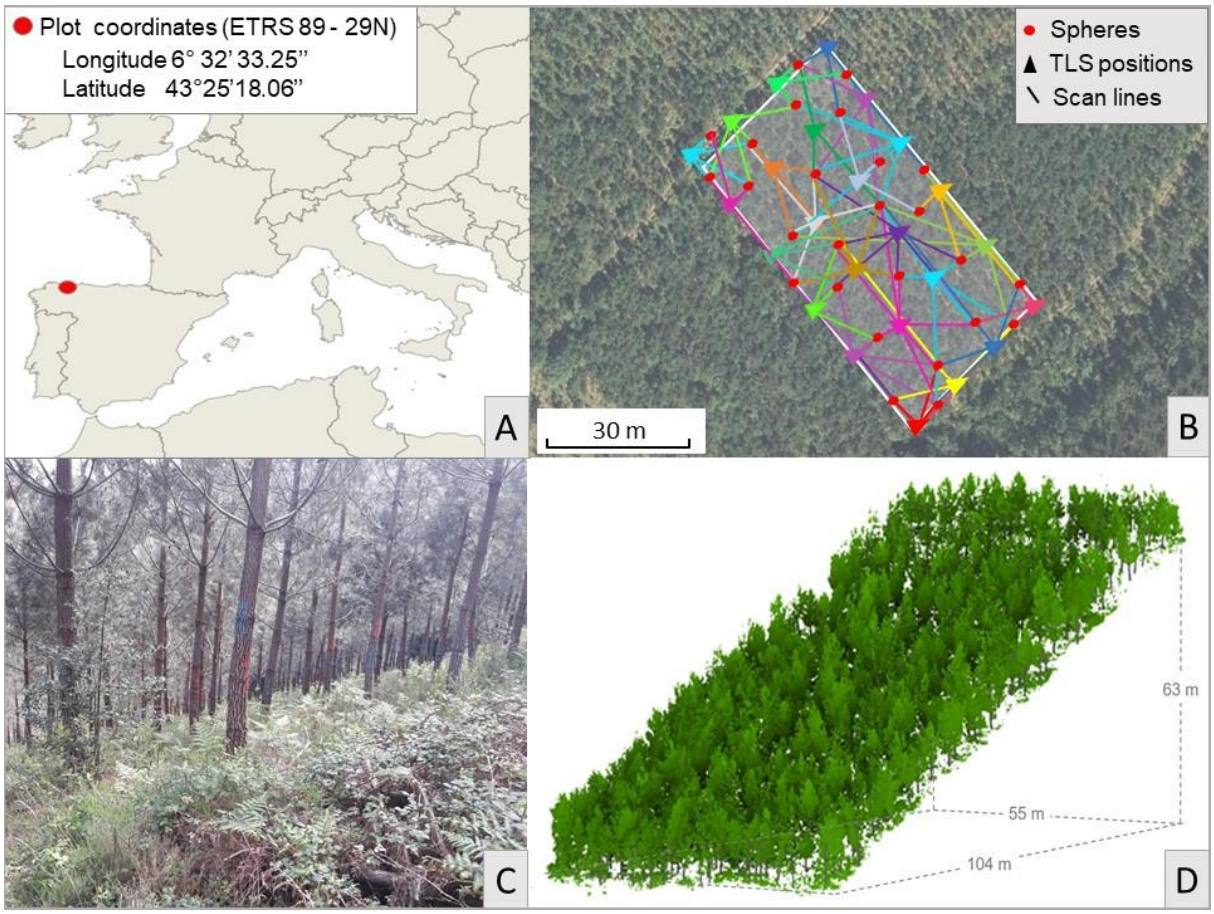

Figure 9.A) Location of the study area B) Schema of the real distribution of the scans and the spheres in the test case plot C) Pinus pinaster stand and understory within the test case plot D) 3D representation of size and slope of the test case plot

Data acquisition was carried out in November 2018 with a TLS model FAROFocus3D (Faro 2018). In total, 24 scans were necessary to ensure the full coverage of the study area and minimize the effect of occlusions. With the aim of merging the point clouds of individual scans into a unified coordinate system, polystyrene spheres of 25 cm diameter fixed to surveying rods were used. Also, the position of the spheres was measured in the field using GNSS (Global Navigation Satellite System), which has an accuracy of 1 cm, thereby ensuring that the unified point cloud had absolute coordinates. The *RMSE* of the registration was 4 mm, and the final matched point cloud obtained for all scans was approximately 150 million points, after removing duplicates within 6 mm. The scanning distribution is shown in Figure 9B. Finally, for all trees within the plot, *dbh* was measured in the field with a calliper (dbh_f) to the nearest 1 mm and total height (h_f) to the nearest 10 cm, using a digital hypsometer (Vertex IV 360º).

2.3.2 Assessing algorithm performance

The performance of the algorithm was assessed from two perspectives: tree detection rates and deviation in the estimation of diameters and tree heights. Tree detection rates were evaluated in terms of completeness and correctness with respect to the tree locations measured with the GNSS+Total station. Completeness was computed as the proportion of the trees within the plot that were detected by the algorithm (number of correctly detected trees divided by the total number of trees in the dataset) and Correctness was calculated as the proportion of elements identified as trees by the algorithm that were actual trees (number of correctly detected trees divided by the total number of elements detected as trees in the dataset). The deviation in the

estimation of both diameter measurements, *dbh* and d_i, and height, *h*, was evaluated by comparing the results obtained from the algorithm and the values obtained using (i) traditional inventory methods and (ii) manual/visual measurements of the point cloud data.
In order to obtain the manual/visual measurements, a graphic interface was designed and implemented.

1) For manual tree height estimations (h_m) each tree is always shown from two different perspectives and the user can identify the highest point from both perspectives before selecting which to use, ensuring misassignments are avoided (i.e., if 'Perspective 1' in Figure 10A was the only available perspective of that specific tree, the h_m estimation would be wrong). The elevation of the selected point above the ground is stored as the total height of each individual.

2) For manual diameter (d_m) estimations, the horizontal distribution of the points included in each section is graphically displayed on the screen. Over each section, the user can draw 3 points (A, B, C) along the section contour, so that a circumference is automatically fitted to them (Figure 10B), after which the diameter and the coordinates of the fitted circle are stored. In the case of *dbh*, the deviation in the diameter estimated by the algorithm is also calculated by comparing it with the direct measurements in the field made with a calliper (428 sections: one per tree). In the case of the diameters along the stem, the algorithm estimations are compared with the manual measurements from the point cloud (9844 sections: 428 trees X 23 sections).

3) With the aim of minimizing the influence of the operator on the estimations, all height measurement and diameter fitting processes were conducted twice, each time by a different operator (Op_1 and Op_2).

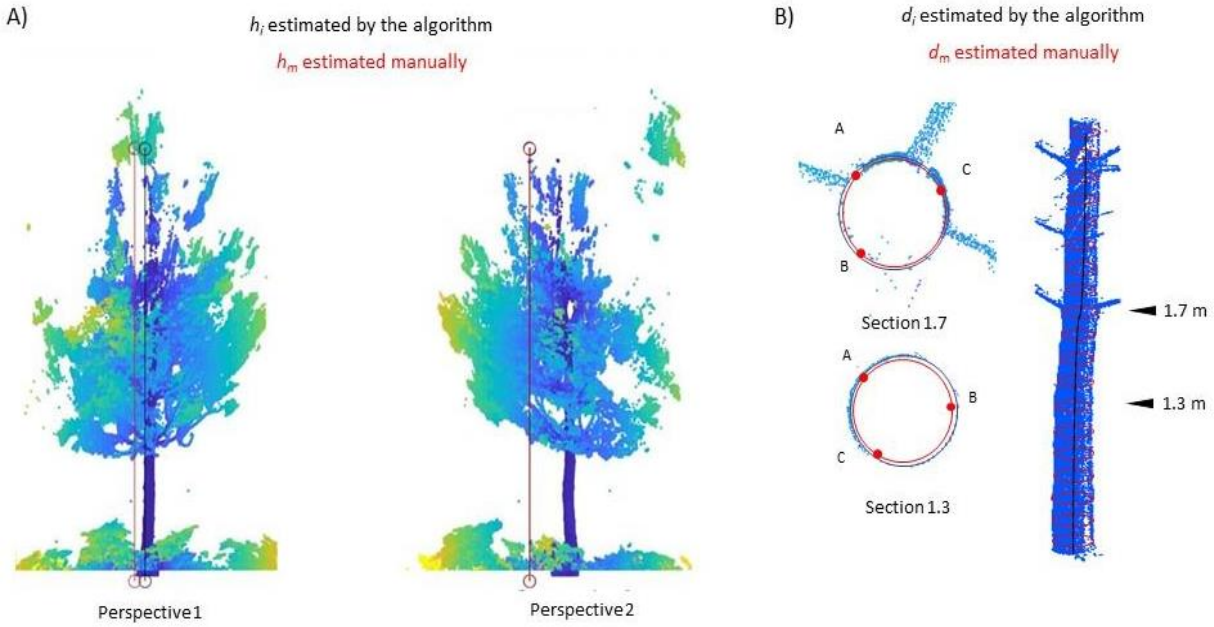

Figure 10. A) Manual total height estimation in the point cloud by marking the highest point in the cloud from two different perspectives B) Manual estimation diameter at different heights in the point cloud, by drawing 3 points (A, B, C) around the section contour.

2.3.3 Experimental results for automatic estimation of dendrometric variables

2.3.3.1 Stem detection rate

All the features detected as trees were actual trees with no false positives present, therefore the correctness of the algorithm is 100% for the dataset. As regards completeness, only 14 trees of the total 428 remained undetected, giving a value of 97%.

2.3.3.2 Total height

The algorithm automatically measured the total height of 98% of the trees. The average values obtained by the algorithm (h), by traditional inventory methods (h_f) and by manual measurement in the point cloud (h_m) as well as their standard deviation, are shown in Table 1. *RMSE* obtained when comparing h with h_f was 1.52 m.

Table 1. Mean and standard deviation (in metres) of the total height obtained from: algorithm (h), traditional inventory methods (h_f) and manual measurements of the point cloud data (h_m).

	h	h_f	h_m
Mean	8.78	10.29	8.72
Standard deviation	1.44	1.48	1.43

Figure 11A shows the differences analysed tree by tree. More precisely, it shows probability density functions for the differences between h, h_f, and h_m. The differences between h and the h_m are less than 0.5 m for 83% of the trees, and less than 1 m for 94%, meaning that the operator and the algorithm each estimate a very similar height in the vast majority of cases. Although differences between h_f and h_m are higher, they are less than 2 metres in 80% of cases.

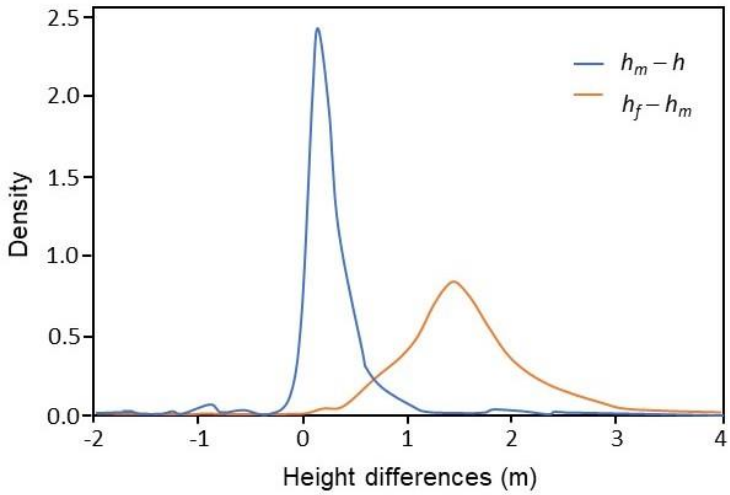

Figure 11. A) Probability density functions for height differences comparing h_m versus h (blue line) and h_f versus h_m (orange line).

2.3.3.3 Diameters along the stem

In this dataset, due to the complexity of the forest stand structure (young trees with a great number of branches, along with high stand density and steep terrain; Figure 12A), the automatic estimation of diameters was carried out from 0.5 to 4.9 m in height (i.e., from the average height of the dense understory to approximately half the average height of the trees in the plot; Figure 12B). The circle fittings were computed for sections with a thickness of 5 cm and spaced 20 cm apart vertically (i.e., 23 sections per tree; Figure 12C)

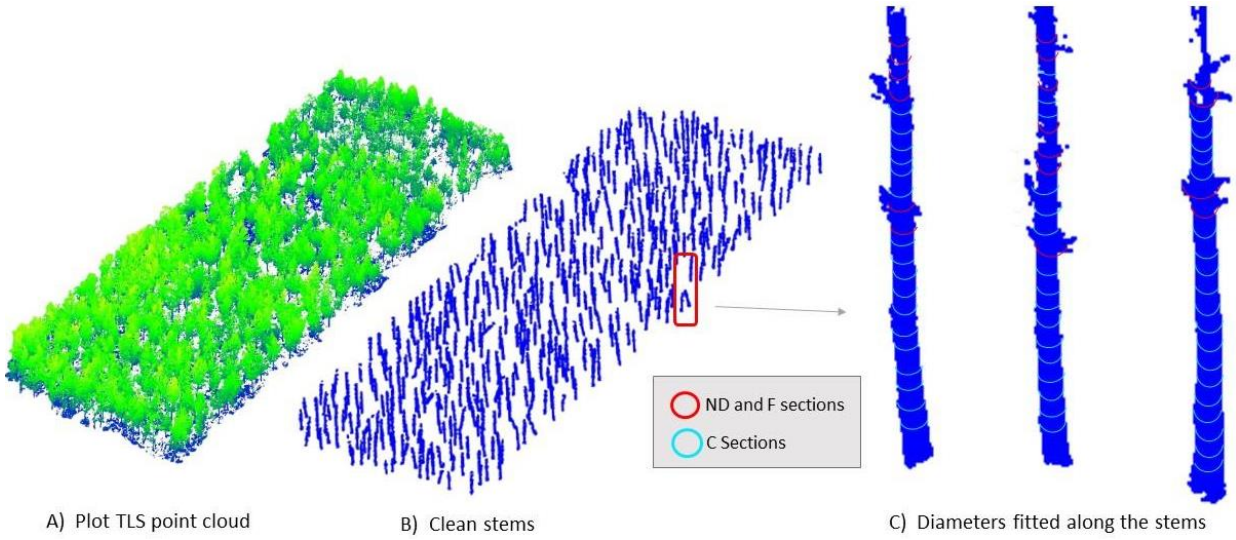

Figure 12. Visual results obtained by the algorithm for the diameter fitting in the study plot: A) initial point cloud B) clean stems C) detail of circle fitting along the stem.

Regarding *dbh*, the algorithm measured it fully automatically in 93% of the trees within the plot, while in the remaining 7%, diameter fitting was not possible or was labelled as F or ND by the validation functions. The *dbh* average value was 17.27 (±3.2 cm) and the *RMSE* was 1.14 cm when compared with $dbh_{f,}$. In absolute terms, 56% of the trees have an error value lower than 1 cm, and this increases to 82% for an error value of less than 2 cm. The distribution of the size of the differences in diameter estimation is shown in Figure 13.

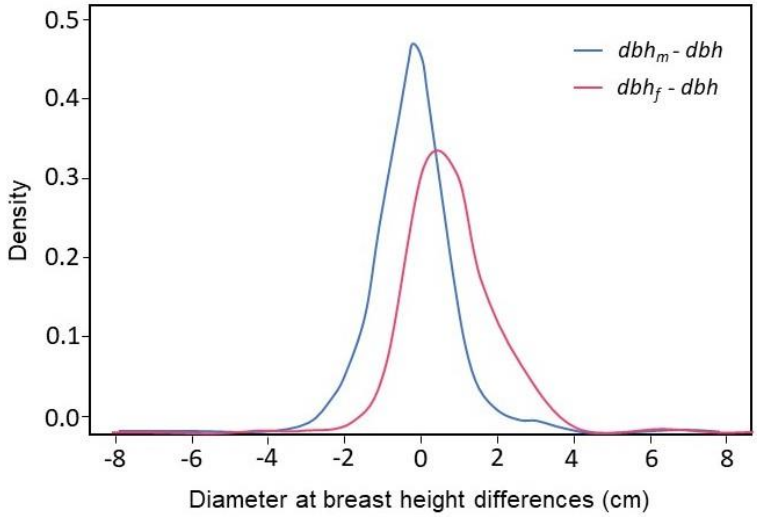

Figure 13. Probability density functions for diameter at breast height differences comparing dbh_m versus dbh (blue line) and dbh_f versus dbh (pink line).

Figure 14 shows the comparison of the diameters along the stem estimations obtained by the algorithm and the manual measurements carried out by the two operators. This comparison has a double aim: (i) comparing Op_1 and Op_2 provides information about the disparity of the different reference measurements and allows the identification and elimination of outliers (in cases where the differences between operators are high) and (ii) the comparison between the algorithm and the operators provides an estimation of the accuracy of the method while allowing the subjectivity associated with the operators' measurements to be considered.

Specifically, Figure 14A shows the differences between the estimations of the two operators in those sections where both were able to see and draw a circle. These differences are approximately of the same order and remain constant along the whole stem: they show apparent symmetric distributions and no bias at any specific height.

Figure 14B and 14C show the differences between the diameter estimations along the stems as calculated by the operators and by the algorithm in the sections that were not flagged for review or elimination by the algorithm. The differences between the two operators are very small according to the average interquartile range (8.2 mm) and remain constant along the stem. However, when the estimations of each operator are compared to those from the algorithm, the interquartile range is slightly higher (Op_1-Alg: 11.2 mm and Op_2-alg: 24.0 mm) and the difference increases with the height of the section. Specifically in the case of *dbh*, *RMSE* was 1.02 cm when compared with dbh_m and the distribution of the size of the differences in diameter estimation is shown in Figure 13 (blue line). On the right of each boxplot the blue line represents the proportion of sections that were used to build the boxplots for each section. The general tendency in each of the 4 boxplots is for the number of sections to decrease with height. This is to be expected because of the presence of low branches and the high density of trees, a combination which makes diameter fittings more difficult higher up the stem, particularly when the branches of the crown begin to appear (at around 2.5 m in this test case).

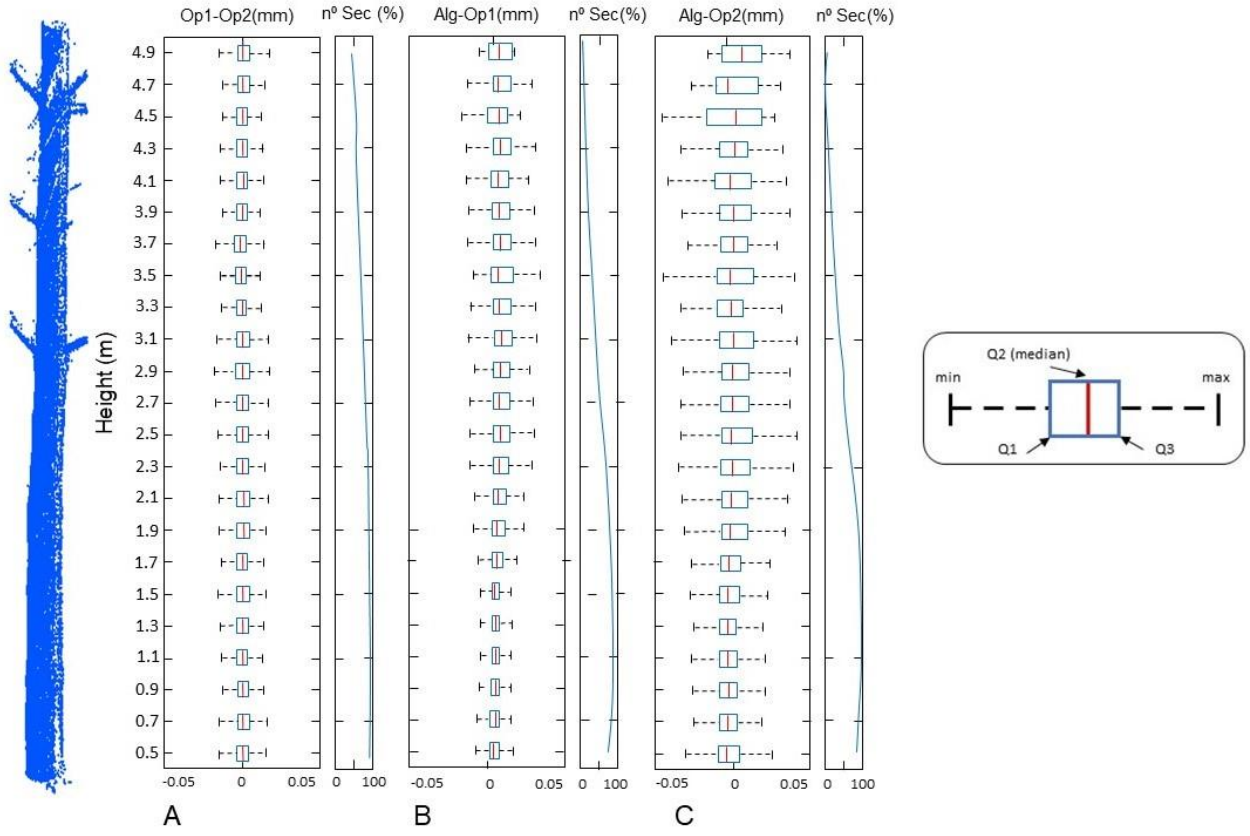

Figure 14. Boxplots of the differences between A) manual estimation of Operator 1 (Op_1) and Operator 2 (Op_2); B) and C) comparison of the manual estimation of Op_1 and Op_2, respectively, with algorithm estimation excluding sections flagged as candidates for review. Q1 and Q2 represent the percentiles, and min and max refer to 1.5 times the interquartile range in mm from the upper and lower quartiles respectively. On the right of each boxplot the blue line represents the number of sections (as a percentage) that were used to build the boxes for each section.

Anomaly detection in stem sections.

Figure 15 shows the distribution of the sections along the stem in terms of how the algorithm classifies them: correct sections (C: grey), flagged (F: magenta), and those where there was not enough data to compute the circle fitting (ND: blue). Also, to assess the performance of the algorithm when identifying ND, and to compare the results with the manual estimations, ND sections have been subdivided into NDa (not enough points for either circle fitting or visual/manual estimation: dark blue) and NDb (not enough points for circle fitting, but sufficient for visual/manual estimation by the operators: pale blue).

As demonstrated in Figure 15, in general terms, the proportion of both F and ND sections is lowest around breast height (1.2-1.6 m) where stems are less affected by occlusions from understory or tree branches, and, in addition, the incidence angle of the LiDAR beams is in general more favourable. In these sections, more than 90% of the diameter estimations are labelled as C, and less than 2% as ND.

The proportion of F sections increases steadily on either side of breast height (i.e., below 1.1. and above 1.5 m), and remains stable above approximately 2.5 m, the average height of the first branches. Conversely, the proportion of ND increases constantly with height from breast height (same increase rate for NDa and NDb up to the last two sections, where NDa becomes much larger than NDb)

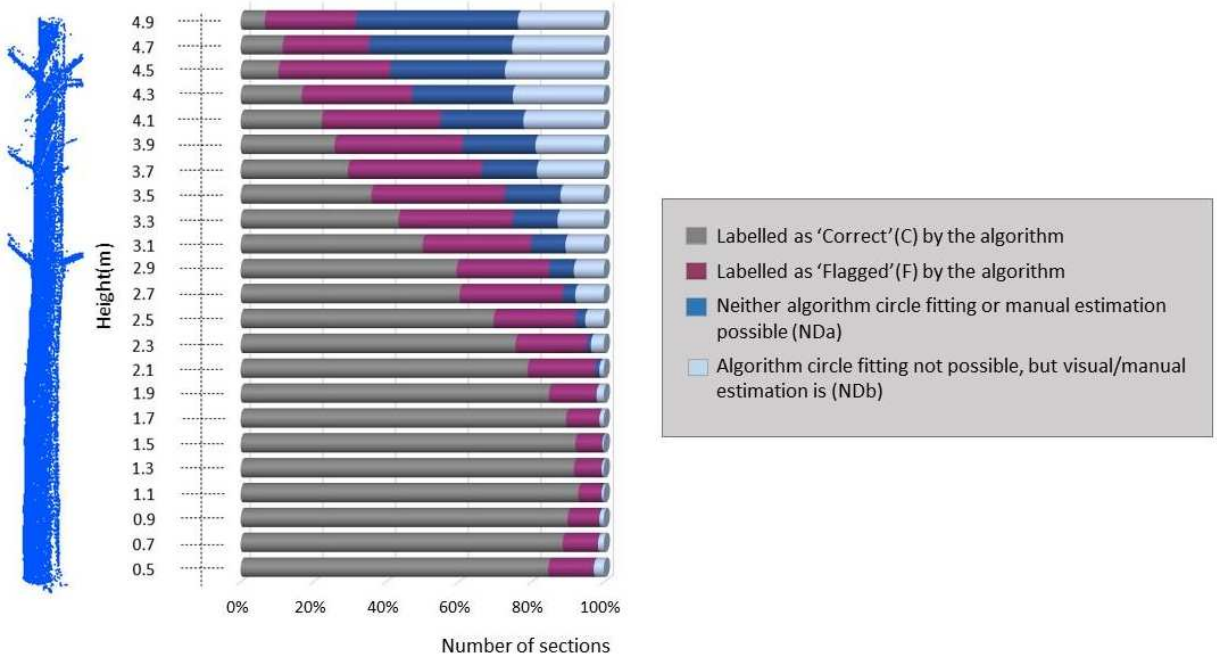

Figure 15. Labelling results obtained by the algorithm expressed in terms of percentage of sections classified into each category

2.3.4 Experimental results for parametrization of volume equations

Selected taper and volume ratio equations were fitted using two datasets that include the following variables for each tree: d_i, h_i and h. The data sets differ in the way in which these three variables have been calculated. In the first (hereafter, "Automatic"), all the variables were estimated automatically by the algorithm. The second (hereafter, "Supervised"), contains the same data as the Automatic, but those sections it labelled as F or ND were substituted by the diameter manually estimated by an operator, i.e., the data from Op_1 and Op_2 that was also used to evaluate the automatic diameter estimations. There were a small number of measurements

which were very different between the operators, and these were considered outliers, and removed from the dataset. However, in general, measurements from the two operators were very close (<5 mm) so the use of data from either of them would provide virtually the same result. On this basis, the diameter from either Op_1 or Op_2 was selected randomly for each section.

Figure 16 shows the scatter plot of the relative diameters (d_i /*dbh*) vs relative heights (h_i/h) that were used for the parameterization of the merchantable volume equations. In both cases there is a reduction in the number of sections that were available for the model parametrization in the upper part of the stems, especially in the top third of the stem. For the Supervised data the situation is slightly better than in the Automatic, because there are more sections in the band of relative height (h_i/h_a), corresponding to 0.60 to 0.80 whereas in the Automatic data there are virtually no sections in that interval. Moreover, there are more sections providing results in the Supervised data and a smaller proportion of outliers than in the Automatic data (7384 vs 5362 sections and a proportion of outliers of 9.7% vs 11.6.%, respectively).

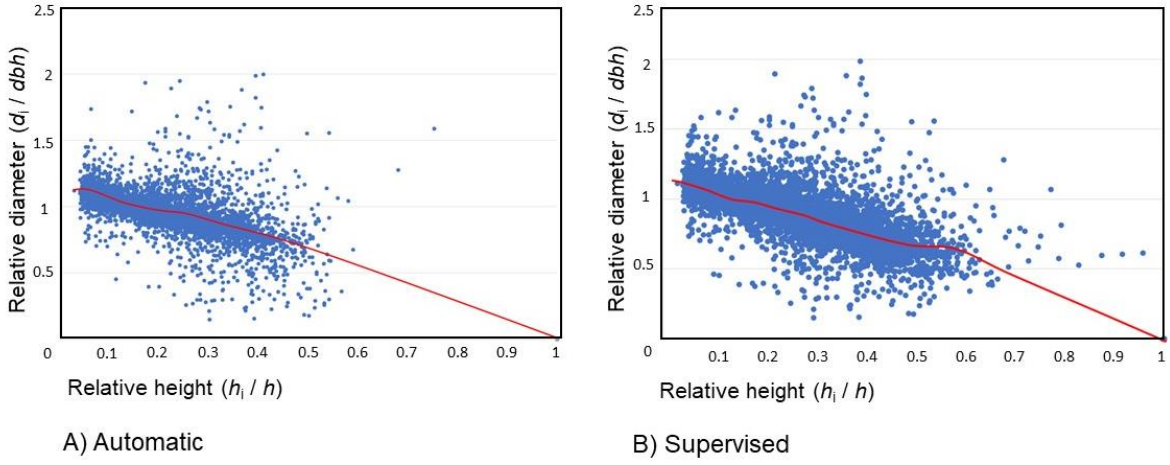

Figure 16. Scatterplots of relative diameter (d_i/dbh) vs relative height (h_i/h), with a local regression smoothing curve (red line) for the two datasets used in fitting merchantable volume equations Note: point (1,0) represents the final section of the stem, where d_i=0 (d_i/d=0) and h_i=h (h_i/h=1).

For both datasets, the algorithm offered the following outputs: parameter estimation, goodness-of-fit statistics and graphical analysis (residual and predicted vs. observed data) of the merchantable volume equations. Looking first at the taper equation system, it did not converge in either of the two data sets due to the lack of sections in the upper third of the stem. From among the volume ratio equations, the algorithm selected for each data set was that with the lowest *AICd* and where all parameters were significant, which in this particular case was the allometric volume equation (eq. 7) and the ratio equation proposed by Clark and Thomas (1984) (eq. 8).

$$v = b_0\, dbh^{b1}\, h^{b2} \qquad \text{eq. 7}$$

$$Ri = exp\,(b_3\, d_i^{b4} dbh^{b5}\,) \qquad \text{eq. 8}$$

where *v* is total over bark stem volume (m^3), calculated as the sum of the volume of all the logs within the stem, and the top of the tree; R_i is the proportion of total volume accounted for at diameter (d_i); *dbh* is diameter at breast height (cm); d_i over bark diameter at height h_i (cm); *h* is total tree height in m, and b_0, b_1, b_2, b_3, b_4 and b_5 are the parameters to be estimated.

Table 2 shows the number of sections used and the comparison of the goodness-of-fit statistics for the volume ratio equation selected by the algorithm, for each of the datasets.

Table 2. Goodness-of-fit statistics of the model fitted in the different data sets.

	Data set	*n*	*P*	*RMSE*	R^2
Total volume equation	Supervised	7382	3	0.0149	0.8480
	Automatic	5362	3	0.0233	0.6714
Ratio equation	Supervised	7384	3	0.1630	0.6759
	Automatic	5362	3	0.1747	0.6382

Note: *n* is the number of sections used for the equation fitting, *P* is the number of parameters in the model, *RMSE* root mean square error, and R^2 is the coefficient of determination.

The Supervised dataset gives better results than the Automatic, especially in the case of the total volume equation. The results demonstrate that a low number of sections, and more specifically their absence in the upper third of the tree, is what is responsible for the drop in the values of the model statistics. Finally, Table 3 shows the estimation of the model parameters which were significant at the 5% level in the two datasets.

Table 3. Parameter estimated for the models fitted in the different data sets.

Data set	Total volume equation			Ratio equation		
	b_0	b_1	b_2	b_3	b_4	b_5
Supervised	0.00008	1.833	0.7875	-0.5664	4.044	-3.797
Automatic	0.000091	1.659	0.9396	-0.7997	3.946	-3.814

Note: b_0, b_1, b_2, b_3, b_4 and b_5 are the estimated parameters in the volume ratio equations.

2.4. DISCUSSION

Comparing the performance of the methodology employed in this work with previous studies is not straightforward as plot size, tree density, forest structure, etc. vary between trials (Cabo et al. 2018a) and all have a strong influence on the results. Moreover, the test case plot has the additional difficulties of high slope, young, and therefore small trees, a tendency of the trees to tortuosity and, particularly, the high density of branches and understory. Despite this, it is possible to establish a range of values obtained by other authors for each dendrometric variable and for volume equations that can serve as a reference for discussion. Regarding tree detection, it is strongly influenced by stem density (Liang and Hyyppä 2013; Thies et al. 2004): the lower the tree density in the sample plot, the higher the detection rate of the stems (Chen et al. 2009). According to Liang et al. (2016), in sparse forests (100–200 stems/ha), the detection rate may reach 100%, while in a forest with a stem density of over 1000 stems/ha, the stem detection rate is generally around 70%. The results obtained in this study for stem individualization are extremely good, with 97% success in a plot with 806 stems/ha. The approach of selecting only the points close to the projection of the stem, based on the estimation of a linear axis for each tree, indeed outperforms previous works by some of the authors (Cabo et al. 2018ab) as it reduces the probability of assigning a tree the height of a higher neighbour tree and eliminates points from branches, leaves or other features around the stem for a more effective diameter estimation.

Regarding the results obtained for the calculation of *h*, most of the differences between the algorithm estimations and the field measurements are between 1 to 2 m. Tree height underestimation using TLS datasets is a common issue (Olofsson and Holmgren 2016), explained

by the fact that the light beam of the sensor is not capable of reaching the top of the crowns, due to foliage obstruction, so the treetops are very often not well defined in the resulting point cloud. Nevertheless, when comparing *h* with h_m, the differences are barely noticeable (6 cm of difference between average values), which indicates that the limitation does not lie with the algorithm, but rather in the nature and quality of the data itself. In cases where *h* needs to be estimated with high accuracy TLS data could be complemented with aerial data, such as LiDAR (Hadas et al. 2017; LaRue et al. 2020; Puletti et al. 2020) or photogrammetric data (Aicardi et al. 2016; Tian et al. 2019) or with a subsample of field measurements in those cases where no remote sensing data is available.

Concerning the *dbh* versus dbh_f comparison, *RMSE* was 1.14 cm, which is compatible with the values of between 0.71 and 2.64 cm reported in previous studies (Hollaus et al. 2019). The difference between Automatic and manual procedures as diameters along the stem increases is also consistent with previous research (Henning and Radtke 2006; Maas et al. 2008) and can be attributed to low point density in higher parts of the stem, the smaller object surface area and obstructions caused by branches and foliage (Liang and Hyyppä 2013). This fact also explains why the most accurate estimations occur in the intermediate part of the tree (between 0.7 and 2.9 m, approximately), which is the interval considered to be "occlusion free". The distribution of anomalous sections (F and ND) follows the same pattern, that is, they are more frequent in the lowest and highest parts of the stem. This problem with diameter estimation in the upper and lower sections could possibly be improved by scanning at higher resolutions, which could lead to better penetration of the foliage, and more laser points. However, any improvement would probably be limited because higher resolutions would still not reduce the occlusion effect (Liang et al. 2016). Stem profile measurement could also be improved by combining diameter measurements retrieved from different sources, or, as shown in the Supervised method used in the test case, by incorporating visual checking or manual fitting in challenging sections if very high accuracy is needed. This might include the possibility of selecting the trees to be used in the parametrization of the equations.

For the parametrization of the merchantable volume equations, the number of sections available, especially in the upper third of the stem, clearly influences the convergence of the stem taper equation and the accuracy of volume estimations. In this particular test case, the use of Supervised data improves on the results obtained with the Automatic data, resulting in an increase of R^2 both in the stem volume equations (from 0.67 to 0.85) and in the ratio equations (from 0.64 to 0.68), as well as the reduction of *RMSE* (from 0.0233 to 0.0149 m^3). When these results are compared with those obtained by destructive techniques in *Pinus pinaster*, where R^2 for stem volume equations ranges between 0.91 and 0.98 (Alegria and Tomé 2011; Yousefpour et al. 2012) and for volume-ratio equations is between 0.80 and 0.89 (Teshome 2005), the values for the same parameter obtained in this study might seem to be low. However, a comparison in absolute terms is not realistic because: (i) in destructive techniques only healthy and standard shaped trees for which there is a full range of measurements along the stem are considered and (ii) in contrast to this study, where all the trees in the plot were considered, in destructive sampling, young trees with erratic growth are generally excluded. Consequently, it is only to be expected that results would be better in study plots with adult trees, low density understory, and the reduced presence of branches.

In terms of time, destructive sampling is by far the most time-consuming step involved in the parametrization of volume equations by means of traditional techniques (Yu et al. 2013). In the case of TLS sampling, only one day would be necessary for a sample of 100-150 trees, which is the number of trees commonly used to adjust merchantable volume equations (Crecente-

Campo et al. 2009). The authors have estimated that only 3 minutes per tree (16GB RAM, i7 4-core 8G processor) is needed to obtain the parametrized volume-ratio equation (including scanning field work), which is a substantial improvement in time compared to destructive methods. Furthermore, in the case of the Supervised dataset, only 20 seconds was necessary to review a complete tree (i.e., 2.5 hours of intense work for all the trees in the test plot). Consequently, the Supervised option is cost-effective in terms of time invested vs improvement in the merchantable volume equations.

This study is eminently methodological, and it has been applied and evaluated in a specific plot of *Pinus pinaster* to assess the performance of the method. The results from a single study plot can be transferred to others as long as they have similar characteristics to the test case plot. However, the strong point of the methodology presented here is that it provides the possibility of parametrizing the volume equations of any tree species or stand typology. The only requirement, is to scan an adequate number of trees (in one or several plots, depending on the scope of the application of the volume equations) so that the algorithm has the necessary input diameters and tree heights (from TLS point clouds) to parametrize the volume equations, after which the algorithm selects the most suitable equation for each case.

From the point cloud processing perspective, the basic principles of tree detection and diameter estimation have already been tested in plots with different characteristics in benchmark studies (Liang et al. 2018; Hollaus, Mokroš, and Wang 2019). These studies describe how more than 20 different algorithms work in a wide variety of scenarios (i.e., different point cloud and vegetation densities, plot configurations and point cloud technologies) and provide very good results when compared with traditional field measurements. However, it is possible that fully automatic approaches for diameter estimations give poorer results in stands with very complex structural or orographic conditions (Liang et al. 2018; Cabo et al. 2018ab; Hollaus, Mokroš, and Wang 2019). In this sense, the methodology here offers contingency alternatives for such complex scenarios: it automatically analyses the coherence of the tree measurements (diameters along the stem), flags anomalous estimations and includes the possibility of the visual checking and correction of flagged measurements. Furthermore, this can be also applied in not-so-complex scenarios, when, for instance, there are few trees available in the TLS datasets and thus problematic or anomalous sections cannot be discarded. What is more, while the methodology selects the most appropriate option (based on statistical indicators: *AICd*), it also offers the possibility of selecting a different model, when, for instance, the reliability of a specific model has been demonstrated to be better for a particular species and/or plot configurations (Westfall and Scott 2010; Menéndez-Miguélez et al. 2014; Saarinen et al. 2019).

Regarding the management of possible measurement errors, in forest inventory modelling it is usual to assume that the independent variables are free of measurement error (Morales-Hidalgo, Kleinn, and Scott 2017). Also, some studies have compared the impact of measurement errors on the parametrization of taper functions when using direct traditional methods and indirect non-destructive methods like TLS (Rodriguez et al. 2014; Marchi et al. 2020; Torresan et al. 2021). Most of these studies concluded that the errors are similar or that they are smaller when using indirect (i.e., remote and non-destructive) measurements. Nevertheless, considering an error model for the independent variables could reinforce the analysis, so this may be something worth exploring in future studies. In the specific case of this study, using error models for the independent variables would, however, affect the automation of the method, as it would involve the need for a specific error model for each scanner and/or stand characteristic, which would potentially impact the simplicity and usability of the method.

CHAPTER 3:

AUTOMATIC ASSESSMENT OF INDIVIDUAL STEM SHAPE PARAMETERS

CHAPTER 3: AUTOMATIC ASSESSMENT OF INDIVIDUAL STEM SHAPE PARAMETERS IN FOREST STANDS FROM TLS POINT CLOUDS: APPLICATION IN *PINUS PINASTER*

3.1. INTRODUCTION

Stem shape is a hugely relevant factor to consider in forestry, as it is closely related to wood quality and has a strong influence on sawmill performance, that is, on the percentage of profitable volume with respect to the volume of the log (Masuda et al. 2021). Consequently, it strongly conditions the use that can be made of a forest stand and its economic sustainability.

The term “stem shape” is usually used generically to refer to a wide range of characteristics, including straightness, conicity, tapering, lean, and even the presence of defects such as bracketing fork and prominences caused by the presence of knots. All these characteristics have great importance in forestry, but the specific importance of straightness and lean is widely recognized from both the scientific and technical perspective (Del Rio et al. 2004; Benneter et al. 2018; MacDonald, Mochan, and Connolly 2009). Stem straightness is particularly significant in forestry because it provides critical information for harvesting and sawing. Stems’ bucking optimization requires the very accurate determination of their shape to enable the cutting points along the stem to be established and to determine merchantable volumes according to particular specifications (Liang et al. 2014). Furthermore, straightness is an important variable in trials, where selecting the straightest provenances is the basis for developing a tree breeding program (MacDonald, Mochan, and Connolly 2009). In the case of lean, its importance was made clear in Thies et al. (2004) and is based on the fact that it influences quality through increasing the proportion of reaction wood (Boschetti et al. 2017); also it is, an expression of the adaptive growth of a tree (Mattheck and Bethge 1998) and a reaction to external loads (i.e., snowfall, stones…) that influences tree growth. Reaction wood (which forms in place of normal wood as a response to gravity meaning its cambial cells are oriented other than vertically) usually has a higher density. Although its mechanical properties are not reduced, it undergoes greater deformations during the drying processes and tends to break more easily; the reason being it is undesirable for wood processing purposes (Murphy, Acuna, and Dumbrell 2010).

To measure the straightness of a stem the most commonly used parameter is sweep, which is traditionally defined as the maximum sagitta per meter of the stem (Hamner, White, and Araman 2007). However, sweep is not the only indicator of straightness; there are others such as sinuosity which are also of great interest. Sinuosity is expressed as the quotient between the line (not necessarily straight) which defines the axis of the stem and the Euclidean distance (straight line) between the end points of the stem (Dwivedi et al. 2019). As for the case of lean, it is defined as the angular deviation of a tree stem from a vertically upright position (Garms et al. 2020).

Fieldwork approaches to collecting data on such variables range from visual classifications made by one or more observers that group trees according to predefined categories, a very common methodology in tree breeding programs, to more evolved systems which use measurements (from calipers, measuring tapes and hypsometers) mainly based on the deviation or lean of the tree axis (Hamner, White, and Araman 2007). However, even with methods that use actual field measurements, results are still subject to observer´s interpretation, which is highly influenced by their experience and the criteria used, as well as by the characteristics of the stand. In the specific case of stem straightness, data on standing trees can also be obtained from localized or national stem curve models (Liang et al. 2014), but their wide scope of application makes them

too imprecise to get accurate results at the individual tree level. Due to all the above, it is difficult to accurately measure complex stem shapes using conventional field investigation methods (del Rio et al. 2004) which is why stem shape variables are not habitually measured as part of regular inventories (Maas et al. 2008). This lack of measurements is especially notable in tree breeding programs of conifers in general (pines in particular) despite stem shape and branch angle assessment being very important (Weng et al. 2017; Wu et al. 2008). In addition to these difficulties, and despite their relevance, in most cases it is not possible or practical to measure the variables implicated in straightness for every single tree in a plot using traditional fieldwork approaches since individual tree measurement is costly and labor intensive (Hyyppä et al. 2020).

The use of remote sensing techniques, and more specifically the use of TLS (Terrestrial Laser Scanning) can be very valuable in the estimation of stem shape. TLS acquires high resolution three-dimensional point clouds of the study area, which provides a reliable representation of the structure of the trees within the stands at the time when data were collected (Liang et al. 2018). The fact that data are collected from the ground makes this technology especially suitable for studying stem profiles. In spite of this, there are only a few studies that have focused their efforts on the calculation of shape variables such as straightness and lean (Murphy, Acuna, and Dumbrell 2010; Warensjo and Rune 2004; Liang and Hyyppä 2013; Olofsson and Holmgren 2016) or to the study of the presence and distribution of branches (Dassot et al. 2012; Kankare et al. 2013; Raumonen, Kaasalainen, Åkerblom, et al. 2013; Zhou et al. 2019) . This may be explained by a combination of issues such as the high price of most scanning devices (Stovall and Atkins 2021) and the lack of algorithms and software applications to calculate shape variables automatically (Molina-Valero et al. 2020) and which also requires expert knowledge to obtain reliable results. However, the general trend is slowly changing, equipment prices are gradually falling (Krok, Kraszewski, and Stereńczak 2020), and the proliferation of methodological developments which automatize data processing and analysis tasks is well under way (Brolly et al. 2021; Disney et al. 2019; Pitkänen, Raumonen, and Kangas 2019). Presumably, then, TLS will be a fundamental technology in forest inventories in the near future (Calders et al. 2020) and will make the automatic measurement of shape variables, such as straightness and lean, possible in regular inventories with minimal effort. For this to happen in a cost-effective and simple way, the automation of point cloud processing with readily available and easy-to-use software capable of extracting information related to important forest attributes is essential (Masuda et al. 2021; Molina-Valero et al. 2020).

The aims of this study are two-fold: (i) To develop a methodology that allows the measurement of straightness (maximum sagitta and sinuosity) and lean automatically at the individual tree level from data captured with TLS; and (ii) to compare the results obtained with measurements made in the field by traditional methods (categorical visual classification that groups trees into classes).

3.2. MATERIALS AND METHODS

3.2.1. Data Collection and Inventory

The study area is located in the autonomous region of Asturias (Northern Spain) (Figure 15A), characterized by an oceanic climate, with abundant rainfall throughout the year and mild temperatures in both winter and summer. The soils are siliceous. The plot where the study was carried out belongs to a network of trials for the National Tree Breeding program of *Pinus pinaster*, a species with a particular tendency to tortuosity. It has an approximate area of 5700 m^2. The terrain is irregular with high slope (>60%) and the presence of various shrub species

such as *Ulex*, *Ericas*, and *Pteridium*, among others (Figure 15B). Both these characteristics contribute to making this study area a challenging one. It was planted in 2005 following an experimental design of four randomized blocks, where 225 families were planted, each family in a row of four trees. Some of the families are from the region of the plantation (Asturias) while others are from various places within Italy, France, Spain, Portugal, and the north of Africa. A genetic thinning (where also fallen trees were removed) was carried out in 2018 resulting in the current number of trees which is 408 (806 stems/ha).

Data acquisition was accomplished in November 2018 using a TLS FAROFocus3D (Faro, 2018). Twenty-four scanning paths were necessary to ensure full coverage and minimize the effect of occlusions. Polystyrene spheres of 25 cm diameter fixed to surveying rods were used to merge the point clouds of individual scans into a unified coordinate system (Figure 17C). Moreover, the position of the spheres was measured in the field using GNSS (Global Navigation Satellite System), thereby ensuring that the unified point cloud had absolute coordinates. The resulting point cloud had approximately 150 million points after removing redundant points within 6 mm (average density ~26,300 points/m^2).

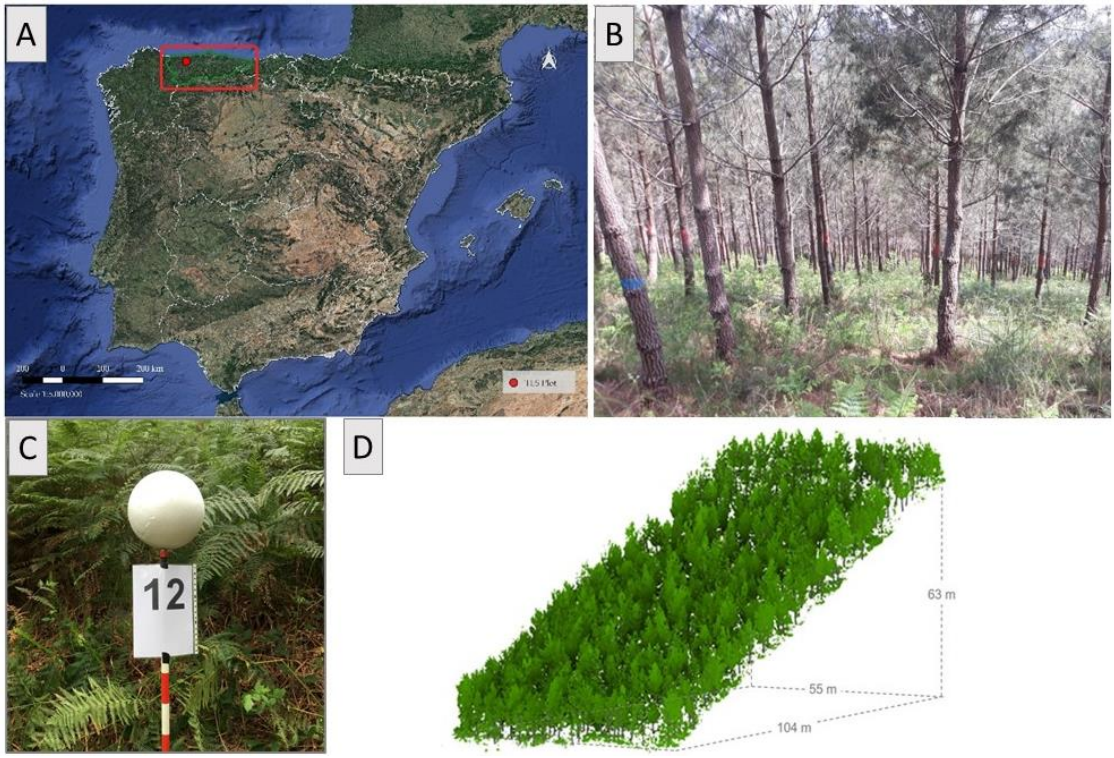

Figure 17.A) Plot situation in northern Spain (Longitude 6°32'33.25 "; Latitude 43°25'18.06" B) Pinus pinaster stand and understory within the plot. C) Polystyrene spheres used for the point cloud georeferentiation. D) Three-dimensional representation of size and slope of the plot.

The point cloud (Figure 17D) was analysed with the methodology for the automatic estimation of *dbh* and *h* described in Chapter 2 (Cabo et al. 2018a; Prendes et al. 2021). As a result, for each tree, measurements of the diameters of the sections along the stem (spaced 20 cm apart, from 0.5 over the ground to 4.9 m) as well as their centers (defined by XYZ coordinates) were automatically obtained (Figure 18A).

Some of the trees did not have the complete range of sections mainly due to (i) the number of points in a section being insufficient to perform the circle fitting or (ii) sections presented anomalies that the methodology detected automatically. In this regard, the methodology

includes several filters to detect anomalies (Cabo et al. 2018a; Prendes et al. 2021) so the potentially 'wrong' sections are flagged for revision by a human operator who checks whether the fitting is correct and/or if it is possible to fit the circle manually.

Moreover, as described in Chapter 2 (Prendes et al. 2021) to have a reference for the data calculated by the algorithm, diameter fitting was manually conducted in the point cloud twice for the same section, each time by a different operator (Op_1 and Op_2). As a result, the centers of the sections for all the individual trees within the plot were available and served two purposes: (i) as reference data to assess the performance of the algorithm and (ii) to correct those sections which were labeled as anomalous by the algorithm (Figure 18A) to ensure data used to estimate stem shape variables were free of outliers (Figure 18B). If a circle obtained and flagged by the algorithm was incorrect but there were enough points to visually estimate its size and position, the operator fitted the circle manually.

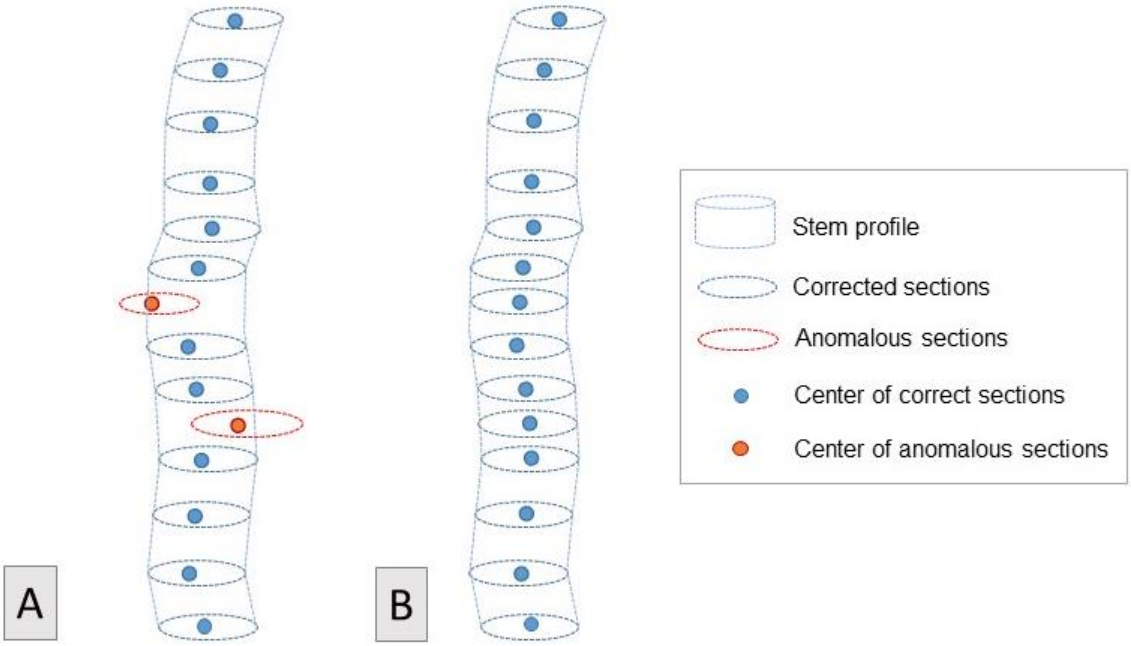

Figure 18. A) Stem sections, defined by their center (XYZ) and radius, automatically calculated by the algorithm presented in [32,33]. In red, the sections labelled as anomalous by the algorithm. B) Stem sections after the correction of the anomalous cases.

In parallel to TLS data acquisition, *dbh* was measured in the field with a caliper, to the nearest 1 mm, and *h*, to the nearest 10 cm, using a digital hypsometer (Vertex IV 360°). As a complement to this inventory data, all the tree stems within the plot were also geo-positioned using the same GNSS as used for the TLS spheres and a total station. This allowed the inventoried trees to be related to those in the point cloud, making comparisons between the two data sources possible. The average *dbh* and *h* for the plot were 17.6 cm and 10.20 m respectively.

Regarding conducting inventories of shape variables in the field (as mentioned in Section 3.1) in tree breeding programs, visual classifications that group the trees according to predefined categories have been widely used as selection criteria over the years to assess stem straightness and lean. In this study, these variables were visually assessed at an individual tree level by a field observer using the classification proposed by del Rio et al. (2004) for *Pinus pinaster* which is detailed in Table 4.

Table 4. Scale of values used as a reference to measure stem shape variables in the field.

Category	Straightness	Lean
1	Straight	Lean not appreciable at first sight
2	Curved in the intermediate or basal zone and less than twice the *dbh*	Lean appreciable up to 15° (referred to the vertical)
3	Curved in the intermediate or basal zone and more than twice the *dbh*	Lean greater than 15° referred to the vertical)

3.2.2. Stem Shape Variables Estimation from TLS Data

As shown in Figure 19, our method automatically calculates the lean angle and straightness parameters (maximum sagitta and sinuosity) from the exact location of the centers of the sections along the stems in a plot. The coordinates of all the sections available for each stem are used to define a polyline that allows the estimation of deviations from ideal straight and/or vertical stem axes.

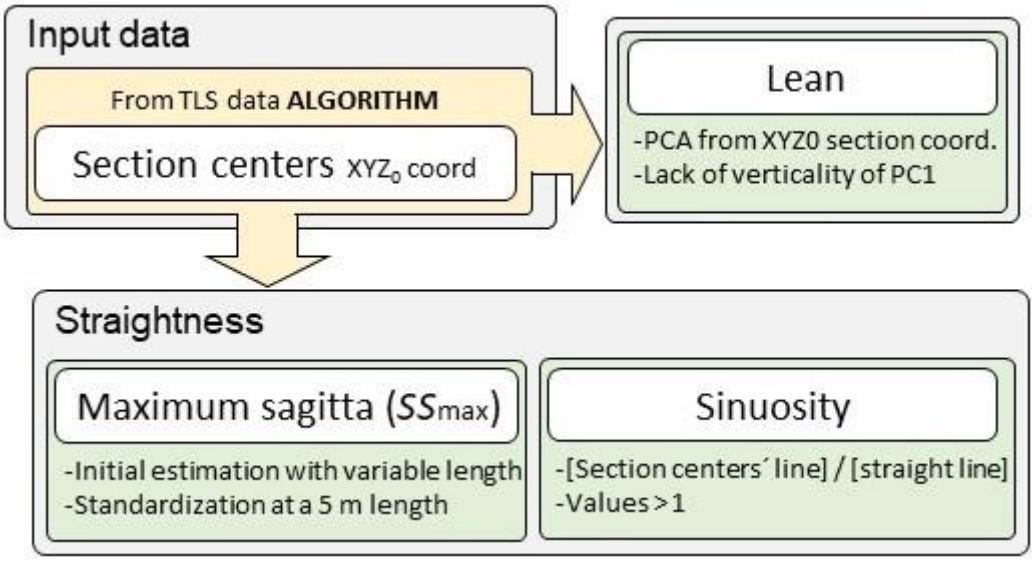

Figure 19. Workflow of the methodology for the automatic estimation of lean and straightness (maximum sagitta and sinuosity) from the coordinates of the section centers along the stems.

The centers of the stem sections for each tree are the only input data necessary for straightness and lean estimations. Each coordinate (XYZ) is stored in an independent array with as many rows as trees in the plot, and as many columns as sections. The workflow for straightness and lean estimations has been implemented in a script written in Python, which enables these variables to be automatically obtained for each individual tree. Consequently, the methodology can be applied in datasets with different characteristics (i.e., species, stand conditions, slope) in a simple and fast way.

3.2.2.1. Straightness

For straightness assessment, the calculation of two variables, maximum sagitta and sinuosity, has been implemented in the methodology. The steps needed for their calculation are explained in detail below.

Maximum sagitta

For each tree, the reference for the sagitta is taken from the straight line segment connecting the centers of the end sections. The sagitta of each section is then calculated as the distance

between the center of the section (Figure 20A) and the straight line segment. The maximum sagitta (hereafter, S_{max}), as well as its position in the stem is identified (Figure 20B).

As explained in Section 3.2.1, some trees do not have data along the full height range (i.e., 23 sections over 4.4 m: from 0.5 to 4.9 m from the ground). In these cases, the sagitta is standardized to the highest height obtained for the dataset (hereafter, standardized height range, i.e., 4.4 m) so that the results obtained for each individual tree within the plot are comparable. To do this, the centers are considered to be distributed around a circumference of radius *R* (Figure 20C). *R* is calculated using the formula that relates the radius of a circumference with the sagitta of its arc and the length of the chord that connects the two ends of the arc. In this case, the sagitta is the S_{max} and the chord is the height range for each tree. From these two variables, *R* can be estimated as in eq.2. Once the value of *R* is known for each tree, the maximum standardized sagitta (hereafter SS_{max}) can be obtained for the standardized height range, this time, by isolating the variable in eq.9.

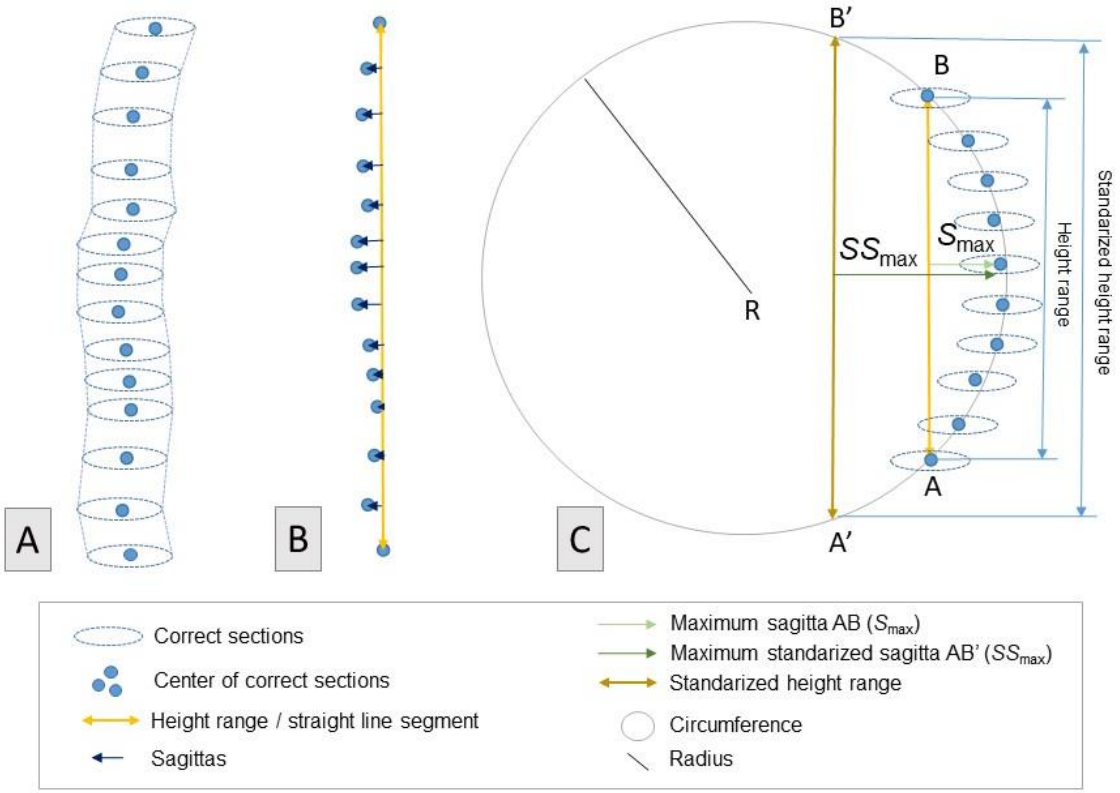

Figure 20. A) Stem sections defined by their center (XYZ) and radius. B) Sagittas calculated for each stem section, defined as the distance from the center of the section to the straight line segment. C) Maximum standardized sagitta calculation considering the centers of the sections to be distributed around a circumference of radius R.

$$\mathrm{R} = \frac{(S_{max}AB) + (Heigth\ range/2)^2}{2 * (S_{max}AB)} \qquad \text{eq. 9}$$

Sinuosity

The sinuosity of a line is calculated as the quotient between its length and the length of a reference line. In the case of a tree, that reference line is the straight line segment that joins the end points of the stem, and its length (*L*) is calculated as the sum of the rectilinear segments

that connect the centers of the stem sections, as in eq.10. According to this, the minimum value for sinuosity is 1, which means no sinuosity.

$$Sinuosity = \frac{L}{Height\ range} \qquad \text{eq. 10}$$

3.2.2.2. Lean

A principal component analysis (PCA) based on the XYZ coordinates of section centers was carried out. When this type of analysis is applied to a 3D point cloud, three principal components (directions), which can be considered as three perpendicular coordinate axes, are created (PC1, PC2, and PC3) (Figure 21A). By definition, PC1 will follow the direction with the greatest variance possible. Since tree stems are eminently linear objects, the direction of the first component follows the direction of the tree axis, and from there, the lean, or lack of verticality, is calculated as in eq. 11 (Figure 21B).

$$\alpha = arctan \frac{|\Delta z|}{\sqrt{\Delta x^2 + \Delta y^2}} \qquad \text{eq. 11}$$

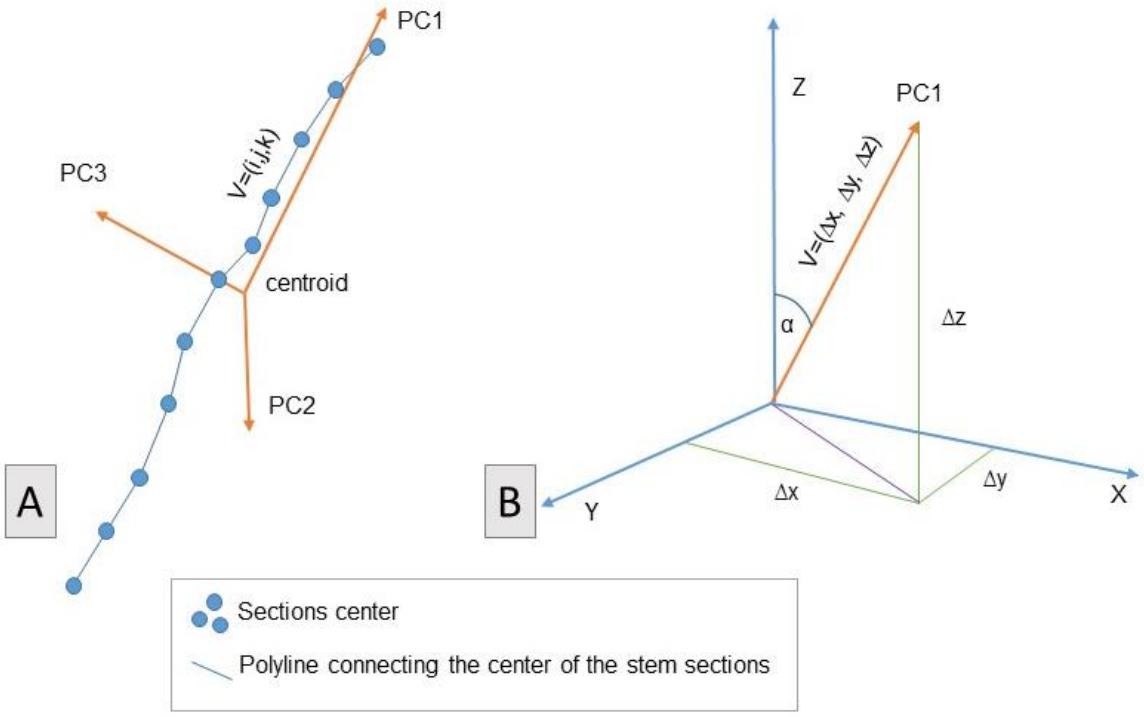

Figure 21.A) Coordinate axis resulting from PCA analysis applied to the stem section centers (B) Calculation of lean angle (α) from PC1 with respect to the vertical.

3.2.3. Validation procedure

The only input data that the methodology uses to estimate the shape variables are the XYZ coordinates of the centers of the sections, and errors will be transmitted to the same variables. Based on that, the methodology´s performance is assessed in terms of error propagation, from the position of the centers of the sections, to the maximum standardized sagitta, sinuosity, and lean. Manual measurements of the centers of the sections (X_{op}, Y_{op}) (see Section 3.2.1.2) have

been considered as ground truth for the comparisons through the workflow explained in Figure 22. In this figure Op_1, Op_2 refer to manual measurements made by two different operators. *Op* refers to a random choice between diameters from Op_1 or from Op_2 that is used to minimize potential biases by either of the operators that might be imperceptible to the naked eye.

The differences between the two operators (Op_1-Op_2) and between the operators and the algorithm (*Op-Alg*) in positioning the sections' centers were calculated. A bootstrap analysis was conducted to study the propagation of the errors from the center of the sections to maximum sagitta, lean, and sinuosity, considering that the distribution of these errors was not known. First, the initial values of these three variables were calculated for each tree given the coordinates (X, Y). Then, 1000 bootstraps samples of dimension *N* x *M* (*N* and *M* being the number of stems and number of sections, respectively) were constructed by resampling with replacement the initial values of the errors for each section. Then, the errors were obtained for each case and added to the initial X, Y coordinates of the centers estimated by the algorithm. With the new coordinates as a starting point, the maximum standardized sagitta, sinuosity, and lean of all the trees were recalculated. Finally, the results obtained were compared with the original estimates of the algorithm. From the differences between them, the density function of the differences was represented graphically, for each scenario and variable (distances between the centers of the sections, maximum standardized sagitta, sinuosity, and lean).

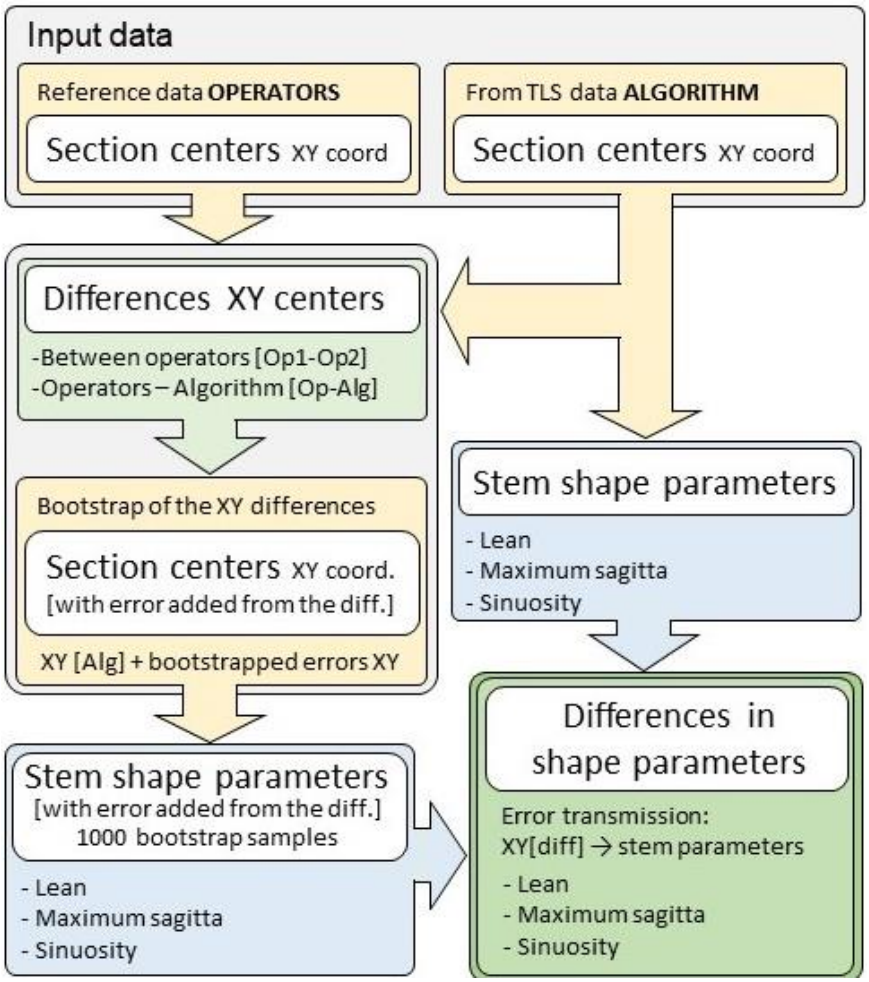

Figure 22. Workflow for the algorithm performance assessment. In yellow: X, Y coordinates of the centers of the sections. In blue: straightness and lean parameters calculated by the algorithm. In green: differences between operators and algorithm in the position of the center of the sections, and in the straightness and lean calculations.

Regarding traditional estimations, comparing a continuous variable (from TLS data) and a categorical one (from a field inventory) is not straightforward due to their different natures. However, it is possible to evaluate if the categorization of the trees in the field as per their straightness and lean follows a similar pattern to that obtained with TLS. The procedure consists of grouping the trees on the plot following the traditional method (Table 4), and then calculating the two shape variables for each tree in each category using the TLS observations. Then, the probability density functions for each variable and for each category were compared. The comparison was done both visually and numerically. Numerical analysis was carried out by analysing the statistics of both variables and through a Tukey-Kramer test (Tukey 1949; Seidel et al. 2021) that compares the individual means from an analysis of variance of several samples with different characteristics.

3.3. RESULTS

3.3.1. Stem Shape Variables from TLS

Once the methodology was tested in the plot, the shape variables were obtained for 385 of the initial 408 trees. The missing trees were either poorly defined in the point cloud or had a very small number of sections. In the first case, it was not possible to apply the methodology to them, while in the second case the results obtained were unreliable. Table 5 summarizes the minimum, maximum, mean, standard deviation, median, and mode of the shape variables estimated by the methodology.

Table 5.Descriptive statistics of shape variables estimated from the TLS point cloud.

	Minimum	Maximum	Mean	Deviation	Median	Mode
Lean	0.150	14.100	4.010	2.604	3.686	1.000
Maximum standardized sagitta (m)	0.020	0.390	0.104	0.058	0.092	0.094
Sinuosity (adimensional)	1.000	1.250	1.008	0.018	1.004	1.003

The range of the lean values was low (14°); the maximum value corresponded to a tree classified as not leaning in the field. These results demonstrate that the trees were mostly slightly inclined. The standard deviation was around 0.5°, with lean values not widely dispersed around the mean. According to the median and mode values, the distribution had negative skew, and the range was small, which means that there was little variability in the lean values.

Regarding maximum standardized sagitta statistics, the trees in the plot can be considered as straight in most cases given their average value of 10.4 cm, which was very close to the average radius of the trees within the plot (8.8 cm). Standard deviation was approximately equivalent to half the mean value, and the distribution negatively skewed in terms of the median and mode values. The range was around 37 cm, indicating considerable variation in the maximum sagitta values. Regarding sinuosity, average values were close to 1 (no sinuosity), while the standard deviation was low, indicating an overall reduced stem tortuosity. The distribution shows negative skewness, and the range is small, which means that there was little variability in the sinuosity values. Figure 23 shows the spatial distribution of the stem-shaped variables obtained in the study plot.

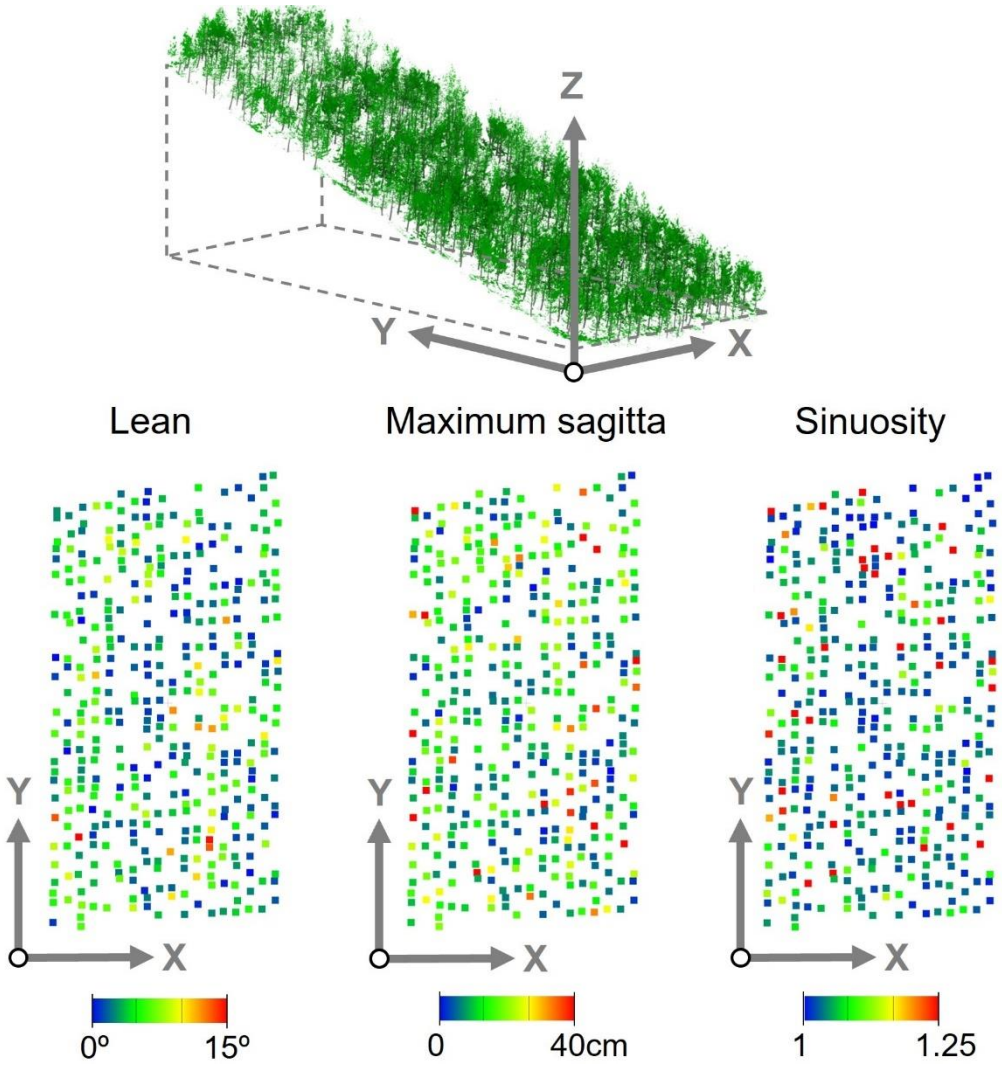

Figure 23. Spatial distribution of the stem-shaped variables (lean, maximum sagitta, and sinuosity) within the study plot. Top: 3D representation of the plot. Bottom: top views of the trees represented by a colored point indicating the stem shape value according to a color scale (blue: lowest value and red highest value within the study plot).

3.3.2. Validation Results

The results of assessing the methodology's performance are shown in Figure 24. The probability density functions obtained as in the procedure explained in Section 3.2.3, were grouped according to the assessed variable and the comparison between operators (Op_1-Op_2) and operators-algorithm (*Op-Alg*).

Regarding the discrepancies between the centers of the sections (Figure 24A), the trend was similar in the two comparisons, with low values in general terms. As expected, the lowest values (less than 2% in 97% of the estimations) were obtained when comparing the estimations of the two operators. When the operator estimations were compared with the algorithm (*Op-Alg*), the discrepancies were slightly higher but still less than 4 cm in 90% of the estimates. The trend was similar for the results obtained for lean (Figure 24B) and maximum standardized sagitta (Figure 24C). For lean, discrepancies were extremely low when comparing Op_1 and Op_2, with less than 0.25° in 99% of the estimates. Regarding *Op-Alg*, the differences were a little higher, but they were still only between −0.5 and 0.5 °, in 95% of the cases, so they were practically insignificant. The same occurred with the maximum standardized sagitta, where the lowest differences were computed for Op_1-Op_2, with 99% of differences in the estimates being below 5 cm. There was a

slight bias in this case showing TLS tended to estimate bigger sagittas than the operators. The comparison between *Op-Alg* showed 92% of differences in the estimates to be below 10 cm. Finally, in the case of sinuosity (Figure 24D), differences between operators were practically negligible (very close to 0) on most occasions, while the differences between algorithm and operators were mostly around −0.015. The distribution was relatively uniform but still had a slight negative bias.

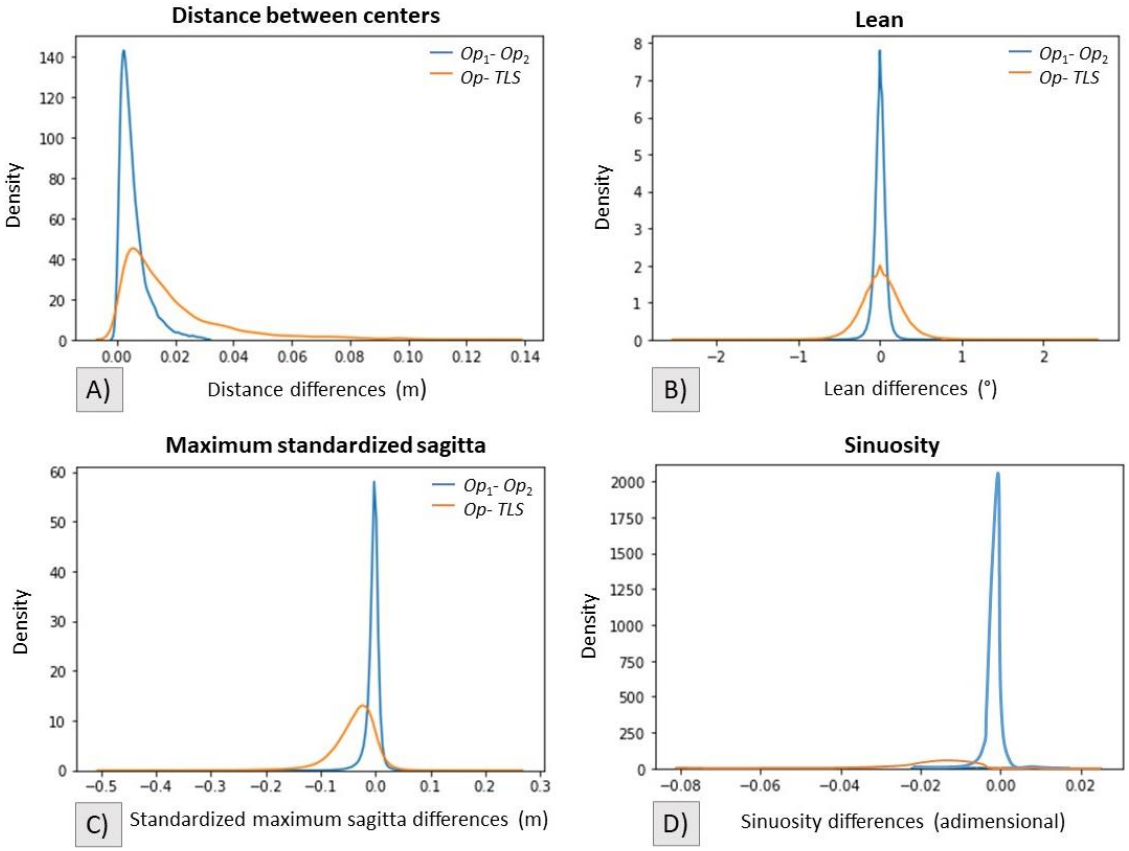

Figure 24. Probability density functions of the error transmission from the centers of the sections to the shape variables as follows: A) Distance between centers (B) Lean C) Maximum Standardized Sagitta (SS_{max}), D) Sinuosity.

As for the comparison with traditional estimations, Figure 25 shows the probability density functions obtained for the trees within the study plot: one for each of the three categories under study established following the criteria in Table 4. Specifically, Figure 25A shows the three curves corresponding to the SS_{max} and Figure 25B shows those relative to the lean. In the case of the SS_{max} there was a high degree of overlap among the three categories, especially 2 and 3, which is an indicator that the boundaries between them were not well defined.

There was a tendency for SS_{max} to increase as category value increased. In category 1, most of the trees were around 5 cm, while in the other two categories, the peak of the density function was slightly shifted to the right, indicating a greater frequency of higher SS_{max} values. In the case of lean, the results were very similar. The curves show a high degree of overlap and reveal a slight decrease in the lean value as the category number increases. Moreover, it is observed that the peak of the distribution is very close to 0° in class 1 and slightly displaced to the left in classes 2 and 3.

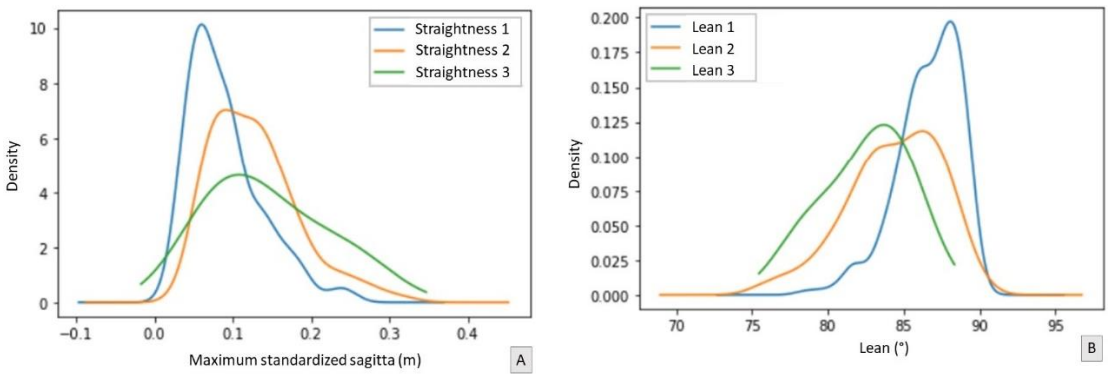

Figure 25. Probability density functions representing the values for SS_{max} (1) and lean (2) obtained by means of the methodology/TLS using the classification from field inventory so that the three categories of trees shown in the graphic could be established.

Table 6 summarizes the descriptive statistics (mean, median, and standard deviation) of the maximum standardized sagitta and lean by category. In view of the results, the trend previously detected in the probability density functions is confirmed by the descriptive statistics. In the case of SS_{max}, mean values increase with the category number. Between categories 1 and 2 the increase is 4.4 cm, while between 2 and 3, it is only 0.5 cm.

In the case of lean, the situation also follows a clear trend: there is a decrease in its value as the field category number increases, which indicates that, in general terms, the trees are more inclined in the higher categories than in the first. The biggest increment in the mean value is between category 1 and 2 (2.28°), while between categories 2 and 3 it is only 1.39°.

Table 6. Maximum standardized sagitta (SS_{max}) and lean statistics obtained for the different categories shown in the probability density functions.

	Maximum Standardized Sagitta (m)					Lean (º)				
	N_S[1]	Mean	Deviation	Minimum	Maximum	N_L[1]	Mean	Deviation	Minimum	Maximum
1	*260*	0.095	0.060	0.020	0.355	272	3.352	2.068	0.149	11.573
2	*120*	0.139	0.080	0.047	0.390	108	5.633	3.051	0.206	14.102
3	*5*	0.144	0.075	0.074	0.256	5	7.026	2.651	4.870	11.314

[1] Note: N_S, N_L are the number of trees included in each category of straightness and lean respectively according to field inventory.

Similar conclusions were obtained by performing a Tukey-Kramer test to compare the means between the three categories. For a significance level $\alpha = 0.05$, the test result showed that it is not possible to assert that there are significant differences between the three categories for SS_{max}. Regarding lean, there was only a significant difference between category 1 and the other two.

3.4. DISCUSSION

This study presents a methodology for the automated measurement of straightness (maximum standardized sagitta and sinuosity) and lean at the individual tree level from data captured with TLS. The results obtained were compared with measurements made in the field employing a categorical visual classification that groups trees into classes according to their degree of straightness and lean.

The methodology performance was assessed in terms of error propagation from the centers of the sections to the maximum standardized sagitta, sinuosity, and lean values. The probability density functions (Figure 24) for comparison between Op_1-Op_2 showed the lowest values of error, as expected. It has been graphically demonstrated that for both comparisons made (Op_1-

Op_2 and *Op-Alg*), the errors have little influence on shape variable estimations, revealing that small errors that may potentially be made regarding the position of the centers of the sections hardly affected the estimation of shape variables. Based on the results, the values obtained for these variables from TLS point clouds with the methodology presented in this study can be considered reasonable. Regarding their spatial distribution, straightness, lean, and sinuosity values do not show any pattern; thus, the differences between trees are mainly associated with genetic factors and not with environmental factors as reported in previous works (Yun et al. 2019; Wang et al. 2019).

In the case of the comparison between the variables obtained by the methodology and those obtained by the categorical classification performed in the field inventory, the results show that there is a clear misclassification between the categories established in the field. Although the results achieved show the mean values tend to increase slightly as the category number increases, (see Table 6) as expected, the statistical analysis shows that there are no differences between any of the groups in the case of straightness and there are only significant differences in the case of group 1 and the other groups in the case of lean. This fact suggests that traditional methods involve constraints which make them unsuitable for accurate analysis at individual tree level, especially in a tree breeding plot, like the one used in this study, where it is crucial to have reliable measurements of the tree's morphology for the correct estimation of individual and family heritability and their genetic correlation between traits.

These results are not entirely unexpected, as several authors have pointed out that manual assessment of stem shape parameters in standing trees is complicated, time-consuming, and costly (Liang and Hyyppä 2013; Mengesha, Hawkins, and Nieuwenhuis 2015). Moreover, comparisons between the results of different studies are difficult due to the variety of methods used to evaluate stem straightness and lean (particularly those based on subjective scales), compounded with variation in testing environments, species, and age at the time of evaluation. These are the main reasons why numerical measurements of quality parameters in standing trees are not yet common for most forest inventories (Mengesha, Hawkins, and Nieuwenhuis 2015). All the above is in line with the high degree of subjectivity in estimates when using exclusively visual classifications that do not rely on any measuring device, thus increasing the risk of error. In the case of the genus *Pine*, when using visual classifications, high heritability in characters related to stem straightness has been reported by several authors. This, however, contrasts with other authors who have reported low heritability (Alia and Majada 2013) in the same characters. Using our methodology on TLS datasets provides, for each shape variable, a numerical value that quantifies it in an absolute and precise manner. Consequently, the subjectivity and ambiguity associated with other alternatives, such as establishing visual categories in the field, disappear, allowing comparisons between different plots, species, or time periods. Besides, based on the results obtained with TLS data, thresholds could be established to define categories if desired. Some authors such as (Garms et al. 2020; Warensjo and Rune 2004) defined a lean value beyond which a tree can be considered as inclined, and the same procedure could be applied to other shape variables. Moreover, the methodology provides estimations for sinuosity, which is difficult to measure in the field by traditional methods. In some studies, such as (Middleton et al. 1989; Espinoza 2009), sinuosity of standing trees was measured by using a combination of visual scoring and assessing the displacement of sections of the stem from the initial direction of growth. Due to the wide range in values, they were averaged and relativized to represent a sinuosity rating for a plot; a very costly and subjective method. However, the methodology presented in this study estimates sinuosity in a very fast and accurate manner.

In this case, a simple characterization of the stems has been made with an eminently practical approach focused on the stem shape variables which are traditionally evaluated. However, the use of TLS point clouds is an extremely powerful tool that offers a three-dimensional reconstruction of the forest at the moment of the scan, which has many advantages (Pitkänen, Raumonen, and Kangas 2019; Cabo et al. 2018b; Torresan et al. 2021). The most obvious is that TLS forest data are permanently available, so multitemporal studies with various objectives can be performed (Liang and Hyyppä 2013; Srinivasan et al. 2014), as well as making it easy for new variables of interest to be studied retrospectively. Moreover, future work could focus on estimating other stem shape variables, like curvature or taper, with the same input data used in this study (i.e., position and diameter of sections along the stems of a forest plot).

Finally, this study provides a new methodology that contributes to the potential availability of information on stem shape and quality in preharvest inventories. On the one hand, this type of information (i) makes possible better value estimations of stems based on a desired specification, (ii) allows the consideration of traits related to stem shape, which influence the yield of merchantable volume, (iii) serves as a starting point for an automated procedure to estimate merchantable volume in standing trees, considering not only diameters at different heights and total height but also stem shape variables, and (iv) facilitates the planning of the bucking of stems into logs using more detailed stem shape data and thereby improves the overall profit that can be obtained from each tree (Garms et al. 2020; Warensjo and Rune 2004; Acuna and Murphy 2005). On the other hand, it has wide applications in the field of tree breeding, where stem straightness and lean are key variables when selecting the best provenances according to wood quality criteria.

CHAPTER 4:

OPTIMAL BUCKING OF STEMS

CHAPTER 4: OPTIMAL BUCKING OF STEMS FROM TERRESTRIAL LASER SCANNING DATA TO MAXIMIZE FOREST VALUE

4.1 INTRODUCTION

To facilitate subsequent processing and maximize merchantable value and volume recovery, trees that are felled in the forest are usually cut into smaller logs (Kivinen 2007). This operation, known as “bucking”, is a critical step in transforming standing timber into final products and plays a fundamental role in determining the profitability of a forestry business (Acuna and Murphy 2005). Bucking decisions at harvest time impact the characteristics, quantity and value of the products (log-types) that can be obtained from the stems. Consequently, poor decisions at this stage may result in substantial value losses, which has been demonstrated in several studies (Labelle and Huß 2018; Pilkerton, Sessions, and Kellogg 2013; Spinelli, Magagnotti, and Nati 2011; G. Murphy 2008; Boston and Murphy 2003).

The allocation of cutting patterns and their implementation through optimal bucking taking into account the individual characteristics of each stem is one of the main goals of, and challenges for forest operation managers. According to Arce et al. (2004), the bucking task is carried out almost exclusively by processor/chainsaw operators based on their experience and intuition, poor decisions compromising the profitability of the forestry business (Silva et al. 2020). Several authors have therefore emphasized the need for a more analytical approach so that bucking patterns are obtained and allocated based on objective measurements that consider the species involved and the characteristics of the stems. Optimal bucking at the individual tree level can be accomplished with various techniques, including dynamic programming (DP), network programming, simulation, and integer linear programming (Pvnematicos and Mann, 1972; Briggs, 1980; Sessions, 1988). Among them, DP is the most common mathematical technique used by researchers and foresters to optimize stem cutting in commercial forests (Jingxin Wang, LeDoux, and McNeel 2004) and it has recently been used in a wide range of studies and applications (Akay 2017; Erber, Stelzer, and Stampfer 2021; Silva et al. 2020; Vanzetti et al. 2019).

One of the main limitations of bucking models is that the input data needed to obtain good results is often unavailable or difficult to collect (Mederski et al. 2018). Usually, preharvest inventory systems provide detailed descriptions of the stems (i.e., diameters) from a small sample of standing or felled trees. However, these sampling procedures are time-consuming, labour intensive, and expensive (Sullivan et al. 2018), and may generate inaccurate data when the sample data are generalised to the whole stand. Moreover, external tree features associated with wood quality, such as curvature and branchiness, may not be appropriately collected by traditional inventory systems (Bukauskas et al. 2019). Modern mechanized harvesters fitted with sensors can also measure stem dimensions at harvest time (da Silva et al. 2022) with the assistance of onboard computers. They can optimally buck each stem according to its dimensions and qualities, log prices, and certain desired specifications to maximize value (Sandak et al. 2019). However, based on market prices, optimally bucking individual stems is unlikely to provide yields that meet order book constraints at the level of the harvest unit or forest stand. Thus, as an alternative adaptive control heuristics imbed an individual stem optimal bucking procedure in an algorithm that can be adjusted to incorporate relative prices and minimum small-end diameter specifications in order to meet order book constraints (Murphy, Marshall, and Bolding 2004). As such, the level of representativeness of the sample data in the case of manual and destructive methods used in pre-harvesting inventories, and the accuracy of

the measurements obtained with sensors as harvesting equipment fells and processes stems will determine the bucking decisions of the remaining stems (Murphy 2008).

Apart from manual and destructive sampling, other alternatives that capture stem data in the field to feed optimal bucking systems also exist. These include, for example, the use of stem taper models (Ko et al. 2019; Zapata-Cuartas, Bullock, and Montes 2021), which are mathematical equations that allow diameters at different heights along the stem to be estimated on the basis of the diameter at breast height (*dbh*) and the total height of the tree (*h*) or stem (Boczniewicz, Mason, and Morgenroth 2022; Ulak et al. 2022). In addition, these models can estimate the height of the stem up to which a specific diameter is to be found, the volume of wood between two diameters or sections of the stem, and the volume up to a particular diameter or commercial height. However, all the above is only possible because a simplification of the stem profile is assumed. For example, where the description of the stems does not include any tree quality feature such as curvature and branchiness, and they are assimilated to a geometric body whose diameter decreases as height increases. Alternatively, the use of remote sensing techniques, more specifically TLS, has proven to be very useful for the estimation of stem attributes (Cabo et al. 2018; Pitkänen, Raumonen, and Kangas 2019; Prendes et al. 2021; Saarinen et al. 2017). The fact that the scanner captures data from the ground enables the acquisition of a high-resolution and accurate point cloud of the stem structure at the individual tree level (Zong et al. 2021).This ability, in turn, makes it possible to measure different attributes along the stem (diameters, heights, branching, etc.) as well as shape variables (straightness, fork, lean, etc.) without the need to fell trees (Liang et al. 2016). These variables of interest are then used directly and efficiently in bucking systems.

In the last fifteen years, there has been increasing interest from the forest industry in laser scanning techniques and the performance of TLS systems for volumetric measurements of timber assortments (Kankare et al. 2014). However, studies where data collected with laser sensors are fed into optimal bucking systems or algorithms are scarce. In the particular case of TLS, Murphy (2008) determined stand value and log product yields using TLS and optimal bucking and then compared the results with estimates from actual stem profiles. The study revealed that TLS-derived estimates of average stand value and log product yields were within 7% of actual estimates. Later on, Murphy et al. (2010) collected information of stem profiles using three methods: (i) TLS scans, (ii) Atlas Cruiser inventory procedure (Atlas Technology, 2010) and (iii) manual measurements after harvesting. TLS volume and value recovery were within 8% and 7%, respectively, of actual harvester recovery, while cruiser volume and value estimates were both within 4% of actual harvester recovery. More recently, Kankare et al. (2014) compared the accuracy of high-density laser scanning techniques to estimate tree-level diameter distribution and timber assortments by combining ALS and TLS for timber assortment estimation. The results showed that accurate tree-level timber assortments and diameter distributions can be obtained using TLS or a combination of TLS and ALS. After the study of Kankare et al. (2014), to our knowledge, no other studies have investigated the potential of TLS data for optimising bucking algorithms. Our study contributes to filling this knowledge gap by investigating the integration of TLS measurements (including log curvature) in an optimal bucking system and providing a tool to measure a forest stand's economic value accurately. The aims of this study are two-fold: (i) to develop and test a non-destructive, fully automated methodology for the optimal bucking of stems, based on their external characteristics (diameters and curvature), which maximize the economic value of a stand using data from TLS point clouds; and (ii) to compare the results obtained by the methodology when TLS-derived curvature is excluded, and when diameters are estimated with a taper equation.

4.2 MATERIAL AND METHODS

4.2.1 Site description and data collection

The study area is located in Villaviciosa, a locality in the autonomous region of Asturias, Northern Spain (43°4'5.00"N 11°27'17.46"W) (Figure 26A). It was established as a pruning trial in winter 2005–2006, on a monospecific, even-aged *Pinus radiata* stand. It was deliberately chosen to represent a young stand (7–11 years old) without previous pruning or thinning treatments and where tree diameters were suitable for pruning interventions. It has an approximate area of 5,000 m^2 with clay-sandy soil, an average slope of 22.3°, and a light presence of shrubs such as *Ulex* and *Pteridium*. A total of 120 trees were measured in the study plot. They had an average *dbh* and *h* of 22.6 cm and 17.7 m, respectively.

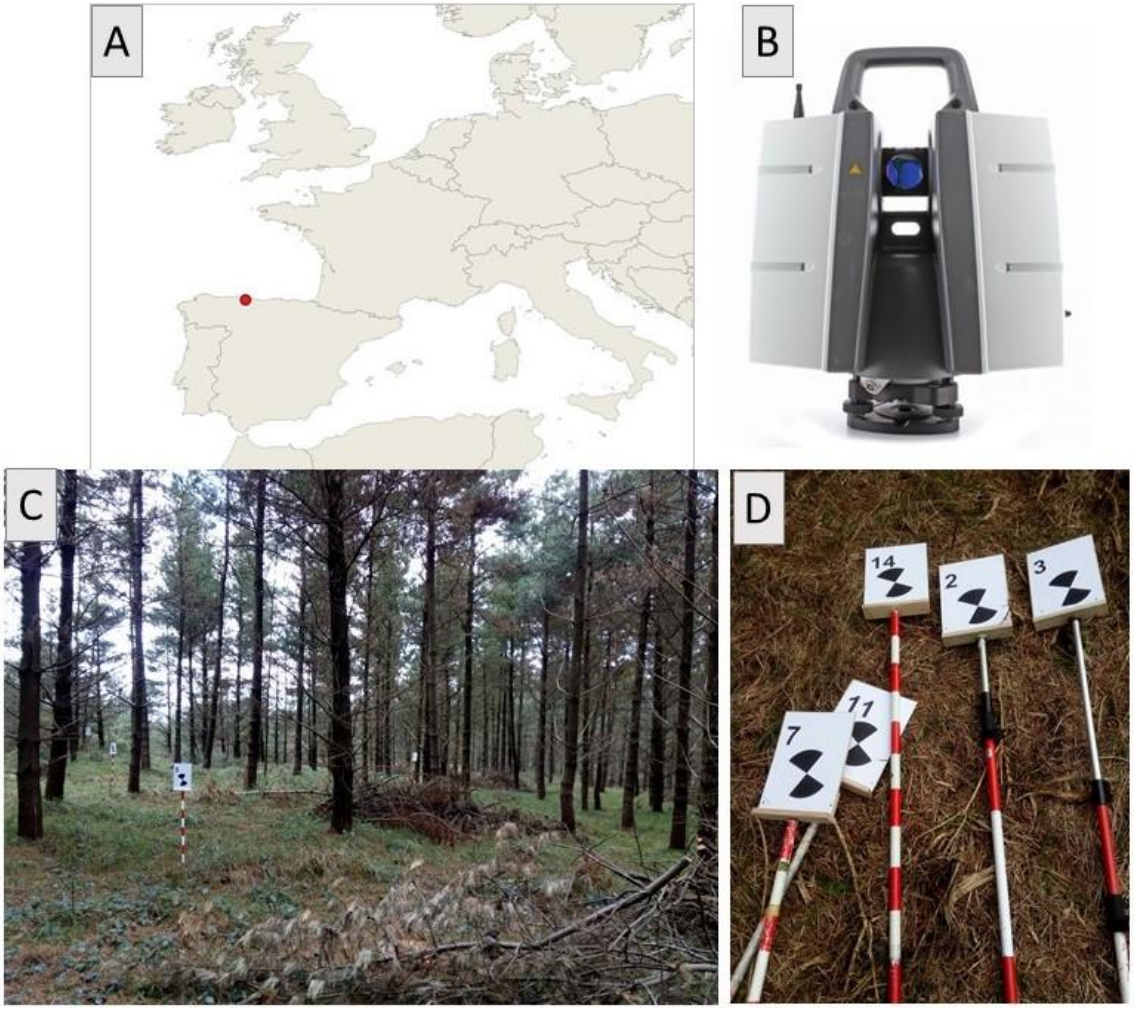

Figure 26. A) Location of the study area B) Leica P40 laser scanner used for data acquisition C) Pinus radiata stand within the study plot D) Wooden targets used for point cloud georeferentiation

Data acquisition on the 120 trees was carried out in February 2018 using a TLS Leica P40 (Leica, 2018) (Figure 26B). Several 12x20 cm targets on surveying rods (Figure 26D) were used to merge individual scan point clouds into a unified coordinate system. Their position was measured using a differential GNSS (Global Navigation Satellite System) Leica Viva GS14 3.75G Performance (Leica, 2021) with dual frequency and centimetric accuracy, thereby providing accurate geolocation for possible future comparisons. The Root Mean Square Error (*RMSE*) of the

registrations was 5 mm and the final unified point cloud had approximately 75 million points, after removal of duplicates within 6 mm of each other.

For all trees in the plot, *dbh* and *h* were measured; *dbh* to the nearest 1 mm with a calliper, and *h* to the nearest 10 cm, using a digital hypsometer (Vertex IV 360º). All individual trees within the plot were also geo-positioned, using the same GNSS used for the TLS targets and a total station, to complement the inventory data.

4.2.2 Diameter estimations along the stem

Diameters along the stem are the primary input of the optimal bucking algorithm, so the resulting bucking pattern is strongly dependent on their values. These diameters were obtained for the trees within the study plot in two different ways: (i) from a stem taper model (ii) from point cloud data collected in the field with the TLS. Both approaches are explained in detail below. A statistical analysis was then carried out to compare the diameters obtained from the two procedures as well as the impact of diameter estimates on the bucking results.

4.2.2.1 Taper model

Diameters along the stem were estimated using the taper model in Canga et al. (2008); a model specifically developed for *Pinus radiata* stands in north-western Spain. The equation builds on the model in Fang et al. (2000) which consists of a compatible system formed by a taper model, a total volume equation, and a merchantable volume equation. The taper model is segmented with two attachment points and three shape factors for each segment. In this context, "compatible" means that the volume computed by the integration of the taper model should be equal to that calculated by a total volume equation (Menéndez-Miguélez et al. 2014). By embedding *dbh* and *h* (from the field inventory) in the taper model, diameters every 10 cm for a height interval between 0.2 and the total height of each tree are obtained as outputs.

4.2.2.2 TLS

In addition, tree point cloud data collected with TLS in the study plot was processed and analysed for the automated estimation of *dbh* and *h* as per the methodology described in Chapter 2 (Cabo et al. (2018a); Prendes et al. (2021)).

As a result, measurements of tree diameters along the stem (spaced 10 cm apart, between 0.2 over the ground and 10 m) and their centers (defined by XYZ coordinates) were automatically obtained. In several cases it was impossible to fit a circle to estimate *dbh* for some stem sections, primarily due to an insufficient number of points or to anomalies present in the stem. In the latter case, a filter-based methodology was developed to detect the anomalies automatically (Cabo et al. 2018; Prendes et al. 2021) such that the potentially wrong sections were flagged for further revision. Available diameters above or below those anomalous sections were used to estimate the missing or flagged sections. Estimating diameters was also problematic in the upper sections of the tree (above 10 m) due to the low definition of the stem contour in areas near the crown, so diameters above that height were completed with the taper model (see Section 4.2.4.6 for more details).

4.2.3. Optimal stem bucking

4.2.3.1 General aspects of the bucking algorithm

Dynamic Programming (DP) was used to optimally buck the stems in our study; it is the most common mathematical technique researchers and foresters use to optimize stem cutting in commercial forests because DP bucking algorithms, in most cases, provide better solutions in

comparison to those generated by a sequential bucking system. The latter procedure is, however, commonly used by field operators, who first try to cut the log with the highest value (i.e., veneer logs). If no extra logs can be cut from this type, they continue with the second-highest value log, then with the third-highest value product, and so on, until the whole stem has been processed. The sequential bucking system only considers the dimensions of the logs and the specifications of the timber products. At the same time, the relative or absolute value of the logs cut is used to guide the priority of the products[1] that will be cut along the stem.

4.2.3.2 Input and output data

Regarding input data, two different files are required to run the DP bucking algorithm: one that provides detailed information on the stems and another that specifies the requirements of each log type (product) that can be cut from the stem. In the first case, the stem file contains information including diameter, volume, and quality (defined by curvature), which are generally detailed for segments of a certain length (i.e., every 10 cm along the stem). This information can be obtained from inventories (manual measurements or collected by sensors) or estimated from taper models. In the second case, the product requirement file specifies the logs' characteristics of each log type. These include large and small end diameters (*LED* and *SED*, respectively), market prices (absolute or relative) for each log type, feasible lengths (one or multiple lengths), and maximum allowable log curvature. This study did not include branchiness and knot size as log type requirements.

4.2.3.3 Bucking optimization

Following the terminology and methodology presented by Taha (2017), the DP recursive computations can be expressed mathematically based on a network representation using *stages* and *states* (nodes). A node is regarded as the information that links the stages together so that the optimal decisions for the remaining stages can be made without re-examining the decisions from previous stages. The proper definition of a node under this approach allows the consideration of each stage separately, guaranteeing that the solution is feasible for all the stages (Taha, 2017). In the stem bucking, the nodes contain the information of the feasible products that can be cut from the stem at a particular stage or position in the stem.

In the mathematical nomenclature of DP, X_i refers to the node of the system at stage *i*. Thus, let $f_i(X_i)$ be the best value to node X_i at stage *i*, and define $V(X_{i-j}, X_i)$ as the value of the variable of interest (i.e., economic value) from node X_{i-j} to node X_i; then f_i is computed from f_{i-j} (j<=i), using the following forward recursive equation (eq. 12):

$$f_i(X_i) = \max\{[f_{i-j}(X_{i-j}) + V(X_{i-j}, X_i)]\},\ \forall i \in i, j \in J \mid j \leq i \ \ and\ j > 0 \qquad \text{eq. 12}$$

Notice that in eq.12, $f_i(X_i)$ must be evaluated for all feasible ($X_{i-j,}X_i$) links. Also, starting at *i* = 1, the recursion sets $f_0(X_0)$ = 0.

Figure 27 shows a practical bucking example with these definitions. The stem has been divided into 6 sections, each 1 m long. Seven stages (S0 to S6) represent potential cutting points where feasible products (represented by nodes) can be cut. Also, A and B represent the quality of each section (A being higher than B), which is determined, for example, by the curvature, presence of branches or stem damage. In the example, at stage 2 (S2), four products (candidate nodes in Figure 27) can be cut, two products of 2 m each (defined by node 4 (Product 1) and node 5

[1] A product is also referred to as a log type, so both terms are used interchangeably throughout the text.

(Product 2) and two products of 1 m each (defined by node 3 (Product 3) and node 6 (Product 4). Each of these four nodes (products) represents a state in S2, and the maximum value from these four cutting alternatives will be considered the best solution at that stage as per eq.12.

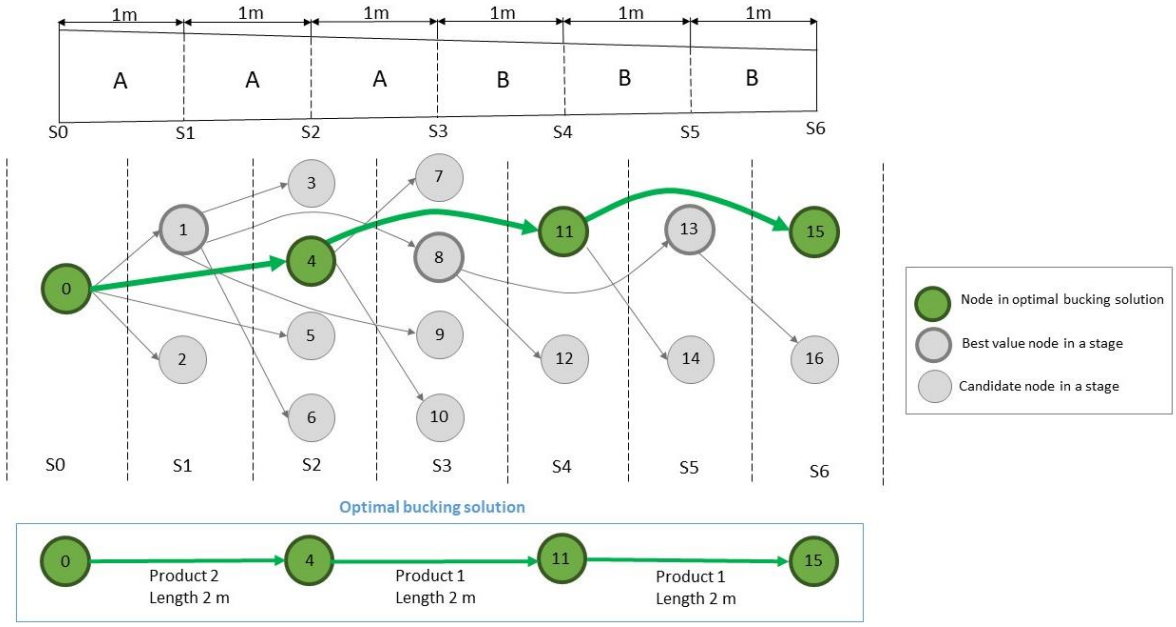

Figure 27. Simplified stem bucking example with the description of stages (S0 to S6) and nodes (states)

Thus, for example, the four equations to be evaluated at stage 2 are as follows eq. 13-16:

$$f_2(X_2 = 3) = \{[f_1(X_1 = 1) + V(X_1 = 1, X_2 = 3)]\} \quad \text{eq. 13}$$

$$f_2(X_2 = 6) = \{[f_1(X_1 = 1) + V(X_1 = 1, X_2 = 6)]\} \quad \text{eq. 14}$$

$$f_2(X_2 = 4) = \{[f_0(X_0 = 0) + V(X_0 = 0, X_2 = 4)]\} \quad \text{eq. 15}$$

$$f_2(X_2 = 5) = \{[f_0(X_0 = 0) + V(X_0 = 0, X_2 = 5)]\} \quad \text{eq. 16}$$

From the four equations, the one with the maximum value for $f_2(X_2)$ will determine the best decision (potential products to be cut) at stage 2. The same procedure must be carried out for the rest of the stages. Notice that under this modelling approach, only one node represents the best solution at each stage (best value nodes in Figure 27). In case there is a 'tie' in value between one or more nodes, some criteria need to be established to determine which is to be considered the maximum value node. Thus, only the arcs that come from best value nodes must be assessed at each stage. In the example, the best value nodes are node 0 (S0), node 1 (S1), node 4 (S2) node 8 (S3), node 11 (S4), node 13 (S5), and node 15 (S6). Also, some arcs between nodes are not feasible since they are associated with logs that do not meet the specifications of a certain product (i.e., quality or *SED*). Like in the case of arcs coming from non-best value nodes, these arcs are also not assessed.

The optimal bucking solution for the whole stem is constructed by connecting the best value nodes, starting from the final stage. In the example, starting from S6, the optimal solution is given by Product 1 of 2 m (arc connecting nodes 15 and 11), a second Product 1 of 2 m (arc connecting nodes 11 and 4) and a Product 2 of 2 m (arc connecting nodes 4 and 0). The optimal solution only includes best value nodes. However, a best value node may not always be part of the optimal bucking solution, as is the case with nodes 1, 8, and 13 in Figure 27.

4.2.4.4 Implementation of the bucking algorithm

The bucking algorithm used in this study corresponds to a variant of the DP algorithm presented in Pnevmaticos and Mann (1972) and Acuna and Murphy (2005) which uses recursive equations to guide the optimization, as described in the previous section.

In the present study, the DP bucking algorithm was programmed in Python language and implemented with a graphical interface using the PyQt5 library. For each type of timber product the system returns the total value, volume, number of logs, as well as average diameters and lengths. It also calculates the total volume and value resulting from the optimal bucking of single or multiple stems. Figure 28 shows a flow diagram of the steps of the programming and implementing of the algorithm for the bucking of a single stem. These steps are summarised below:

0) After importing the product specification and market files, all the variables that are used in the algorithm are initialized. These include the number of log types, log lengths per log type, number of segments, and length of each segment (i.e., 10 cm). A segment is equivalent to a section as presented in the practical example in 2.4.3. Also, the temporary stage (variable *TS* in Figure 28) is initially set to 0 (the base of the tree).

1) Starting from the base of the tree, a log of the first product is assessed. Also, a new *TS* is calculated by adding the current temporary length and the length of the log being assessed. Since some log types accept more than one valid length, these lengths and their corresponding *TS*s are evaluated one by one. At a specific *TS*, there could be more than one product and length, and these correspond to the nodes in the DP terminology.

2) If the *TS* calculated in (1) exceeds the commercial height of the stem, a log of the next product is assessed; otherwise, the process moves to Step (3).

3) The *SED* and curvature of the log being assessed are checked. In the procedure, for each individual log that can potentially be cut, the reference for the sagitta is taken from the straight line segment connecting the centers of the end sections (Prendes et al., 2022). The sagitta of each section is then calculated as the distance between the center of the section and the straight line segment. Subsequently, the maximum sagitta is identified and compared to the maximum allowable curvature.

4) The value (*VAL*) of the log being assessed at the current *TS* is calculated using the recursive equation presented in 4.2.4.3. If *VAL* is higher than the current best value (*BVAL*) at that *TS*, *BVAL* and best log are updated; otherwise, the process moves to Step (5).

5) If there are still valid lengths for the log being assessed, a new valid length is assessed starting from Step (1); otherwise, the process moves to Step (6).

6) If there still log types to be assessed, a new log type and its corresponding valid lengths are assessed starting from Step (1); otherwise, the process moves to Step (7).

7) If the current segment exceeds the number of stem segments, the algorithm stops; otherwise, the procedure is repeated for the next segment commencing from Step (1).

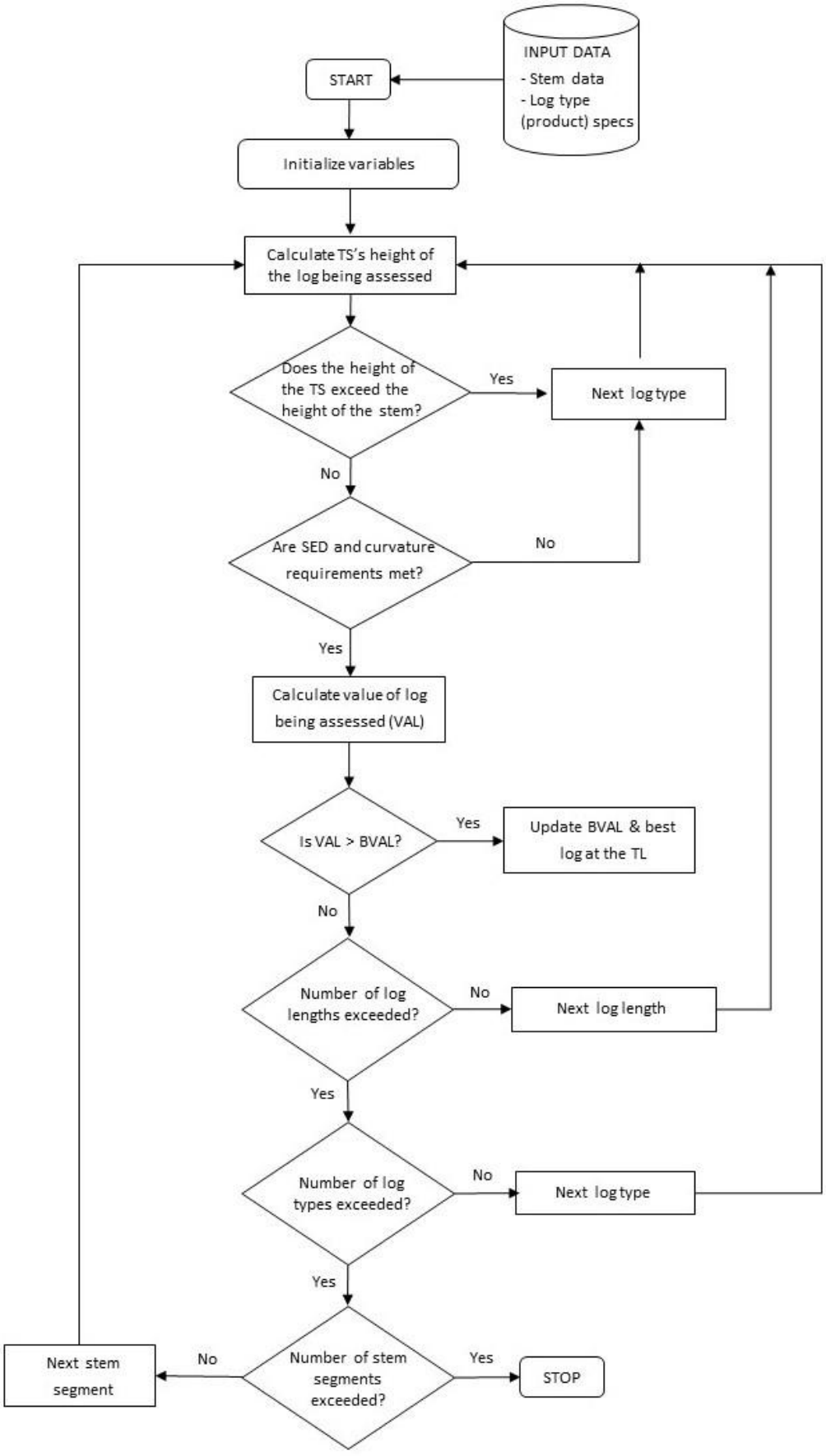

Figure 28. Flow diagram of the DP bucking algorithm implemented in the study.

4.2.4.5 Log types (timber products) incorporated in the optimal bucking algorithm

The optimal bucking algorithm included some of the most common log types produced in Asturias (Spain) for *Pinus radiata* trees as input. Their characteristics are shown in Table 7. The specifications of the log types and prices were obtained from the "Observatory of forest products prices" report, which was prepared by COSE (Confederation of Forestry Organizations of Spain) as part of the RedFor project (García-Márquez, 2014). As for the log type Fibre (pulpwood), this is not a very common product for *Pinus radiata* in Asturias. However, it was included in the study since it represents a potential future commercial opportunity for Asturias and other provinces in northern Spain (ASPAPEL, 2021). The price of this log type was estimated based on personal communications with local sawmill managers and the authors' own knowledge. All the stem wood that could not be included in any of the five log types was considered waste, with an economic value equal to 0.

Table 7. Market log specifications for Pinus radiata logs in Asturias

Log-type	Min *SED* (cm)	Valid lengths (m)	Max curvature* (cm)	Price (€/m^3)
Veneer	28.0	2.5/3.0	5.0	60.0
Saw log 1	25.0	2.5/3.0/5.0/6.0	2.0	50.0
Saw log 2	22.0	2.5/3.0/5.0	3.0	45.0
Saw log 3	20.0	2.5/3.0	3.0	40.0
Fibre	6.0	Variable length between 2.5-5.0 m in multiples of 10 cm	0.0	25.0
Waste		NA	NA	0.0

4.2.4.6 Datasets analysed and compared

Three stem input data sets were used to feed the bucking algorithm. One was generated using a taper model (dataset A), and two were obtained from a point cloud acquired from TLS, one where curvature was excluded, the other where it was included (datasets B and C, respectively).

1. Dataset A: the diameters of each stem were estimated every 10 cm using the taper model presented in section 4.2.2.1 (Figure 29A). For this data set, trees were assumed to be completely straight

2. Dataset B: the diameters of each stem were estimated every 10 cm from the TLS point cloud as explained in section 4.2.2.2 (Figure 29B). Due to the low definition of the stem contour in areas near the crown, the diameters were completed using estimates provided by the taper equation above 10 m. For this data set, trees were also assumed to be completely straight. This dataset resembles the measurement of trees on the ground after they are felled, where diameters but not shape measurements are recorded, and it also represents the simplest input data which can be obtained with TLS, that is, diameters.

3. Dataset C: This data set is similar to dataset B, but with the addition of the coordinates of the center (XYZ) for each stem section/diameter (Figure 29C). This new parameter enabled the inclusion of a maximum curvature constraint (Table 7) for each log type in the bucking algorithm, so the trees/logs here are not considered to be straight.

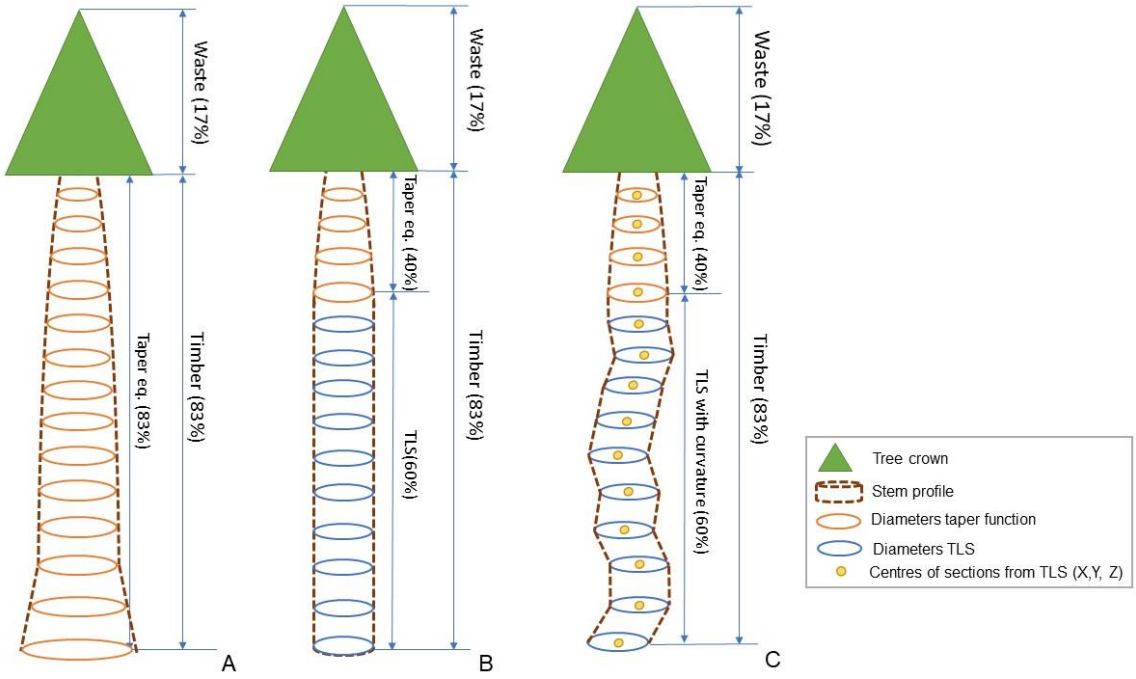

Figure 29. Profile of the trees for datasets A, B, C used to feed the optimal bucking algorithm

4.3.2.6 Comparing the optimal bucking results from the three datasets

Diameters along the stem are one of the critical parameters in the optimal bucking algorithm. Consequently, differences in diameter between the TLS point cloud (hereafter d_{TLS}) and the taper model (d_{taper}) were assessed in terms of (i) a PDF (Probability Density Function) of the differences between $d_{TLS} - d_{taper}$ (ii) a double line plot representing average diameter value per stem section obtained through the taper model and from TLS. It is worth mentioning that the PDF is used to specify the probability of the random variable (in this case, the difference in diameter) falling within a particular range of values.

After completing the runs of the optimal bucking algorithm on datasets A, B and C, the results were compared in terms of number of logs, length of the logs, total volume, and total merchantable value. This comparison provided insights into the impact of using different techniques of estimating diameters along the stem, especially when including curvature constraints. Special attention was paid to the *LED* and *SED* of each log type (the difference between them being related to taper) and the curvature value in the case of dataset C. The analysis was performed by conducting a Tukey-Kramer test (Seidel et al. 2021; Tukey,1949) that compared the differences of the individual means from the *LED* and *SED* for each log type and identified any significant differences among the three datasets.

Finally, all the logs of one type within the same tree were added in order to have one value per log type and tree. Subsequently, a PDF for the volume and value per tree and dataset type was calculated for each of the 120 trees within the study plot. This also allowed comparisons by log type and dataset.

4.3. RESULTS

4.3.1 Difference in diameter estimated with the taper model and the TLS

The PDF curve for the difference between d_{TLS} and d_{taper} is shown in Figure 30. The curve has a normal distribution and reveals minor differences in diameter measurements using the two systems, with most of the differences ranging between -0.05 and +0.05 m. In percentage terms, 43.5% of the sections presented a diameter difference below or equal to 1 cm. That percentage increased to 72.5 % for differences below or equal to 2 cm and 87% for differences lower than or equal to 3 cm. The *RMSE* was 2.68 cm.

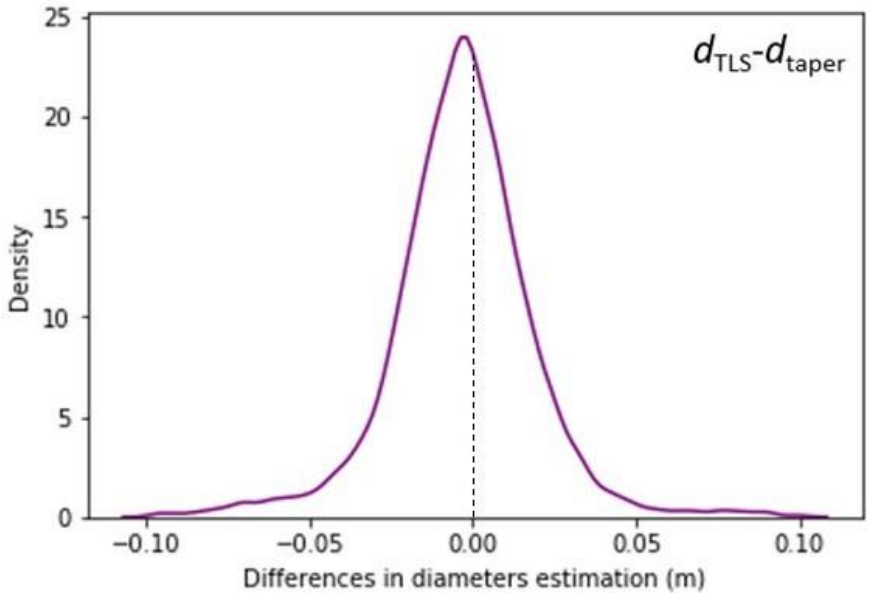

Figure 30. PDF for the difference between diameters estimated using TLS and taper model

The curves in Figure 31 show the average diameter value per section obtained using the taper model (yellow) and TLS (blue). At first glance, it is evident that the curve for the TLS diameters is smoother than in the case of the taper model. Unlike the taper model (yellow) curve, the small peaks of the blue line indicate that as the height increases, diameter does not in fact decrease in a constant manner, and indeed they sometimes increase in comparison to the previous data point.

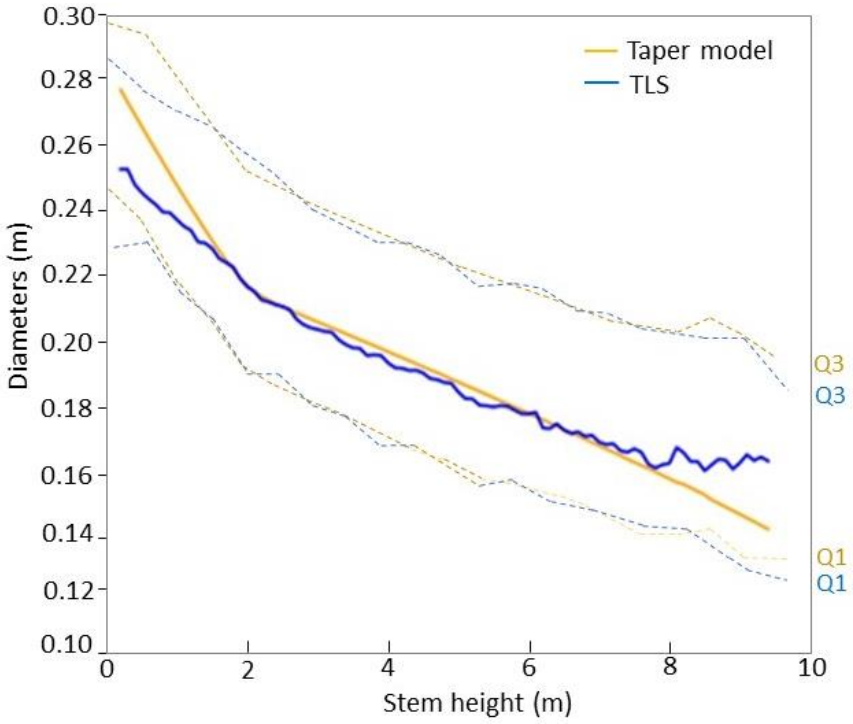

Figure 31. Line plot representing average diameter value per section obtained using the taper model (yellow) and TLS (blue). Q1 and Q3 refer to the dotted lines which represent Quartile 1 and 3 respectively for the taper model (yellow) and TLS (blue)

Compared to the TLS curve, the taper model tends to overestimate diameters in the bottom sections of the stem (between 0-1.8 m) and underestimate diameters in the upper sections of the stem (6 -10 m). As for the rest of the stem (1.9–5.9 m), the differences are quite low, with diameters estimated by the taper model being very close to those obtained with TLS.

4.3.2 Optimal economic value and volume estimated for each dataset

The optimal bucking algorithm only considered those sections with a diameter greater than 6 cm; below that they were considered waste. Regarding the results of the bucking algorithm, on average, 17% and 83% of the stem length corresponded, respectively, to waste and commercial timber. In the case of datasets B and C, not all diameters along the stem were obtained from the TLS point cloud due to the low definition of the stem contour in areas near the crown (see 4.2.4.6). On average, 40% of all diameters in B and C were estimated with the taper model (upper sections of the stems), while the remaining 60% of the stem diameters were calculated from the TLS point cloud.

After optimally bucking the 120 trees, the total value amounted to €1467.71, €1467.38, and €1379.14 for datasets A, B, and C, respectively. Table 8 shows the descriptive statistics of volume and value per tree for the three datasets (i.e., excluding waste). According to the results, both value and volume per tree were greater for dataset A than for datasets B and C. As expected, dataset C gave the lowest value and volume per tree due to the additional curvature constraint included in this scenario.

Table 8. Descriptive statistics of volume and value per tree from the three datasets evaluated A) Taper model B) TLS and C) TLS + curvature

Dataset	Volume (m^3/tree)					Value (€/tree)				
	Mean	Median	Dev	Min	Max	Mean	Median	Dev	Min	Max
A	0.364	0.331	0.174	0.058	0.916	12.23	9.86	8.73	1.33	44.27
B	0.351	0.314	0.164	0.059	0.907	12.22	9.60	8.20	1.33	44.27
C	0.346	0.314	0.162	0.059	0.907	11.49	9.44	7.71	1.33	44.27

4.3.2.1 Optimal bucking by log type

Table 9 summarizes the average values of the main attributes of each log type in datasets A, B and C. Specifically, it contains: the average log *SED* and *LED*, the difference between their values (*LED-SED*), their position in the stem with respect to the ground (Z_{SED}, Z_{LED}), and log length. For dataset C, the mean curvature and its range (in cm) are also shown.

Table 9. Average values of log attributes in datasets A, B, C

Dataset		Veneer	Saw log 1	Saw log 2	Saw log 3	Fibre
A	***LED* (cm)**	38.2	33.1	28.8	25.0	16.8
	***SED* (cm)**	29.1	26.0	23.1	20.5	12.1
	***LED-SED* (cm)**	9.1	7.1	5.7	4.5	4.7
	Z_{SED}	3.9	4.1	4.7	5.7	10.7
	Z_{LED}	0.6	1.2	1.9	2.9	7.1
	Length (cm)	3.34	3.34	3.36	3.35	3.35
B	***LED* (cm)**	29.4	27.8	26.1	23.2	16.2
	***SED* (cm)**	29.2	26.2	22.9	20.6	11.3
	***LED-SED* (cm)**	0.2	1.6	3.2	2.6	4.9
	Z_{SED}	3.9	4.6	5.1	5.7	11.3
	Z_{LED}	0.7	1.8	2.3	3.1	7.7
	Length	2.5	3.08	3.08	3.11	3.15
C	***LED* (cm)**	29.2	27.0	26.3	23.1	16.7
	***SED* (cm)**	29.1	26.0	23.3	20.6	11.9
	***LED-SED* (cm)**	0.1	1	3	2.5	4.8
	Z_{SED}	4.0	5.3	4.9	5.4	10.9
	Z_{LED}	1.1	2.7	2.2	2.8	7.2
	Length	3.13	2.95	3.12	3.15	3.16
	Curvature (cm)	3.20[0-14.2]	1.38 [0-1.8]	2.26 [0-3.0]	2.08 [0-3.0]	2.09 [0-12.3]

The difference between *SED* and *LED* can be considered a proxy of the taper/conicity of the different log types. In comparison to datasets B and C, larger differences between *SED* and *LED* were obtained in dataset A for all log types except for the log type Fibre (pulpwood). The most significant differences in dataset A were observed for the two most valuable log types (Saw log 1 and Veneer) since these products are mostly cut from the bottom sections of the stem (see Z_{SED} and Z_{LED} values). For a significance level of $\alpha = 0.05$, the Tukey test showed statistically significant differences in *SED* and *LED* between datasets A and B and between datasets A and C, but not between datasets B and C. In the case of the log type Fibre, there were no significant differences between any dataset because most logs are obtained from the upper parts of the stem, where diameters are the same irrespective of the dataset. For the 120 trees within the study plot, the results obtained after running the bucking algorithm on datasets A, B and C are presented in Figures 32 and 33.

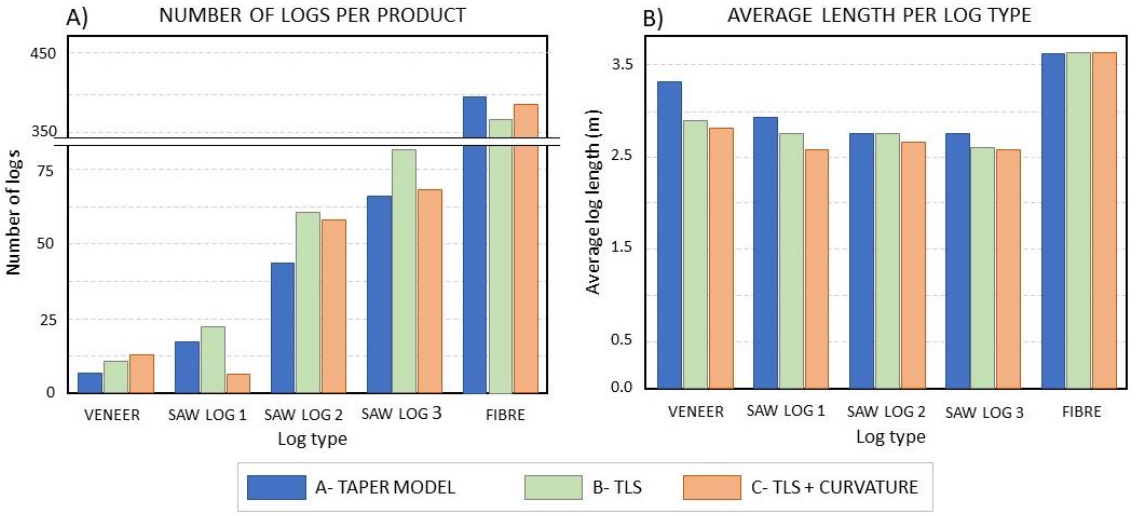

Figure 32. A) Number of logs per product obtained for datasets A, B and C. B) Average length per log type (m). Note the double horizontal line represents a break in the vertical scale to make the figure easier to understand.

Figure 32A compares the number of logs obtained for each product. The numerical results were as follows:

- Dataset A: 534 logs in total (Veneer: 6; Saw log 1: 18; Saw log 2: 45; Saw log 3: 67; Fibre:398)
- Dataset B: 546 logs in total (Veneer: 12; Saw log 1: 21; Saw log 2: 62; Saw log 3: 84; Fibre:367)
- Dataset C: 536 logs in total (Veneer: 14; Saw log 1: 6; Saw log 2: 61; Saw log 3: 69; Fibre: 386).

Regarding the average length of the logs (Figure 32B), the longest logs were obtained for dataset A, followed by datasets B and C, irrespective of the log type. In the case of the log type Fibre, the length of the logs was almost the same in the three datasets.

Similarly, Figure 33A compares the total volume by log type obtained in each dataset. When all the products were included, the total volume obtained for datasets A, B, and C were, respectively, 43.2, 41.2, and 40.7 m^3. Regardless of the dataset used, most of the volume was related to the log type Fibre, followed by the log types Saw log 2 and Saw log 3. The volume of log type Fibre was more than three times larger than that of log types Saw log 2 and Saw log 3, and more than seven times larger than that of log types Saw log 1 and Veneer. The same trend was observed when quantifying the total value by log type (Figure 33B). In this case, the total value of log type Fibre was about twice as much as that of log types Saw log 2 and Saw log 3 and about six times greater than that of log types Saw log 1 and Veneer.

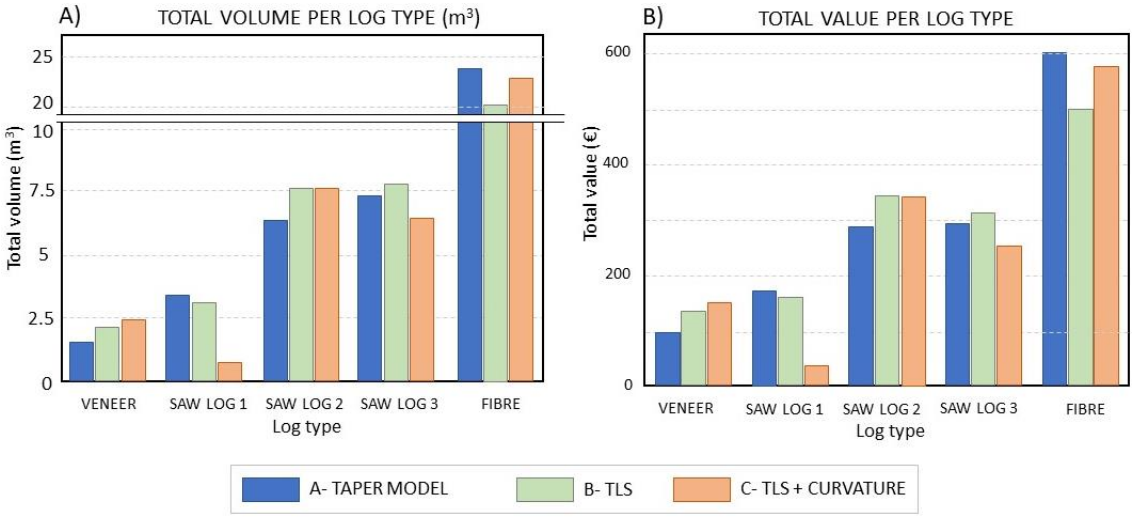

Figure 33. A) Total volume per log type obtained for datasets A, B and C. B) Total value per log type in euros. Note the double horizontal line represents a break in the vertical scale to make the figure easier to understand

As can be seen in Figures 32A and 32B, except for the log type Fibre, more logs were obtained for dataset B than for dataset A. Likewise, except for log types Saw log 1 and Fibre, the volume and value were greater for dataset B than for dataset A. In the case of log type Saw log 1, the increased number of logs in the dataset B did not result in a greater volume or value than in dataset A since the logs of this type in the former dataset were shorter and had smaller diameters. In the case of dataset C, both the total value and volume were lower than in datasets A and B. As expected, the inclusion of a curvature restriction in the bucking algorithm resulted in a reduced volume and value of log types Saw log 1, Saw log 2, and Saw log 3 in comparison to datasets A and B. However, in contrast to dataset B, it also resulted in more logs and a greater volume and value for log types Veneer and Fibre, which had the least stringent curvature constraints.

Figure 34 shows the distribution of the PDFs of volume and value by log type and dataset. The peaks in the PDF curves indicates the most frequent value. Overall, the volume and value in each dataset follow a very similar distribution with a peak (or two in the case of dataset A) and some overlap between curves. The overlap between curves of different categories (log types) is more evident for volume than for value, and it is more pronounced in the case of dataset C. In contrast, dataset A has less overlap, which is reflected in a wider range of values across the log volume and log value spectrum. This is particularly true in the case of the log type Veneer and to a lower extent in the case of the log type Saw log 1. These are the two most valuable products, and also those with a greater variation in their distributions among the datasets.

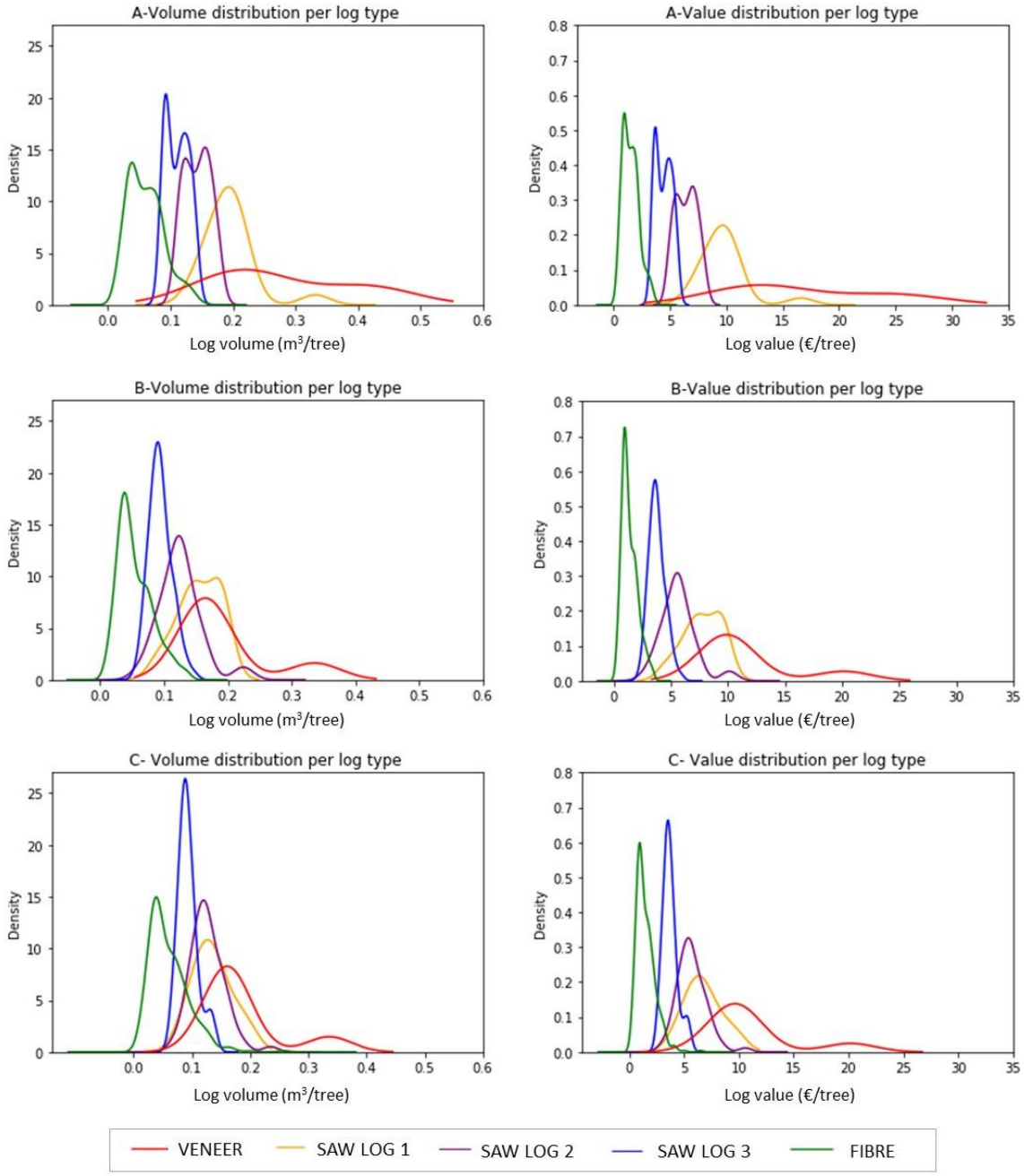

Figure 34. PDF distribution of volume (left side) and value (right side) by log type in the three datasets evaluated

4.4 DISCUSSION

This study presents a methodology for the optimal bucking of stems based on TLS data. Designed as a procedural workflow, it automatically estimates the external variables needed for stem bucking (i.e., diameters and curvature of the logs) and implements a DP-based optimal bucking algorithm.

The bucking results obtained for dataset C, which comprised TLS data and log curvature, were compared with the those obtained for data estimated from a taper model (dataset A) and data collected with a TLS but that excluded log curvature from the bucking algorithm (dataset B). The total value was practically the same for datasets A and B, and it declined slightly (6%) for dataset C. However, the number of logs, their length, and total value and volume associated with each product presented differences between the three datasets. The origin of these differences lies

fundamentally in: (i) the values of the diameters that feed the bucking algorithm and (ii) the consideration or not of the curvature constraint in the bucking algorithm.

Regarding stem diameters, differences between the taper equation and TLS were minor, with an *RMSE* of only 2.68 cm. However, the distribution of the differences along the stem was not homogeneous. In comparison to TLS, on average, the taper equation overestimated diameters in the bottom parts of the stem and underestimated them in the top parts. This is explained because the taper equation used in this study (Canga et al. 2008) is a mathematical model which likens the stem to a cone frustum for all the trees within the plot and therefore, it does not reflect in detail the variability of their morphology (see Figure 29A). Conversely, in the case of TLS, the point cloud is a three-dimensional representation of the trees within the plot obtained from their direct measurement without intermediate models or assumptions (Gollob, Ritter, and Nothdurft 2020). As confirmed by previous studies such as (Hollaus, Mokroš, and Wang 2019; Liang et al. 2016), the diameters obtained with TLS are more reliable and realistic than those estimated by a taper equation. In addition, our methodology includes the section centers, which is a big development compared with other studies that only report the diameters (Heinzel and Huber 2017; Oveland et al. 2017; Pitkänen, Raumonen, and Kangas 2019b). Knowing the XYZ coordinates of the section centers provides valuable information on the curvature of the stem, which represents a key parameter in bucking algorithms that facilitate improved cutting decisions.

In the specific case of the study plot, the better definition of diameters along the stem provided by TLS allows the algorithm to identify a larger number of logs, but which are shorter, in dataset B than in dataset A, except for log type Fibre. Particularly at the base of the tree, the larger diameters estimated by the taper model (dataset A) lead to a greater proportion of longer logs for the most valuable log types: Saw log 1 and Veneer (see Table 9, dataset A). In dataset A, the algorithm also maximized value by cutting longer logs in all the product categories, and more logs in the Fibre category since this product is the least restrictive regarding minimum *SED.*

The inclusion of a curvature constraint in dataset C notably affected the results, leading to a substantial reduction in the number of log types that involve greater curvature restriction. This is exemplified by the reduced number of Saw log 1 logs (max. curvature < 2cm) in dataset C compared to dataset B, while the number of the less restrictive log types (Fibre and Veneer) is higher. Because of the more restrictive curvature constraint associated with all saw log types, the bucking algorithm maximises each tree's value by cutting more logs in the Fibre and Veneer categories, and shorter logs in all the saw log categories.

The wood volume in a product category is closely related to the number and diameter of logs in that category and, to a lesser extent, to length. When the volume and value distribution are assessed by log type (see Figure 33), minor differences in diameters result in notable differences in the proportions of the different products. Using taper equations (dataset A), the range of value and volume is slightly greater than in the other two datasets, and logs of more volume and value are reported due to the volume overestimation in the bottom sections of the stem. The latter also has implications for other products, such as Veneer, which shows a higher volume and value than in the datasets using TLS data (B and C). The inclusion of the curvature constraint (dataset C) reduces the volume and value of the most restrictive log type (Saw log 1), which shows an overlap with Saw log 2 in the distribution curve (see Figure 34). However, on the plus side, logs that would be cut as Saw log 2 using datasets A and B are cut as Saw log 1 in dataset C as they meet the curvature constraint, which results in an increased total value. Several authors (Liang et al. 2018; Malinen et al. 2007) have pointed out that log shape is a critical factor that

significantly conditions the use timber is put to as well as its processing. More specifically, the bucking optimization of logs requires the accurate determination of curvature that allows the cutting points along the stem and the commercial volume to be determined according to particular specifications (Erber et al. 2021). Thus, including curvature restrictions in the bucking algorithm contributes to obtaining a more realistic total value that is not overestimated (Rummukainen et al. 2021).

Despite the important benefits discussed, the empirical results reported here should be considered in light of certain limitations. Firstly, the optimal bucking algorithm was tested in a single plot consisting primarily of young homogeneous trees, which resulted in a low number of high-value log types. A better understanding of the performance of bucking algorithms will require that our methodology is tested in a wider range of forest conditions. This should include different species and forest management regimes, with trees of various sizes (i.e., height and diameter) and quality features (i.e., tree form and branchiness). Secondly, tree defects such as heavy branches or multiple stems were not included in the bucking algorithm. Future studies should include these tree quality parameters, since they represent a critical aspect to consider in optimal bucking procedures because of their impact on the value of timber assortments and volume recovery (Malinen et al. 2007; Marenče et al. 2020).

CHAPTER 5:

FINAL CONCLUSIONS

CHAPTER 5: CONCLUSIONS

5.1 CONCLUSIONS (IN ENGLISH)

In this PhD thesis three algorithms based on TLS point clouds for use in precision forestry inventories were developed. They cover key issues in forestry, namely: volume equation parametrization, stem shape variables assessment and optimal bucking. They also share some common characteristics which favour their use in forest inventory and planning tasks: (1) they aim to be applicable to any terrestrial point cloud, irrespective of the sensor used to acquire the data; (2) they are applicable to any species; (3) they are scalable, so can be applied to a single tree, a plot or a whole forest; and (4) they are written in Python programming language, a widespread open-source language, which facilitates their use by multiple users.

The algorithms presented here allow the construction of extremely accurate 3D single tree models. As a result, the variables needed for precision forestry inventories are obtained automatically and without the intervention of an operator, thus avoiding the subjectivity associated with traditional measurement techniques. The diameter of the stem and center coordinates (XYZ) of any section along the stem are calculated automatically from TLS measurements. The only limitation is the impossibility of obtaining diameter measurements for the top part of trees because of laser range (in the case of tall trees) and/or a very leafy crown. What is more, the total height of the tree can be measured with an acceptable error range.

Of the variables estimated from TLS data with the algorithms developed, two in particular, diameter along the stem and height, are the main inputs for parametrizing volume equations. Consequently, the availability of accurate diameters strongly influences both the type of merchantable volume equation that can be fitted and the degree of uncertainty in their estimation. The algorithm specifically developed to estimate these two variables issues a warning when uncertainty in the calculation of a diameter is high. As expected, the manual review of flagged sections for review or elimination improved the volume estimation, although the results obtained with the fully automatic approach are still suitable for parametrizing equations when a high degree of accuracy in the merchantable volume estimation is not necessary. The proposed methodology and the algorithm developed to implement it are robust to errors in estimating the centers of the sections, which, together with diameters along the stem, constitutes the basis for estimating two variables that characterize the shape of the tree: straightness and lean. The estimated values of these two variables provided by our approach clearly outperform those obtained by means of classical field techniques, to the point of opening a door to the integration of shape variables in standard forest inventories

Finally, making available accurate estimations of variables that describe stems in detail in terms of diameter, height and shape has great applicability in the optimal bucking of stems, and is a big step forward compared with existing methodologies such as taper models. The low capacity of traditional methodologies to reflect variability in morphological characteristics at the individual tree level suggests that their use should be restricted to situations where TLS data are not accessible, and/or to estimate diameters in the upper sections of trees when point cloud data is not available. The results of the study constitute a starting point towards automatic optimal bucking in standing trees in an operational environment, which is of great interest in forestry organizations.

In general terms, the algorithms presented in this PhD have shown very promising results and demonstrate the convenience of using laser scanner point cloud-based models over traditional

field methods for forest inventory in terms of speed of data collection, data volume, accuracy and reliability of the estimated variables.

Future lines of work

The algorithms developed in this work have been tested in single plots of species of the *Pinus* genus, so the systematic investigation of larger test sites with different scanning techniques, forest species and conditions is desirable. In addition to this, in the case of the optimal bucking algorithm, future work should consider parameters connected to the quality of wood such as branchiness or presence of knots in the wood.

Finally, testing the algorithms' performance in other types of terrestrial point clouds such as photogrammetric and/or mobile laser scanner point clouds would also be advisable.

5.5 CONCLUSIONES (EN ESPAÑOL)

En esta tesis doctoral se desarrollaron tres algoritmos basados en nubes de puntos TLS para su uso en inventarios forestales de precisión. Todos ellos se centran en asuntos claves de la ciencia forestal , como son: la parametrización de ecuaciones de volumen, la estimación de variables de forma del tronco y el tronzado óptimo de los fustes. También comparten algunas características comunes que favorecen su uso en tareas de inventario y planificación forestal: (1) pretenden ser aplicables a cualquier nube de puntos terrestre, independientemente del sensor utilizado para adquirir los datos; (2) son aplicables a cualquier especie; (3) son escalables, por lo que se pueden aplicar a un solo árbol, una parcela o un bosque completo; y (4) están escritos en lenguaje de programación Python, un lenguaje de código abierto muy extendido, lo que facilita su uso por parte de usuarios con diferentes perfiles.

Los algoritmos presentados en esta tesis, permiten la creación de modelos 3D de árbol individual extremadamente detallados Como resultado, las variables necesarias para los inventarios forestales de precisión se obtienen de forma automática y sin la intervención de un operador, evitando así la subjetividad asociada a las técnicas de medición tradicionales. El diámetro del fuste y las coordenadas del centro (XYZ) de cualquier sección a lo largo del mismo se calculan automáticamente a partir de las mediciones realizadas con el TLS. La única limitación es la imposibilidad de obtener medidas de diámetros en la parte superior de los árboles debido al rango de alcance del láser (que es insuficiente en el caso de árboles altos) y/o la existencia de una copa muy frondosa. Además, la altura total del árbol se puede medir con un margen de error aceptable.

De las variables estimadas a partir de los datos TLS con los algoritmos desarrollados, dos en particular, el diámetro a lo largo del fuste y la altura, son las principales entradas para parametrizar las ecuaciones de volumen. En consecuencia, la disponibilidad de diámetros precisos influye fuertemente tanto en el tipo de ecuación de volumen comercial que se puede ajustar como en el grado de incertidumbre en su estimación. El algoritmo desarrollado específicamente para estimar estas dos variables dispone de un sistema para etiquetar aquellas secciones donde la incertidumbre en el cálculo del diámetro es alta. Como era de esperar, la revisión manual de las secciones marcadas para su revisión o eliminación mejoró la estimación del volumen, aunque los resultados obtenidos con el enfoque completamente automático siguen siendo adecuados para parametrizar ecuaciones cuando no es necesario un alto grado de precisión en la estimación del volumen comercial. La metodología propuesta y el algoritmo desarrollado para implementar dicha metodología son robustos a los errores en la estimación de los centros de las secciones, lo que, junto con los diámetros a lo largo del fuste, constituye la base para estimar dos variables que caracterizan la forma del árbol: la rectitud y la inclinación. Los valores estimados de estas dos variables proporcionados por nuestro enfoque superan claramente a los obtenidos mediante técnicas de medición clásicas, hasta el punto de abrir un camino hacia la integración de la medición de variables de forma en los inventarios forestales estándar.

Finalmente, el hecho de disponer de estimaciones precisas de variables que describen los fustes en detalle en términos de diámetro, altura y forma tiene una gran aplicabilidad en el tronzado óptimo de los fustes y es un gran paso adelante en comparación con las metodologías existentes, como las funciones de perfil. La baja capacidad de las metodologías tradicionales para reflejar la variabilidad en las características morfológicas a nivel de árbol individual sugiere que su uso debería restringirse a situaciones en las que los datos TLS no son accesibles y/o a la estimación de diámetros en las secciones superiores de los fustes cuando no hay nubes de puntos

disponibles. Los resultados del estudio constituyen un punto de partida hacia la implementación del tronzado óptimo automático en árboles en pie en un entorno operativo, que es de gran interés para las organizaciones forestales.

En términos generales, los algoritmos presentados en esta tesis doctoral han mostrado resultados muy prometedores y demuestran la conveniencia de usar modelos basados en nubes de puntos de escáner láser sobre los métodos de campo tradicionales para el inventario forestal en términos de velocidad de recopilación de datos, volumen de datos, precisión y fiabilidad de las variables estimadas.

Líneas futuras de trabajo

Los algoritmos desarrollados en este trabajo se han evaluado en parcelas individuales compuestas por especies del género *Pinus*, por lo que sería deseable la investigación sistemática en parcelas más grandes con diferentes técnicas de toma de datos, especies y condiciones forestales. Además de lo anterior, en el caso del algoritmo de tronzado óptimo, el trabajo futuro debería considerar parámetros como la ramificación de los fustes o la presencia de nudos puesto que están muy relacionados con la calidad de la madera.

Finalmente, también sería recomendable evaluar el comportamiento de los algoritmos en otro tipo de nubes de puntos terrestres, como las nubes fotogramétricas y/o las procedentes de escáneres láser móviles.

BIBLIOGRAPHIC REFERENCES

Acuna, Mauricio A., and Glen E. Murphy. 2005. “Optimal Bucking of Douglas Fir Taking into Consideration External Properties and Wood Density.” *New Zealand Journal of Forestry Science* 35 (2): 139–152.

Alberdi, Iciar, Isabel Cañellas, and Roberto Vallejo Bombín. 2017. “The Spanish National Forest Inventory: History, Development, Challenges and Perspectives.” *Pesquisa Florestal Brasileira* 37 (91): 361–368.

Alegria, Cristina, and Margarida Tomé. 2011. “A Set of Models for Individual Tree Merchantable Volume Prediction for Pinus Pinaster Aiton in Central Inland of Portugal.” *European Journal of Forest Research* 130 (5). Springer: 871–879.

Álvarez González, Juan Gabriel, Klaus von Gadow, and Pedro Real Hermosilla. 2001. “Modelización Del Crecimiento y La Evolución de Bosques.” IUFRO.

Alia, Ricardo and Juan Majada. 2013. “Phenotyping for the Future and the Future of Phenotyping.” *Novel Tree Breeding*. PublINIA Madrid, Spain, 53e62.

Andersen, Hans-Erik, Robert J. McGaughey, and Stephen E. Reutebuch. 2005. “Estimating Forest Canopy Fuel Parameters Using LIDAR Data.” *Remote Sensing of Environment* 94 (4): 441–449.

Apostol, Bogdan, Serban Chivulescu, Albert Ciceu, Marius Petrila, Ionut-Silviu Pascu, Ecaterina Nicoleta Apostol, Stefan Leca, Adrian Lorent, Mihai Tanase, and Ovidiu Badea. 2018. “Data Collection Methods for Forest Inventory: A Comparison between an Integrated Conventional Equipment and Terrestrial Laser Scanning.” *Annals of Forest Research* 61 (2): 189–202.

Apostol, Bogdan, Marius Petrila, Adrian Lorenţ, Albert Ciceu, Vladimir Gancz, and Ovidiu Badea. 2020. “Species Discrimination and Individual Tree Detection for Predicting Main Dendrometric Characteristics in Mixed Temperate Forests by Use of Airborne Laser Scanning and Ultra-High-Resolution Imagery.” *Science of The Total Environment* 698. Elsevier: 134074.

Aubry-Kientz, Mélaine, Raphaël Dutrieux, Antonio Ferraz, Sassan Saatchi, Hamid Hamraz, Jonathan Williams, David Coomes, Alexandre Piboule, and Grégoire Vincent. 2019. “A Comparative Assessment of the Performance of Individual Tree Crowns Delineation Algorithms from ALS Data in Tropical Forests.” *Remote Sensing* 11 (9). MDPI: 1086.

Akay, Abdullah Emin. 2017. “Potential Contribution of Optimum Bucking Method to Forest Products Industry.” *European Journal of Forest Engineering* 3 (2): 61–65.

Arce, Julio Eduardo, Patricio MacDonagh, and Ramón Alejandro Friedl. 2004. “Optimal Bucking Pattern Generation through Cutting Algorithms Applied to Individual Stems.” *Revista Árvore* 28 (2). SciELO Brasil: 207–217.

ASPAPEL (Spanish Association of Pulp, Paper and Cardboard Manufacturers). 2021. "Sustainability report: The decarbonised bi-circularity of the paper industry". December 2021 Edition. Available in: http://www.aspapel.es/content/memoria-de-sostenibilidad-del-papel-2021 (Accessed online 4th April 2021)

Atlas Technology. 2010. https://integral.co.nz/cruiser-inventory-assessment/. Rotorua, New Zeland. (Accessed online 25thFebruary 2022)

Bagaram, Martin B., Diego Giuliarelli, Gherardo Chirici, Francesca Giannetti, and Anna Barbati. 2018. “UAV Remote Sensing for Biodiversity Monitoring: Are Forest Canopy Gaps Good Covariates?” *Remote Sensing* 10 (9). MDPI: 1397.

Barker, Martin G., and Michelle A. Pinard. 2001. “Forest Canopy Research: Sampling Problems, and Some Solutions.” In *Tropical Forest Canopies: Ecology and Management*, 23–38. Springer.

Benneter, Adam, David I. Forrester, Olivier Bouriaud, Carsten F. Dormann, and Jürgen Bauhus. 2018. “Tree Species Diversity Does Not Compromise Stem Quality in Major European Forest Types.” *Forest Ecology and Management* 422. Elsevier: 323–337.

Bi, Huiquan, and Yushan Long. 2001. “Flexible Taper Equation for Site-Specific Management of Pinus Radiata in New South Wales, Australia.” *Forest Ecology and Management* 148 (1–3). Elsevier: 79–91.

Birant, Derya, and Alp Kut. 2007. “ST-DBSCAN: An Algorithm for Clustering Spatial–Temporal Data.” *Data & Knowledge Engineering* 60 (1): 208–221.

Bitterlich, Walter. 1984. *The Relascope Idea. Relative Measurements in Forestry.* Commonwealth Agricultural Bureaux.

Boczniewicz, Daniel, Euan G. Mason, and Justin A. Morgenroth. 2022. “Developing Fully Compatible Taper and Volume Equations for All Stem Components of Eucalyptus Globoidea Blakely Trees in New Zealand.” *New Zealand Journal of Forestry Science* 52.

Boschetti, Walter Torezani Neto, Rubens Chaves de Oliveira, Ana Márcia Macedo Ladeira Carvalho, and Maria Fernanda Vieira Rocha. 2017. “The Effect of Reaction Wood on the Properties of Eucalyptus Kraft Pulp–Part II.” *Nordic Pulp & Paper Research Journal* 32 (3). De Gruyter: 428–435.

Boston, Kevin, and Glen Murphy. 2003. “Value Recovery from Two Mechanized Bucking Operations in the Southeastern United States.” *Southern Journal of Applied Forestry* 27 (4). Oxford University Press: 259–263.

Bourgouin, Maurane, Osvaldo Valeria, and Nicole J. Fenton. 2022. “Predictive Mapping of Bryophyte Diversity Associated with Mature Forests Using LiDAR-Derived Indices in a Strongly Managed Landscape.” *Ecological Indicators* 136. Elsevier: 108585.

Boyd, D. S., and F. M. Danson. 2005. “Satellite Remote Sensing of Forest Resources: Three Decades of Research Development.” *Progress in Physical Geography* 29 (1). Sage Publications Sage CA: Thousand Oaks, CA: 1–26.

Breidenbach, Johannes, Aksel Granhus, Gro Hylen, Rune Eriksen, and Rasmus Astrup. 2020. “A Century of National Forest Inventory in Norway–Informing Past, Present, and Future Decisions.” *Forest Ecosystems* 7 (1). Springer: 1–19.

Briggs, David George. 1980. *A Dynamic Programming Approach to Optimizing Stem Conversion*. University of Washington.

Brolly, Gábor, Géza Király, Matti Lehtomäki, and Xinlian Liang. 2021. “Voxel-Based Automatic Tree Detection and Parameter Retrieval from Terrestrial Laser Scans for Plot-Wise Forest Inventory.” *Remote Sensing* 13 (4). Multidisciplinary Digital Publishing Institute: 542.

Bufton, Jack L. 1989. “Laser Altimetry Measurements from Aircraft and Spacecraft.” *Proceedings of the IEEE* 77 (3). IEEE: 463–477.

Buján, Sandra, Eduardo González-Ferreiro, Fabián Reyes-Bueno, Laura Barreiro-Fernández, Rafael Crecente, and David Miranda. 2012. “Land Use Classification from Lidar Data and Ortho-Images in a Rural Area.” *The Photogrammetric Record* 27 (140): 401–422.

Bukauskas, Aurimas, Paul Mayencourt, Paul Shepherd, Bhavna Sharma, Caitlin Mueller, Pete Walker, and Julie Bregulla. 2019. “Whole Timber Construction: A State of the Art Review.” *Construction and Building Materials* 213. Elsevier: 748–769.

Burkhart, Harold E. 1977. “Cubic-Foot Volume of Loblolly Pine to Any Merchantable Top Limit.” *Southern Journal of Applied Forestry* 1 (2). Oxford University Press: 7–9.

Cabo, Carlos, Antero Kukko, Silverio García-Cortés, Harri Kaartinen, Juha Hyyppä, and Celestino Ordoñez. 2016. “An Algorithm for Automatic Road Asphalt Edge Delineation from Mobile Laser Scanner Data Using the Line Clouds Concept.” *Remote Sensing* 8 (9): 740.

Cabo, Carlos, Celestino Ordóñez, Carlos A. López-Sánchez, and Julia Armesto. 2018a. “Automatic Dendrometry: Tree Detection, Tree Height and Diameter Estimation Using Terrestrial Laser Scanning.” *International Journal of Applied Earth Observation and Geoinformation* 69: 164–174.

Cabo, Carlos, Susana Del Pozo, Pablo Rodríguez-Gonzálvez, Celestino Ordóñez, and Diego González-Aguilera. 2018b. “Comparing Terrestrial Laser Scanning (TLS) and Wearable Laser Scanning (WLS) for Individual Tree Modeling at Plot Level.” *Remote Sensing* 10 (4): 540.

Calders, Kim, Jennifer Adams, John Armston, Harm Bartholomeus, Sebastien Bauwens, Lisa Patrick Bentley, Jerome Chave, F. Mark Danson, Miro Demol, and Mathias Disney. 2020. “Terrestrial Laser Scanning in Forest Ecology: Expanding the Horizon.” *Remote Sensing of Environment* 251. Elsevier: 112102.

Canga, Elena. 2008. "Growth and production of regular *Pinus radiata* d.don pine forests in Asturias". *Dissertation*. University of Oviedo.

Cao, Quang V., Harold E. Burkhart, and Timothy A. Max. 1980. “Evaluation of Two Methods for Cubic-Volume Prediction of Loblolly Pine to Any Merchantable Limit.” *Forest Science* 26 (1). Oxford University Press: 71–80.

Chen, Yunhao, Wei Su, Jing Li, and Zhongping Sun. 2009. “Hierarchical Object Oriented Classification Using Very High Resolution Imagery and LIDAR Data over Urban Areas.” *Advances in Space Research* 43 (7): 1101–1110.

Choudhry, Harsh, and Glen O’Kelly. 2018. “Precision Forestry: A Revolution in the Woods.” *Basic Materials, Paper & Forest Products*.

Clark, Alexander, and Charles E. Thomas. 1984. “Weight Equations for Southern Tree Species: Where We Are and What Is Needed.” USDA Forest Service.

Clutter, Jerome L. 1980. “Development of Taper Functions from Variable-Top Merchantable Volume Equations.” *Forest Science* 26 (1). Oxford University Press: 117–120.

Corbane, Christina, Stefan Lang, Kyle Pipkins, Samuel Alleaume, Michel Deshayes, Virginia Elena García Millán, Thomas Strasser, Jeroen Vanden Borre, Spanhove Toon, and Förster Michael. 2015. “Remote Sensing for Mapping Natural Habitats and Their Conservation Status–New Opportunities and Challenges.” *International Journal of Applied Earth Observation and Geoinformation* 37. Elsevier: 7–16.

Corral-Rivas, José Javier, Ulises Diéguez-Aranda, Sacramento Corral Rivas, and Fernando Castedo Dorado. 2007. “A Merchantable Volume System for Major Pine Species in El Salto, Durango (Mexico).” *Forest Ecology and Management* 238 (1–3): 118–129.

Crecente-Campo, Felipe, Alberto Rojo Alboreca, and Ulises Diéguez-Aranda. 2009. “A Merchantable Volume System for *Pinus Sylvestris* L. in the Major Mountain Ranges of Spain.” *Annals of Forest Science* 66 (8): 808.

da Silva, Josiane Maria, Lucas Santos Santana, Carlos Eduardo Silva Volpato, Ana Beatriz Alves da Silva, and Tauan Bonin Goiz. 2022. “Assertiveness of a log length sensor allocated in different positions on the harvester head.” *Floresta* 52 (2): 294–303.

Dash, Jonathan P., Grant D. Pearse, and Michael S. Watt. 2018. "UAV Multispectral Imagery Can Complement Satellite Data for Monitoring Forest Health." *Remote Sensing* 10 (8). MDPI: 1216.

Dassot, Mathieu, Aurélie Colin, Philippe Santenoise, Meriem Fournier, and Thiéry Constant. 2012. "Terrestrial Laser Scanning for Measuring the Solid Wood Volume, Including Branches, of Adult Standing Trees in the Forest Environment." *Computers and Electronics in Agriculture* 89: 86–93.

de Conto, Tiago, Kenneth Olofsson, Eric Bastos Görgens, Luiz Carlos Estraviz Rodriguez, and Gustavo Almeida. 2017. "Performance of Stem Denoising and Stem Modelling Algorithms on Single Tree Point Clouds from Terrestrial Laser Scanning." *Computers and Electronics in Agriculture* 143: 165–176.

Del Rio, Miren, Felipe Bravo, Valentín Pando, Gemma Sanz, and Rosario Sierra de Grado. 2004. "Influence of Individual Tree and Stand Attributes in Stem Straightness in *Pinus Pinaster* Ait. Stands." *Annals of Forest Science* 61 (2). EDP Sciences: 141–148.

Demaerschalk, J. P. 1972. "Converting Volume Equations to Compatible Taper Equations." Forest Science 18 (3). Oxford University Press: 241–245

Disney, M., A. Burt, Kim Calders, C. Schaaf, and A. Stovall. 2019. "Innovations in Ground and Airborne Technologies as Reference and for Training and Validation: Terrestrial Laser Scanning (TLS)." *Surveys in Geophysics* 40 (4). Springer: 937–958.

Dobre, Alexandru Claudiu, Ionuț-Silviu Pascu, Ștefan Leca, Juan Garcia-Duro, Carmen-Elena Dobrota, Gheorghe Marian Tudoran, and Ovidiu Badea. 2021. "Applications of TLS and ALS in Evaluating Forest Ecosystem Services: A Southern Carpathians Case Study." *Forests* 12 (9). MDPI: 1269.

Dwivedi, Pranjal, Eric Sucre, Eric C. Turnblom, and Robert B. Harrison. 2019. "Investigating Relationships between Nutrient Concentrations, Stem Sinuosity, and Tree Improvement in Douglas-Fir Stands in Western Washington." *Forests* 10 (7). Multidisciplinary Digital Publishing Institute: 541.

Erber, Gernot, Stefan Stelzer, and Karl Stampfer. 2021. "Evaluation of a Novel Mobile Device App for Value-Maximized Bucking by Chainsaw." *International Journal of Forest Engineering*. Taylor & Francis, 1–11.

Espinoza, Jesus Alberto. 2009. "Genetic and Nutritional Effects on Stem Sinuosity in *Loblolly Pine*." *Dissertation.* North Carolina State University.

Fang, Zixing, Bruce E. Borders, and Robert L. Bailey. 2000. "Compatible Volume-Taper Models for Loblolly and Slash Pine Based on a System with Segmented-Stem Form Factors." *Forest Science* 46 (1): 1–12.

Fahey, Robert Timothy, Jason Tallant, Christopher Michael Gough, Brady S. Hardiman, J. Atkins, and Cynthia M. Scheuermann. 2016. "Comparison of Aerial and Terrestrial Remote Sensing Techniques for Quantifying Forest Canopy Structural Complexity and Estimating Net Primary Productivity." In *AGU Fall Meeting Abstracts*, 2016:B53J-07.

Fairweather, Stephen E. 1994. "Field Tests of the Criterion 400 for Hardwood Tree Diameter Measurements." *Northern Journal of Applied Forestry* 11 (1). Oxford University Press: 29–31.

Faro 2018. URL: http://www.faro.com (Accessed 31st December 2018)

Fardusi, Most Jannatul, Francesco Chianucci, and Anna Barbati. 2017. "Concept to Practice of Geospatial-Information Tools to Assist Forest Management and Planning under Precision Forestry Framework: A Review." *Ann. Silvic. Res* 41 (1): 3–14.

Fraser, R. H., and Z. Li. 2002. "Estimating Fire-Related Parameters in Boreal Forest Using SPOT VEGETATION." *Remote Sensing of Environment* 82 (1): 95–110.

Fröhlich, Christofer, and Markus Mettenleiter. 2004. "Terrestrial Laser Scanning—New Perspectives in 3D Surveying." *International Archives of Photogrammetry, Remote Sensing and Spatial Information Sciences* 36 (Part 8): W2.

Fang, Zixing, Bruce E. Borders, and Robert L. Bailey. 2000. "Compatible Volume-Taper Models for Loblolly and Slash Pine Based on a System with Segmented-Stem Form Factors." *Forest Science* 46 (1): 1–12.

Gabriel, Richard S. 2017. "The Use of Terrestrial Laser Scanning and Computer Vision in Tree Level Modeling."

Garms, Cory G., Chase H. Simpson, Christopher E. Parrish, Michael G. Wing, and Bogdan M. Strimbu. 2020. "Assessing Lean and Positional Error of Individual Mature Douglas-Fir (Pseudotsuga Menziesii) Trees Using Active and Passive Sensors." *Canadian Journal of Forest Research* 50 (11). NRC Research Press 1840 Woodward Drive, Suite 1, Ottawa, ON K2C 0P7: 1228–1243.

Ghimire, Suman, Fotios Xystrakis, and Nikos Koutsias. 2017. "Using Terrestrial Laser Scanning to Measure Forest Inventory Parameters in a Mediterranean Coniferous Stand of Western Greece." *PFG–Journal of Photogrammetry, Remote Sensing and Geoinformation Science* 85 (4). Springer: 213–225.

Ghosh, Sujit Madhab, Mukunda Dev Behera, and Somnath Paramanik. 2020. "Canopy Height Estimation Using Sentinel Series Images through Machine Learning Models in a Mangrove Forest." *Remote Sensing* 12 (9). MDPI: 1519.

Gollob, Christoph, Tim Ritter, and Arne Nothdurft. 2020. "Comparison of 3D Point Clouds Obtained by Terrestrial Laser Scanning and Personal Laser Scanning on Forest Inventory Sample Plots." *Data 5* (4). Multidisciplinary Digital Publishing Institute: 103.

Gonzalez de Tanago, Jose, Alvaro Lau, Harm Bartholomeus, Martin Herold, Valerio Avitabile, Pasi Raumonen, Christopher Martius, Rosa C. Goodman, Mathias Disney, and Solichin Manuri. 2018. "Estimation of Above-Ground Biomass of Large Tropical Trees with Terrestrial LiDAR." *Methods in Ecology and Evolution* 9 (2): 223–234.

González-Olabarria, José-Ramón, Francisco Rodríguez, Alfredo Fernández-Landa, and Blas Mola-Yudego. 2012. "Mapping Fire Risk in the Model Forest of Urbión (Spain) Based on Airborne LiDAR Measurements." *Forest Ecology and Management* 282: 149–156.

Hackenberg, Jan, Christopher Morhart, Jonathan Sheppard, Heinrich Spiecker, and Mathias Disney. 2014. "Highly Accurate Tree Models Derived from Terrestrial Laser Scan Data: A Method Description." *Forests* 5 (5): 1069–1105.

Hadas, Edyta, Andrzej Borkowski, Javier Estornell, and Przemyslaw Tymkow. 2017. "Automatic Estimation of Olive Tree Dendrometric Parameters Based on Airborne Laser Scanning Data Using Alpha-Shape and Principal Component Analysis." GIScience & Remote Sensing 54 (6). Taylor & Francis: 898–917.

Hamner, Peter, Marshall S. White, and Philip A. Araman. 2007. "The Frequency and Level of Sweep in Mixed Hardwood Saw Logs in the Eastern United States." *Forest Products Journal. 57 (9): 23-27.*

Hauglin, Marius, Terje Gobakken, Rasmus Astrup, Liviu Ene, and Erik Naesset. 2014. "Estimating Single-Tree Crown Biomass of Norway Spruce by Airborne Laser Scanning: A Comparison of

Methods with and without the Use of Terrestrial Laser Scanning to Obtain the Ground Reference Data." *Forests* 5 (3): 384–403.

Heinzel, Johannes, and Markus O. Huber. 2017. "Detecting Tree Stems from Volumetric TLS Data in Forest Environments with Rich Understory." *Remote Sensing* 9 (1). Multidisciplinary Digital Publishing Institute: 9.

Henning, Jason G., and Philip J. Radtke. 2006. "Detailed Stem Measurements of Standing Trees from Ground-Based Scanning Lidar." *Forest Science* 52 (1): 67–80.

Herrera, Jonnier F., Alonso Barrios, Ana M. López, and Víctor Nieto. 2015. "Generación de Patrones de Corte Óptimos Para Árboles Individuales a Partir de Productos Demandados En Plantaciones Comerciales." *Colombia Forestal* 18 (2). Facultad del Medio Ambiente y Recursos Naturales, Universidad Distrital: 193–206.

Hollaus, Markus, Martin Mokroš, and Yunsheng Wang. 2019. "International Benchmarking of Terrestrial Image-Based Point Clouds for Forestry." In *Geophysical Research Abstracts*. Vol. 21.

Holopainen, M., M. Vastaranta, V. Kankare, M. Räty, M. Vaaja, X. Liang, X. Yu, J. Hyyppä, H. Hyyppä, and R. Viitala. 2011. "Biomass Estimation of Individual Trees Using Stem and Crown Diameter TLS Measurements." *ISPRS-International Archives of the Photogrammetry, Remote Sensing and Spatial Information Sciences* 3812: 91–95.

Holopainen, Markus, and Jouni Kalliovirta. 2006. "Modern Data Acquisition for Forest Inventories." In *Forest Inventory*, 343–362. Springer.

Hopkinson, Chris, Laura Chasmer, Colin Young-Pow, and Paul Treitz. 2004. "Assessing Forest Metrics with a Ground-Based Scanning Lidar." *Canadian Journal of Forest Research* 34 (3). NRC Research Press Ottawa, Canada: 573–583.

Hyyppä, Eric, Antero Kukko, Risto Kaijaluoto, Joanne C. White, Michael A. Wulder, Jiri Pyörälä, Xinlian Liang, Xiaowei Yu, Yunsheng Wang, and Harri Kaartinen. 2020. "Accurate Derivation of Stem Curve and Volume Using Backpack Mobile Laser Scanning." *ISPRS Journal of Photogrammetry and Remote Sensing* 161. Elsevier: 246–262.

Jarron, Lukas R., Nicholas C. Coops, William H. MacKenzie, Piotr Tompalski, and Pamela Dykstra. 2020. "Detection of Sub-Canopy Forest Structure Using Airborne LiDAR." *Remote Sensing of Environment* 244. Elsevier: 111770.

Jung, Sung-Eun, Doo-Ahn Kwak, Taejin Park, Woo-Kyun Lee, and Seongjin Yoo. 2011. "Estimating Crown Variables of Individual Trees Using Airborne and Terrestrial Laser Scanners." *Remote Sensing* 3 (11): 2346–2363.

Kangas, Annika, and Matti Maltamo. 2006. *Forest Inventory: Methodology and Applications*. Vol. 10. Springer Science & Business Media.

Kankare, Ville, Jari Vauhkonen, Topi Tanhuanpää, Markus Holopainen, Mikko Vastaranta, Marianna Joensuu, Anssi Krooks, Juha Hyyppä, Hannu Hyyppä, and Petteri Alho. 2014. "Accuracy in Estimation of Timber Assortments and Stem Distribution–A Comparison of Airborne and Terrestrial Laser Scanning Techniques." *ISPRS Journal of Photogrammetry and Remote Sensing* 97: 89–97.

Kankare, Ville, Markus Holopainen, Mikko Vastaranta, Eetu Puttonen, Xiaowei Yu, Juha Hyyppä, Matti Vaaja, Hannu Hyyppä, and Petteri Alho. 2013. "Individual Tree Biomass Estimation Using Terrestrial Laser Scanning." *ISPRS Journal of Photogrammetry and Remote Sensing* 75. Elsevier: 64–75.

Kivinen, Veli-Pekka. 2007. “Design and Testing of Stand-Specific Bucking Instructions for Use on Modern Cut-to-Length Harvesters.” *Dissertationes Forestales*.

Ko, Chiung, Jin Taek Kang, Yeong Mo Son, and Dong-Geun Kim. 2019. “Estimating Stem Volume Using Stem Taper Equation for Quercus Mongolica in South Korea.” *Forest Science and Technology* 15 (2). Taylor & Francis: 58–62.

Kotilainen, Juha, and Teijo Rytteri. 2011. “Transformation of Forest Policy Regimes in Finland since the 19t^{h} Century.” *Journal of Historical Geography* 37 (4). Elsevier: 429–439.

Kovácsová, Petronela, and Mária Antalová. 2010. “Precision Forestry–Definition and Technologies.” Šumarski List 134 (11–12). *Hrvatsko šumarsko društvo*: 603–610.

Krok, Grzegorz, Bartolomiej Kraszewski, and Krzysztof Stereńczak. 2020. “Application of Terrestrial Laser Scanning in Forest Inventory–an Overview of Selected Issues.” Instytut Badawczy Lesnictwa (Forest Research Institute), Sekocin Stary, Poland.

Kukko, Antero, Harri Kaartinen, Juha Hyyppä, and Yuwei Chen. 2012. “Multiplatform Approach to Mobile Laser Scanning.” Proceedings of the International Archives of the Photogrammetry, *Remote Sensing and Spatial Information Sciences* 39: B5.

Labelle, Eric, and Linus Huß. 2018. “Creation of Value through a Harvester On-Board Bucking Optimization System Operated in a Spruce Stand.” *Silva Fennica* 52 (3).

Larsen, David R. 2017. “Simple Taper: Taper Equations for the Field Forester.” In*: Kabrick, John M.; Dey, Daniel C.; Knapp, Benjamin O.; Larsen, David R.; Shifley, Stephen R.; Stelzer, Henry E., Eds. Proceedings of the 20th Central Hardwood Forest Conference; 2016 March 28-April 1; Columbia, MO. General Technical Report NRS-P-167. Newtown Square, PA: US Department of Agriculture, Forest Service, Northern Research Station: 265-278.*, 265–278.

LaRue, Elizabeth A., Franklin W. Wagner, Songlin Fei, Jeff W. Atkins, Robert T. Fahey, Christopher M. Gough, and Brady S. Hardiman. 2020. “Compatibility of Aerial and Terrestrial LiDAR for Quantifying Forest Structural Diversity.” *Remote Sensing* 12 (9). Multidisciplinary Digital Publishing Institute: 1407.

Laurin, Gaia Vaglio, Nicola Puletti, William Hawthorne, Veraldo Liesenberg, Piermaria Corona, Dario Papale, Qi Chen, and Riccardo Valentini. 2016. “Discrimination of Tropical Forest Types, Dominant Species, and Mapping of Functional Guilds by Hyperspectral and Simulated Multispectral Sentinel-2 Data.” *Remote Sensing of Environment* 176: 163–176.

Lechner, Alex M., Giles M. Foody, and Doreen S. Boyd. 2020. “Applications in Remote Sensing to Forest Ecology and Management.” *One Earth* 2 (5). Elsevier: 405–412.

Leica. 2021. https://leica-geosystems.com/es-es/products/laser-scanners (Accessed 3rd May, 2021)

Li, Dandan, Haotian Guo, Weiwei Jia, and Fan Wang. 2021. “Analysis of Taper Functions for Larix Olgensis Using Mixed Models and TLS.” *Forests* 12 (2). MDPI: 196.

Li, Linyuan, Xihan Mu, Maxime Soma, Peng Wan, Jianbo Qi, Ronghai Hu, Wuming Zhang, Yiyi Tong, and Guangjian Yan. 2020. “An Iterative-Mode Scan Design of Terrestrial Laser Scanning in Forests for Minimizing Occlusion Effects.” *IEEE Transactions on Geoscience and Remote Sensing*. IEEE.

Li, Yingchang, Mingyang Li, Chao Li, and Zhenzhen Liu. 2020. “Forest Aboveground Biomass Estimation Using Landsat 8 and Sentinel-1A Data with Machine Learning Algorithms.” *Scientific Reports* 10 (1). Nature Publishing Group: 1–12.

Liang, Xinlian, and Juha Hyyppä. 2013. “Automatic Stem Mapping by Merging Several Terrestrial Laser Scans at the Feature and Decision Levels.” *Sensors* 13 (2): 1614–1634.

Liang, Xinlian, Antero Kukko, Harri Kaartinen, Juha Hyyppä, Xiaowei Yu, Anttoni Jaakkola, and Yunsheng Wang. 2014. “Possibilities of a Personal Laser Scanning System for Forest Mapping and Ecosystem Services.” *Sensors* 14 (1): 1228–1248.

Liang, Xinlian, Juha Hyyppä, Antero Kukko, Harri Kaartinen, Anttoni Jaakkola, and Xiaowei Yu. 2014. “The Use of a Mobile Laser Scanning System for Mapping Large Forest Plots.” *IEEE Geoscience and Remote Sensing Letters* 11 (9). IEEE: 1504–1508.

Liang, Xinlian, Juha Hyyppä, Harri Kaartinen, Markus Holopainen, and Timo Melkas. 2012. “Detecting Changes in Forest Structure over Time with Bi-Temporal Terrestrial Laser Scanning Data.” *ISPRS International Journal of Geo-Information* 1 (3). Multidisciplinary Digital Publishing Institute: 242–255.

Liang, Xinlian, Juha Hyyppä, Harri Kaartinen, Matti Lehtomäki, Jiri Pyörälä, Norbert Pfeifer, Markus Holopainen, Gábor Brolly, Pirotti Francesco, and Jan Hackenberg. 2018. “International Benchmarking of Terrestrial Laser Scanning Approaches for Forest Inventories.” *ISPRS Journal of Photogrammetry and Remote Sensing* 144: 137–179.

Liang, Xinlian, Ville Kankare, Juha Hyyppä, Yunsheng Wang, Antero Kukko, Henrik Haggrén, Xiaowei Yu, et al. 2016. “Terrestrial Laser Scanning in Forest Inventories.” *ISPRS Journal of Photogrammetry and Remote Sensing*, Theme issue “State-of-the-art in photogrammetry, remote sensing and spatial information science,” 115 (May): 63–77.

Lim, Kevin, Paul Treitz, Michael Wulder, Benoît St-Onge, and Martin Flood. 2003. “LiDAR Remote Sensing of Forest Structure.” *Progress in Physical Geography* 27 (1). Sage Publications Sage CA: Thousand Oaks, CA: 88–106.

Maas, Hans-Gerd, Anne Bienert, St Scheller, and E Keane. 2008. “Automatic Forest Inventory Parameter Determination from Terrestrial Laser Scanner Data.” *International Journal of Remote Sensing* 29 (5): 1579–1593.

MacDonald, Elspeth, Shaun Mochan, and Thomas Connolly. 2009. “Validation of a Stem Straightness Scoring System for Sitka Spruce (*Picea Sitchensis* (Bong.) Carr.).” *Forestry* 82 (4). Oxford University Press: 419–429.

Maier, B., D. Tiede, and L. Dorren. 2008. “Characterising Mountain Forest Structure Using Landscape Metrics on LiDAR-Based Canopy Surface Models.” In *Object-Based Image Analysis*, 625–643. Springer.

Maltamo, Matti, Erik Næsset, and Jari Vauhkonen. 2014. “Forestry Applications of Airborne Laser Scanning.” *Concepts and Case Studies. Managing Forest Ecosystems* 27. Springer: 460.

Marchi, Maurizio, Roberto Scotti, Giulia Rinaldini, and Paolo Cantiani. 2020. “Taper Function for Pinus Nigra in Central Italy: Is a More Complex Computational System Required?” *Forests* 11 (4). Multidisciplinary Digital Publishing Institute: 405.

Masuda, Hiroshi, Yuichiro Hiraoka, Kazuto Saito, Shinsuke Eto, Michinari Matsushita, and Makoto Takahashi. 2021. “Efficient Calculation Method for Tree Stem Traits from Large-Scale Point Clouds of Forest Stands.” *Remote Sensing* 13 (13). Multidisciplinary Digital Publishing Institute: 2476.

Mattheck, C., and K. Bethge. 1998. “The Mechanical Survival Strategy of Trees.” *Arboricultural Journal* 22 (4). Taylor & Francis: 369–386.

Mederski, Piotr S., Mariusz Bembenek, Zbigniew Karaszewski, Zenon Pilarek, and Agnieszka Lacka. 2018. “Investigation of Log Length Accuracy and Harvester Efficiency in Processing of Oak Trees.” *Croatian Journal of Forest Engineering: Journal for Theory and Application of Forestry Engineering* 39 (2). Fakultet šumarstva i drvne tehnologije Sveučilišta u Zagrebu: 173–181.

Menéndez-Miguélez, María, Elena Canga, Pedro Álvarez-Álvarez, and Juan Majada. 2014. “Stem Taper Function for Sweet Chestnut (*Castanea Sativa* Mill.) Coppice Stands in Northwest Spain.” *Annals of Forest Science* 71 (7): 761–770.

Mengesha, Taye, Michael Hawkins, and Maarten Nieuwenhuis. 2015. “Validation of Terrestrial Laser Scanning Data Using Conventional Forest Inventory Methods.” *European Journal of Forest Research* 134 (2). Springer: 211–222.

Middleton, George., Carter, B. D. Munro, and J. F. G. Mackay. 1989. “Losses in Timber Values Associated with Distorted Growth in Immature Douglas-Fir.” *FRDA Report*.

Mielcarek, Milosz, Krzysztof Stereńczak, and Anahita Khosravipour. 2018. “Testing and Evaluating Different LiDAR-Derived Canopy Height Model Generation Methods for Tree Height Estimation.” *International Journal of Applied Earth Observation and Geoinformation* 71. Elsevier: 132–143.

Mohammed, Habiba Ibrahim, Zulkepli Majid, and Linda Ngozi Izah. 2018. “Terrestrial Laser Scanning for Tree Parameters Inventory.” *IOP Conference Series: Earth and Environmental Science* 169 (July): 012096.

Molina-Valero, Juan Alberto, Maria José Ginzo Villamayor, Manuel Antonio Novo Pérez, Juan Gabriel Álvarez-González, Fernando Montes, Adela Martínez-Calvo, and César Pérez-Cruzado. 2020. “FORTLS: An R Package for Processing TLS Data and Estimating Stand Variables in Forest Inventories.” In *Environmental Sciences Proceedings*, 3:38. Multidisciplinary Digital Publishing Institute.

Morales-Hidalgo, D., C. Kleinn, and C. T. Scott. 2017. “Voluntary Guidelines on National Forest Monitoring.” FAO.

Morin, David, Milena Planells, Dominique Guyon, Ludovic Villard, Stéphane Mermoz, Alexandre Bouvet, Hervé Thevenon, Jean-François Dejoux, Thuy Le Toan, and Gérard Dedieu. 2019. “Estimation and Mapping of Forest Structure Parameters from Open Access Satellite Images: Development of a Generic Method with a Study Case on Coniferous Plantation.” *Remote Sensing* 11 (11). MDPI: 1275.

Murphy, Glen E., Mauricio A. Acuna, and Ian Dumbrell. 2010. “Tree Value and Log Product Yield Determination in Radiata Pine (*Pinus Radiata*) Plantations in Australia: Comparisons of Terrestrial Laser Scanning with a Forest Inventory System and Manual Measurements.” *Canadian Journal of Forest Research* 40 (11): 2223–2233.

Murphy, Glen, Hamish Marshall, and M. Chad Bolding. 2004. “Adaptive Control of Bucking on Harvesters to Meet Order Book Constraints.” *Forest Products Journal* 54 (12). Forest Products Society: 114.

Murphy, Glen. 2008. “Determining Stand Value and Log Product Yields Using Terrestrial Lidar and Optimal Bucking: A Case Study.” *Journal of Forestry* 106 (6). Oxford University Press Bethesda, MD: 317–324.

Nasberg, Mikael. 1985. "Mathematical programming model for optimal log bucking". *Dissertation* (132. 200) Linkoping University, Sweden.

Newnham, R. M. 1992. “Variable-Form Taper Functions for Four Alberta Tree Species.” *Canadian Journal of Forest Research* 22 (2): 210–223.

Olofsson, Kenneth, and Johan Holmgren. 2016. “Single Tree Stem Profile Detection Using Terrestrial Laser Scanner Data, Flatness Saliency Features and Curvature Properties.” *Forests* 7 (9): 207.

Oveland, Ivar, Marius Hauglin, Terje Gobakken, Erik Naesset, and Ivar Maalen-Johansen. 2017. “Automatic Estimation of Tree Position and Stem Diameter Using a Moving Terrestrial Laser Scanner.” *Remote Sensing* 9 (4): 350.

Oviedo-de la Fuente, Manuel, Carlos Cabo, Celestino Ordóñez, and Javier Roca-Pardiñas. 2021. “A Distance Correlation Approach for Optimum Multiscale Selection in 3D Point Cloud Classification.” Mathematics 9 (12). Multidisciplinary Digital Publishing Institute: 1328.

Pang, Lifeng, Yongpeng Ma, Ram P. Sharma, Shawn Rice, Xinyu Song, and Liyong Fu. 2016. “Developing an Improved Parameter Estimation Method for the Segmented Taper Equation through Combination of Constrained Two-Dimensional Optimum Seeking and Least Square Regression.” *Forests* 7 (9). Multidisciplinary Digital Publishing Institute: 194.

Parresol, Bernard R., James E. Hotvedt, and Quang V. Cao. 1987. “A Volume and Taper Prediction System for Bald Cypress.” *Canadian Journal of Forest Research* 17 (3): 250–259.

Pascu, Ionuț-Silviu, Alexandru-Claudiu Dobre, Ovidiu Badea, and Mihai Andrei Tanase. 2020. “Retrieval of Forest Structural Parameters from Terrestrial Laser Scanning: A Romanian Case Study.” *Forests* 11 (4). MDPI: 392.

Pfeifer, Norbert, and Christian Briese. 2007. “Geometrical Aspects of Airborne Laser Scanning and Terrestrial Laser Scanning.” *International Archives of Photogrammetry, Remote Sensing and Spatial Information Sciences* 36 (3/W52). ISPRS Vienna, Austria: 311–319.

Pfeifer, Norbert, and Daniel Winterhalder. 2004. “Modelling of Tree Cross Sections from Terrestrial Laser Scanning Data with Free-Form Curves.” *International Archives of Photogrammetry, Remote Sensing and Spatial Information Sciences* 36 (Part 8): W2.

Picard, Nicolas, Laurent Saint-André, and Matieu Henry. 2012. *Manual for Building Tree Volume and Biomass Allometric Equations: From Field Measurement to Prediction*. FAO/CIRAD.

Pilkerton, Stephen J., John Sessions, and Loren D. Kellogg. 2013. “Development of Efficient Cutting Patterns to Maximize Value with a Log-Allocation Constraint.” *International Journal of Forest Engineering* 24 (1). Taylor & Francis: 42–52.

Pitkänen, Timo P., Pasi Raumonen, and Annika Kangas. 2019. “Measuring Stem Diameters with TLS in Boreal Forests by Complementary Fitting Procedure.” *ISPRS Journal of Photogrammetry and Remote Sensing* 147. Elsevier: 294–306.

Pnevmaticos, Shaun and Sebastian Mann. 1972. "Dynamic programming in tree bucking". *Forest Products Journal* 22(2), 26–30.

Prada, Marta, Elena Canga, Juan Majada, and Celia Martínez-Alonso. 2022. “Canopy Characterization of Sweet Chestnut Coppice in the North of Spain from Lidar Data.” *European Journal of Forest Research* 141 (2). Springer: 267–279.

Prendes, Covadonga, Carlos Cabo, Celestino Ordoñez, Juan Majada, and Elena Canga. 2021. “An Algorithm for the Automatic Parametrization of Wood Volume Equations from Terrestrial Laser Scanning Point Clouds: Application in *Pinus Pinaster*.” *GIScience & Remote Sensing*. Taylor & Francis, 1–21.

Prendes, Covadonga, Elena Canga, Celestino Ordoñez, Juan Majada, Mauricio Acuna, and Carlos Cabo. 2022. “Automatic Assessment of Individual Stem Shape Parameters in Forest Stands from TLS Point Clouds: Application in Pinus Pinaster.” *Forests* 13 (3). MDPI: 431.

Puletti, Nicola, Mirko Grotti, Carlotta Ferrara, and Francesco Chianucci. 2020. "Lidar-Based Estimates of Aboveground Biomass through Ground, Aerial, and Satellite Observation: A Case Study in a Mediterranean Forest." *Journal of Applied Remote Sensing* 14 (4). International Society for Optics and Photonics: 044501.

Raumonen, Pasi, Eric Casella, Kim Calders, Sue Murphy, Markku Åkerblom and Mikko Kaasalainen. 2015. "Massive-scale tree modelling from TLS data". *ISPRS Annals of Photogrammetry, Remote Sensing & Spatial Information Sciences* 2.

Raumonen, Pasi, Mikko Kaasalainen, Markku Åkerblom, Sanna Kaasalainen, Harri Kaartinen, Mikko Vastaranta, Markus Holopainen, Mathias Disney, and Philip Lewis. 2013. "Fast Automatic Precision Tree Models from Terrestrial Laser Scanner Data." *Remote Sensing* 5 (2): 491–520.

Reed, David D., and Edwin J. Green. 1984. "Compatible Stem Taper and Volume Ratio Equations." *Forest Science* 30 (4). Oxford University Press: 977–990.

Rodríguez, Francisco, Iñigo Lizarralde Torre, and Felipe Bravo Oviedo. 2015. "Comparison of Stem Taper Equations for Eight Major Tree Species in the Spanish Plateau." Forest Systems 24 (3). Instituto Nacional de Investigación y Tecnología Agraria y Alimentaria (INIA): 2Rodriguez, Francisco, Inigo Lizarralde, Alfredo Fernández-Landa, and Sonia Condés. 2014. "Non-Destructive Measurement Techniques for Taper Equation Development: A Study Case in the Spanish Northern Iberian Range." European Journal of Forest Research 133 (2). Springer: 213–223.

Rodríguez-Puerta, Francisco, Esteban Gómez-García, Saray Martín-García, Fernando Pérez-Rodríguez, and Eva Prada. 2021. "UAV-Based LiDAR Scanning for Individual Tree Detection and Height Measurement in Young Forest Permanent Trials." *Remote Sensing* 14 (1). MDPI: 170.

Rogan, John, and DongMei Chen. 2004. "Remote Sensing Technology for Mapping and Monitoring Land-Cover and Land-Use Change." *Progress in Planning* 61 (4). Pergamon: 301–325.

Roughgarden, J., Steven W. Running, and Pamela A. Matson. 1991. "What Does Remote Sensing Do for Ecology?" *Ecology* 72 (6). JSTOR: 1918–1922.

RTA2017-00063-C04-02.2017. Research project: Evaluation of relevant characters for the sustainable management of *Pinus Pinaster* Ait. and its interaction with new climate scenarios. INIA. (National Institute of Agrarian Research). Main researcher: Juan Pedro Majada Guijo.

Saarinen, Ninni, Ville Kankare, Jiri Pyörälä, Tuomas Yrttimaa, Xinlian Liang, Michael A. Wulder, Markus Holopainen, Juha Hyyppä, and Mikko Vastaranta. 2019. "Assessing the Effects of Sample Size on Parametrizing a Taper Curve Equation and the Resultant Stem-Volume Estimates." *Forests* 10 (10). Multidisciplinary Digital Publishing Institute: 848.

Saarinen, Ninni, Ville Kankare, Mikko Vastaranta, Ville Luoma, Jiri Pyörälä, Topi Tanhuanpää, Xinlian Liang, Harri Kaartinen, Antero Kukko, and Anttoni Jaakkola. 2017. "Feasibility of Terrestrial Laser Scanning for Collecting Stem Volume Information from Single Trees." *ISPRS Journal of Photogrammetry and Remote Sensing* 123: 140–158.

SADEI, 2018. Statistical Yearbook of Asturias. Asturian Institute of Statistics. Regional Ministry of Rural Development and Natural Resources. Government of the Principality of Asturias, Oviedo.

Salas, Christian, Mauricio Reyes, and Claudia Bassaber. 2005. "Measurement of Upper-Stem Diameters with Bitterlich Mirror Relascope and Finnish Parabolic Caliper: Effects in Volume Estimations." *Bosque (Valdivia)* 26 (2). SciELO Chile: 81–90.

Sandak, Jakub, Anna Sandak, Stefano Marrazza, and Gianni Picchi. 2019. "Development of a Sensorized Timber Processor Head Prototype–Part 1: Sensors Description and Hardware

Integration." *Croatian Journal of Forest Engineering: Journal for Theory and Application of Forestry Engineering* 40 (1). Fakultet šumarstva i drvne tehnologije Sveučilišta u Zagrebu: 25–37.

Santopuoli, Giovanni, Mirko Di Febbraro, Mauro Maesano, Marco Balsi, Marco Marchetti, and Bruno Lasserre. 2020. "Machine Learning Algorithms to Predict Tree-Related Microhabitats Using Airborne Laser Scanning." *Remote Sensing* 12 (13). MDPI: 2142.

Seidel, Dominik, Peter Annighöfer, Christian Ammer, Martin Ehbrecht, Katharina Willim, Jan Bannister, and Daniel P. Soto. 2021. "Quantifying Understory Complexity in Unmanaged Forests Using TLS and Identifying Some of Its Major Drivers." *Remote Sensing* 13 (8). Multidisciplinary Digital Publishing Institute: 1513.

Sessions, John. 1988. "Making Better Tree-Bucking Decisions in the Woods." *Journal of Forestry* 86 (10). Oxford University Press: 43–45.

Silva, Rodrigo Freitas, Marcelo Otone Aguiar, Mayra Luiza Marques da Silva, Gilson Fernandes da Silva, and Adriano Ribeiro de Mendonça. 2020. "SISFLOR: A Computational system to determine the optimal tree bucking." *Revista Engenharia Na Agricultura-Reveng* 28: 192–201.

Smith, W. Brad. 2002. "Forest Inventory and Analysis: A National Inventory and Monitoring Program." *Environmental Pollution* 116. Elsevier: S233–S242.

Spinelli, Raffaele, Natascia Magagnotti, and Carla Nati. 2011. "Work Quality and Veneer Value Recovery of Mechanised and Manual Log-Making in Italian Poplar Plantations." *European Journal of Forest Research* 130 (5). Springer: 737–744.

Spurr, Stephen Hopkins. 1952. "Forest Inventory." Ronald Press

Srinivasan, Shruthi, Sorin C. Popescu, Marian Eriksson, Ryan D. Sheridan, and Nian-Wei Ku. 2014. "Multi-Temporal Terrestrial Laser Scanning for Modeling Tree Biomass Change." *Forest Ecology and Management* 318. Elsevier: 304–317.

Stovall, Atticus EL, and Jeff W. Atkins. 2021. "Assessing Low-Cost Terrestrial Laser Scanners for Deriving Forest Structure Parameters." Preprints.

Sullivan, Martin JP, Simon L. Lewis, Wannes Hubau, Lan Qie, Timothy R. Baker, Lindsay F. Banin, Jerôme Chave, Aida Cuni-Sanchez, Ted R. Feldpausch, and Gabriela Lopez-Gonzalez. 2018. "Field Methods for Sampling Tree Height for Tropical Forest Biomass Estimation." *Methods in Ecology and Evolution* 9 (5). Wiley Online Library: 1179–1189.

Sun, Yuan, Xinlian Liang, Ziyu Liang, Clive Welham, and Weizheng Li. 2016. "Deriving Merchantable Volume in Poplar through a Localized Tapering Function from Non-Destructive Terrestrial Laser Scanning." *Forests* 7 (4): 87.

Taha, Hamdy.2017. "Operations Research: An Introduction", 10th Edition. *Pearson Education Limited*. London. ISBN 13: 978-1-292-16554-7. 843.

Teshome, Tesfaye. 2005. "A Ratio Method for Predicting Stem Merchantable Volume and Associated Taper Equations for Cupressus Lusitanica, Ethiopia." *Forest Ecology and Management* 204 (2–3). Elsevier: 171–179.

Thies, Michael, and H. Spiecker. 2004. "Evaluation and Future Prospects of Terrestrial Laser Scanning for Standardized Forest Inventories." *Forest* 2 (2.2). Citeseer: 1.

Thies, Michael, Norbert Pfeifer, Daniel Winterhalder, and Ben GH Gorte. 2004b. "Three-Dimensional Reconstruction of Stems for Assessment of Taper, Sweep and Lean Based on Laser Scanning of Standing Trees." *Scandinavian Journal of Forest Research* 19 (6): 571–581.

Tian, Jiarong, Tingting Dai, Haidong Li, Chengrui Liao, Wenxiu Teng, Qingwu Hu, Weibo Ma, and Yannan Xu. 2019. "A Novel Tree Height Extraction Approach for Individual Trees by Combining

TLS and UAV Image-Based Point Cloud Integration." *Forests* 10 (7). Multidisciplinary Digital Publishing Institute: 537.

Tomppo, Erkki, Thomas Gschwantner, Mark Lawrence, Ronald E. McRoberts, K. Gabler, K. Schadauer, C. Vidal, A. Lanz, G. Ståhl, and E. Cienciala. 2010. "National Forest Inventories." *Pathways for Common Reporting. European Science Foundation* 1. Springer: 541–553.

Torresan, Chiara, Francesco Pelleri, Maria Chiara Manetti, Claudia Becagli, Cristiano Castaldi, Monica Notarangelo, and Ugo Chiavetta. 2021. "Comparison of TLS against Traditional Surveying Method for Stem Taper Modelling. A Case Study in European Beech (*Fagus Sylvatica* L.) Forests of Mount Amiata." *Annals of Silvicultural Research* 46 (2).

Trincado, Guillermo, and Harold E. Burkhart. 2006. "A Generalized Approach for Modeling and Localizing Stem Profile Curves." *Forest Science* 52 (6): 670–682.

Trincado, Guillermo, Klaus Von Gadow, and Victor Sandoval. 1997. "Estimación de Volumen Comercial En Latifoliadas." *Bosque* 18 (1): 39–44.

Tukey, John W. 1949. "Comparing Individual Means in the Analysis of Variance." *Biometrics*. JSTOR, 99–114.

Ulak, Sunita, Keshav Ghimire, Rabindra Gautam, Shes Kanta Bhandari, Krishna Prasad Poudel, Yajna Prasad Timilsina, Dhirendra Pradhan, and Thakur Subedi. 2022. "Predicting the Upper Stem Diameters and Volume of a Tropical Dominant Tree Species." *Journal of Forestry Research*. Springer, 1–13.

Van Leeuwen, Martin, and Maarten Nieuwenhuis. 2010. "Retrieval of Forest Structural Parameters Using LiDAR Remote Sensing." *European Journal of Forest Research* 129 (4). Springer: 749–770.

Vauhkonen, Jari, Matti Maltamo, Ronald E. McRoberts, and Erik Næsset. 2014. "Introduction to Forestry Applications of Airborne Laser Scanning." In *Forestry Applications of Airborne Laser Scanning*, 1–16. Springer.

Van Deusen, Paul C., Alfred D. Sullivan, and Thomas G. Matvey. 1981. "A Prediction System for Cubic Foot Volume of Loblolly Pine Applicable through Much of Its Range." *Southern Journal of Applied Forestry* 5 (4). Oxford University Press: 186–189.

Vanzetti, Nicolás, Diego Broz, Jorge M. Montagna, and Gabriela Corsano. 2019. "Integrated Approach for the Bucking and Production Planning Problems in Forest Industry." *Computers & Chemical Engineering* 125. Elsevier: 155–163.

Warensjo, M., and Göran Rune. 2004. "Stem Straightness and Compression Wood in a 22-Year-Old Stand of Container-Grown Scots Pine Trees." *Silva Fennica* 38 (2). Citeseer: 143–153.

Wang, Jiamin, Xinxin Chen, Lin Cao, Feng An, Bangqian Chen, Lianfeng Xue, and Ting Yun. 2019. "Individual Rubber Tree Segmentation Based on Ground-Based LiDAR Data and Faster R-CNN of Deep Learning." *Forests* 10 (9). Multidisciplinary Digital Publishing Institute: 793.

Wang, Kai, Wei-Ning Xiang, Xulin Guo, and Jianjun Liu. 2012. "Remote Sensing of Forestry Studies." *Global Perspectives on Sustainable Forest Management*. IntechOpen, 205–216.

Wang, Jingxin, Chris B. LeDoux, and Joseph McNeel. 2004. "Optimal Tree-Stem Bucking of Northeastern Species of China."

Wilkes, Phil, Alvaro Lau, Mathias Disney, Kim Calders, Andrew Burt, Jose Gonzalez de Tanago, Harm Bartholomeus, Benjamin Brede, and Martin Herold. 2017. "Data Acquisition Considerations for Terrestrial Laser Scanning of Forest Plots." *Remote Sensing of Environment* 196: 140–153.

Westfall, J. A., and C. T. Scott. 2010. "Taper Models for Commercial Tree Species in the Northeastern United States." *Forest Science* 56 (6): 515–528. Oxford University Press.

Weng, Yuhui, Randy Ford, Zaikang Tong, and Marek Krasowski. 2017. "Genetic Parameters for Bole Straightness and Branch Angle in Jack Pine Estimated Using Linear and Generalized Linear Mixed Models." *Forest Science* 63 (1). Oxford University Press Oxford, UK: 111–117.

Wu, H. X., M. Ivkovic, W. J. Gapare, A. C. Matheson, B. S. Baltunis, M. B. Powell, and T. A. McRae. 2008. "Breeding for Wood Quality and Profit in Pinus Radiata: A Review of Genetic Parameter Estimates and Implications for Breeding and Deployment." *New Zealand Journal of Forestry Science* 38 (1): 56–87.

Xie, Bo, Chunxiang Cao, Min Xu, Xinwei Yang, Robert Shea Duerler, Barjeece Bashir, Zhibin Huang, Kaimin Wang, Yiyu Chen, and Heyi Guo. 2022. "Improved Forest Canopy Closure Estimation Using Multispectral Satellite Imagery within Google Earth Engine." *Remote Sensing* 14 (9). MDPI: 2051.

Xu, Dandan, Haobin Wang, Weixin Xu, Zhaoqing Luan, and Xia Xu. 2021. "LiDAR Applications to Estimate Forest Biomass at Individual Tree Scale: Opportunities, Challenges and Future Perspectives." *Forests* 12 (5). Multidisciplinary Digital Publishing Institute: 550.

You, Lei, Shouzheng Tang, Xinyu Song, Yuancai Lei, Hao Zang, Minghua Lou, and Chongyang Zhuang. 2016. "Precise Measurement of Stem Diameter by Simulating the Path of Diameter Tape from Terrestrial Laser Scanning Data." *Remote Sensing* 8 (9): 717.

Yu, X., X. Liang, J. Hyyppä, V. Kankare, M. Vastaranta, and M. Holopainen. 2013. "Stem Biomass Estimation Based on Stem Reconstruction from Terrestrial Laser Scanning Point Clouds." *Remote Sensing Letters* 4 (4): 344–353.

Yun, Ting, Kang Jiang, Hu Hou, Feng An, Bangqian Chen, Anna Jiang, Weizheng Li, and Lianfeng Xue. 2019. "Rubber Tree Crown Segmentation and Property Retrieval Using Ground-Based Mobile LiDAR after Natural Disturbances." *Remote Sensing* 11 (8). Multidisciplinary Digital Publishing Institute: 903.

Zapata-Cuartas, Mauricio, Bronson P. Bullock, and Cristian R. Montes. 2021. "A Taper Equation for Loblolly Pine Using Penalized Spline Regression." *Forest Science* 67 (1). Oxford University Press US: 1–13.

Zhang, Tian, Wanchang Zhang, Ruizhao Yang, Yimo Liu, and Masoud Jafari. 2021. "CO2 Capture and Storage Monitoring Based on Remote Sensing Techniques: A Review." *Journal of Cleaner Production* 281. Elsevier: 124409.

Zhang, Yuzhen, Jun Ma, Shunlin Liang, Xisheng Li, and Manyao Li. 2020. "An Evaluation of Eight Machine Learning Regression Algorithms for Forest Aboveground Biomass Estimation from Multiple Satellite Data Products." *Remote Sensing* 12 (24). MDPI: 4015.

Zhao, Qingxia, Shichuan Yu, Fei Zhao, Linghong Tian, and Zhong Zhao. 2019. "Comparison of Machine Learning Algorithms for Forest Parameter Estimations and Application for Forest Quality Assessments." *Forest Ecology and Management* 434. Elsevier: 224–234.

Zhou, Junjie, Hongqiang Wei, Guiyun Zhou, and Lihui Song. 2019. "Separating Leaf and Wood Points in Terrestrial Laser Scanning Data Using Multiple Optimal Scales." *Sensors* 19 (8). MDPI: 1852.

Zong, Xin, Tiejun Wang, Andrew K. Skidmore, and Marco Heurich. 2021. "The Impact of Voxel Size, Forest Type, and Understory Cover on Visibility Estimation in Forests Using Terrestrial Laser Scanning." *GIScience & Remote Sensing* 58 (3). Taylor & Francis: 323–339